

Institute of Animal Pathology
Faculty of Veterinary Medicine
Ludwig Maximilians University Munich
Chair: Prof. Dr. Walter Hermanns

Doctoral Studies Performed in the
Institute of Neuropathology and Prion Research
Faculty of Medicine
Ludwig Maximilians University Munich
Under Supervision of Prof. Dr. Hans Kretzschmar

Studies on Pathogenic Mechanisms of Prion Diseases and Evaluation of Prion Strains Properties

A Thesis
Submitted for the
Doctor Degree in Veterinary Medicine
Faculty of Veterinary Medicine
Ludwig Maximilians University Munich

From
Mohamed Karmi Hussein Mahmoud
Aswan-Egypt

Munich 2009

Gedruckt mit Genehmigung der Tierärztlichen Fakultät
Der Ludwig Maximilians University Munich

Dekan: Universität-Professor Dr. J. Braun
Referent: Universität-Professor Dr. W. Hermanns
Koreferent: Universität-Professor Dr. W. Klee

Tag der Promotion: 6. Februar 2009

This work is dedicated to
my parents, my wife and my son Abd El-Rahman

Table of Contents	Page
1. Introduction.....	13
1.1. The Prion.....	13
1.2. The Prion Diseases and Neurodegeneration.....	15
1.3. Conversion and Aggregation of Prion Protein.....	17
1.4. Neuropathology of the Prion Protein.....	19
1.5. Biochemical Analysis of the Prion Protein.....	20
1.6. Mutations and Polymorphisms of the PrP-Gene.....	21
1.7. Effect of the Codon 129 Polymorphism on Human Susceptibility.....	22
1.8. Species Barrier and Strain Diversibility of Prions.....	24
1.9. Potential Abilities of Classical and Atypical Human TSE Strains.....	26
to Propagate in Transgenic Mice	
1.10. Alteration of Atypical TSE biological Properties after Transmission.....	28
to Humanized Mice	
1.11. Potential Similarities and Links between Atypical TSE Cases and.....	29
other Known Prion Protein	
1.12. Aim of the Work.....	29
2. Material and Methods.....	31
2.1. Materials.....	31
2.1.1. Chemicals.....	31
2.1.2. Biologicals.....	32
2.1.3. Buffers for Sample Preparation.....	33
2.1.4. Buffers for SDS-PAGE and Western Blot analysis.....	34
2.1.5. Buffers for FACS analysis.....	35
2.1.6. DNA Isolation Kits and PCR reagents.....	35
2.1.7. Consumables.....	36
2.1.8. Equipments.....	37
2.2. Methods.....	38
3.1.1. Construction of EGFP-PrP Transgene.....	38
2.2.2. Generation of Transgenic Mice.....	39
2.2.3. Infection of Transgenic Mice.....	39
2.2.4. Determination of Incubation Times.....	41
2.2.5. SDS-PAGE and Western Blot analysis of Infected Animals.....	41

2.2.6. Histology and Immunohistochemistry.....	43
2.2.7. Determination of Lesion Profiles “Scoring”.....	44
2.2.8. FACS analysis of EGFP-PrP transgenic mice.....	44
2.2.9. <i>In Vitro</i> Conversion Assay of EGFP-PrP.....	46
2.2.10. Confocal Laser Scanning Microscopy “LSM”.....	46
2.2.11. Rescue Studies on transgenic F35 Mice.....	47
2.2.12. Genotyping of HuM, HuV and LL mice.....	47
3. Results.....	50
3.1. Investigation of Pathogenic Mechanisms of Prion Diseases using.....	50
TransgenicMice expressing EGFP-PrP	
3.1.1. Expression of EGFP-PrP in EGFP-PrP Transgenic Mice.....	50
3.1.2. FACS analysis of EGFP-PrP Mice.....	51
3.1.3. <i>In Vitro</i> Conversion Assay and Susceptibility of EGFP-PrP Mice.....	51
to Scrapie Infection	
3.1.4. Rescue Studies using F35 Mice.....	53
3.1.5. Incubation Times of Infected EGFP-PrP Mice.....	55
3.1.6. Biochemical Analysis of infected EGFP-PrP Mice.....	55
3.1.7. Histology and Immunohistochemistry of Infected Brain Tissue.....	56
3.1.8. Confocal Laser Scanning Microscopy of Infected Brain Tissue.....	58
3.2. Evaluation of Prion Strains Properties using Transgenic Mice Expressing....	60
Human PrP	
3.2.1. Susceptibility and Incubation Times of Humanized and LL Mice.....	60
to Various Human TSE Strains	
3.2.2. Neuropathology and Lesion Profiling.....	64
3.2.3. Biochemical Analysis of infected Humanized and LL Mice.....	68
4. Discussion.....	73
4.1. Investigation of Pathogenic Mechanisms of Prion Diseases using.....	73
Transgenic Mice expressing EGFP-PrP	
4.2. Evaluation of Prion Strains Properties using Transgenic Mice Expressing....	78
Human and LL Mice	
5. Summary.....	84
6. Zusammenfassung.....	86

7. References.....	88
8. Curriculum Vitae.....	103
9. Acknowledgment.....	105

List of Figures	Page
Figure 1: The phgGFP-PrP Fusion Protein Transgene Construct.....	38
Figure 2: EGFP-PrP L42 transgene construct.....	39
Figure 3: Pronucleus injection of EGFP-PrP in nuclei of Oocytes.....	39
Figure 4: Confocal laser scanning microscopy of EGFP-PrP transgenic mice..... showing different Expression Patterns of EGFP-PrP	50
Figure 5: FACS analysis of EGFP-PrP-24 mice showing positive cells in..... transgenic samples	51
Figure 6: Analysis of stable clones of RK13 cells transfected with phg EGFP-..... PrP L42 construct.	52
Figure 7: <i>In vitro</i> conversion assay of EGFP-PrP.....	53
Figure 8: Illustration showing structure of F35-PrP truncated gene with deletion.... of 32-234 residues	54
Figure 9: Histopathological effects of F35-PrP truncated gene on mice.....	54
Figure 10: Survival data of scrapie infected EGFP-PrP/wt-PrP-mice.....	55
Figure 11: Western Blot of scrapie infected EGFP-PrP/wt-PrP mice.....	56
Figure 12: Histology by H&E and Immunohistochemistry by CDC1 & L42.....	57
Figure 13: Histology by H&E and Immunohistochemistry by CDC1 & L42.....	57
Figure 14: Cerebellum of infected mice showing strongly fluorescent aggregates.... distributed throughout the molecular and granular cell layers, but more abundant in the molecular cell layer in comparison with non-infected mice, which were negative for aggregates.	58
Figure 15: Cerebellum of infected mice showing strongly fluorescent aggregates.... distributed throughout the molecular and granular cell layers, but more abundant in the molecular cell layer in comparison with non-infected mice, which were negative for aggregates.	59
Figure 16: Cerebral cortex and basal ganglia of infected mice showing a lot of..... fluorescent aggregates distributed widely in nervous tissue in comparison with non-infected mice, which were negative for aggregates.	59
Figure 17: Incubation times of humanized mice infected with TSE strains.....	62
Figure 18: Comparison of incubation times between different TSE strains.....	63
Figure 19: Comparison of incubation times between HuMM and HuVV mice..... infected with different TSE strains	64
Figure 20: Incubation times of LL mice infected with two different GSS strains.....	64

(a & b)

Figure 21: Immunocytochemical pattern of PrP deposition (A-C) and astrogliosis....65 (D) in the hippocampus of LL mice inoculated with GSS-b 729 days post inoculation	
Figure 22: Immunocytochemical patterns of PrP deposition in LL mice.....65	
Figure 23: Immunocytochemistry showing patterns of PrP deposition human.....66 transgenic mice	
Figure 24: Immunocytochemistry showing patterns of PrP deposition (A&C).....66 and astrogliosis (B&D) in the hippocampus and thalamus of HuVV mice inoculated with sCJD MM1, 601 days post inoculation	
Figure 25: Histological sections (H&E) showing extensive spongiosis in the.....67 medulla (A) and thalamus (B) in HuVV mice inoculated with sCJD MM1, 586 days post inoculation	
Figure 26: Lesion Profiles for the different sCJD, vCJD and GSS Strains.....68	
Figure 27: Western Blot of HuVV Groups Infected with different TSE Strains.....70	
Figure 28: Western Blot of HuMM Groups Infected with different TSE Strains.....71	
Figure 29: Western Blot of LL Groups Infected with different TSE Strains.....72	

List of Tables	Page
Table 1: Chemicals.....	31
Table 2: Biologicals.....	32
Table 3: Buffers for sample preparation.....	33
Table 4: Buffers for SDS-PAGE and western blot analysis.....	34
Table 5: Buffers for FACS analysis.....	35
Table 6: DNA isolation kits and PCR reagents.....	35
Table 7: Consumables.....	36
Table 8: Equipments.....	37
Table 9: Groups of human transgenic mice, HuMM and HuVV inoculated with.....	41
different TSE strains of human prions	
Table 10: PCR-programme for genotyping of HuM, HuV and HuMV mice.....	48
Table 11: PCR-programme for genotyping of LL mice.....	49
Table 12: Time Score of Incubation Times of HuMM and HuVV mice after.....	61
Infection with sCJD MM1 (a&b), sCJD MM2 (a&b) and vCJD (a&b).	
Table 13: Incubation Times and Glycoform Types of HuMM and HuVV mice after...	61
infection with sCJD MM1 (a&b), sCJD MM2 (a&b) and vCJD (a&b).	

List of Abbreviations

AA	Amino acid
AEF	Amyloid enhancing factors
Asn	Asparagine
BHK	Baby hamster kidney fibroblast cells
bp	Base pair
BSA	Bovine serum albumin
BSE	Bovine spongiform encephalopathy
CDC1	Epitope on the prion protein for antibody binding
CHO	Chinese hamster ovary cells
CJD	Creutzfeldt - Jakob disease
CNS	Central nervous system
CWD	Chronic wasting disease
DdeI	Restriction enzyme
DNA	Deoxyribonucleic acid
d.p.i.	Days post infection
DY	Drowsy prion strain isolated from mink
ECL	Enhanced chemiluminescence reagent
EEG	Electroencephalography
EGFP	Enhanced green fluorescent protein
ER	Endoplasmic reticulum
FACS	Fluorescent-activated cell sorting
fCJD	Familial Creutzfeldt-Jakob disease
FFI	Fatal familial insomnia
FSC	Forward scattering count
FVB	Wild type mice (sensitive for <u>F</u> riend Leukemia <u>V</u> irus <u>B</u> strain)
F35	Mice with deletion of codon 32-135 of PrP gene
GPI	Glycosylphosphatidylinositol
GPS	Gas phase sequencing
GSS	Gerstmann-Sträussler-Scheinker syndrome
H&E	Haematoxyline and Eosin stain
HGH	Human growth hormone
Hu	Human
HuMM	Methionine homozygous humanized transgenic mice

HuVV	Valine homozygous humanized transgenic mice
HY	Hyper prion strain isolated from mink
I.Block	Bovine serum used for blocking of membrane
IgG	Immunoglobulin G
L42	Epitope on human prion protein
Leu	Leucine
LG	Group of LL mice
LL	Homozygous for Leucine residue at codon 101 of PrP gene
LOD	Logarithm (base 10) of odds used for genetic linkage study
LSB	Laemmli sample buffer
LSM	Laser scanning microscopy
M	Methionine
mA	Milliampere
ME7	Scrapie prion strain
MG	Group of MM mice
MM	Homozygous for methionine at codon 129 of PrP gene
Mo	Mause
MS	Mass spectrometry
NEBuffer	Used with restriction endonucleases
NspI	Restriction enzyme
ORF	Open reading frame of the gene
PBS	Phosphate buffered saline
P102L	Change of proline into leucine at codon 102 of PrP gene
PCR	Polymerase chain reaction
phg	Half genomic construct
PK	Proteinase K enzyme
PMSF	Phenylmethanesulphonyl fluoride
PRNP	Prion protein gene
Pro	Proline
PrP	Prion protein
PrP ^C	Cellular prion protein
PrP ^{Sc}	Scrapie prion protein
PrP27-30	Fragment of prion protein 27-30 bp long after PK digestion
PrP%	Mice without prion protein

PVDF	Polyvinylidene fluoride
R1&R2	Gated regions in FACS analysis
RML	Rocky Mountain Laboratory Scrapie Strain
RK13	Rabbit kidney cells
³⁵ S	Radioactive sulfur 35
sCJD	Sporadic Creutzfeldt-Jakob disease
SD	Standard deviation
SDS-PAGE	Sodium dodecyl sulfate polyacrylamide gel electrophoresis
SHa	Syrian hamster
SSC	Side scattering count
Taq	Polymerase enzyme
Tg	Transgenic
TME	Transmissible mink encephalopathy
TSE	Transmissible spongiform encephalopathy
UV	Ultraviolet rays
V	Valine amino acid
VG	Group of VV mice
VV	Homozygous for valine at codon 129 of PrP gene
vCJD	Variant Creutzfeldt-Jakob disease
Wt-BKG	Wild-type background
w/v	Weight per volume
X-ray	Roentegen rays
3F4	Clone of prion protein
4H11	Clone of prion protein
22L	Scrapie prion strain
101LL	Mutation at codon101 of PrP gene homozygous for Leucine
129 MM	Homozygous for methionine at codon 129 of PrP gene
129 VV	Homozygous for valine at codon 129 of PrP gene
Δ	Gene deletion

1. Introduction

1.1. The Prion

Prions are unprecedented infectious pathogens that cause a group of invariably fatal neurodegenerative diseases mediated by an entirely novel mechanism. Prions are devoid of nucleic acid and seen to be composed exclusively of a modified isoform of PrP designated PrP^{Sc}. The normal, cellular PrP, denoted PrP^C, is converted into PrP^{Sc} through a process whereby a portion of its α -helical and coil structure is refolded into β -sheet. This structural transition is accompanied by profound change in the physicochemical properties of the PrP (1,3,4,20). The name Prion is derived from its definition as a ***proteinaceous infectious*** particle that lacks nucleic acid (1,4,25,26,27,28).

The Prion was defined as an infectious pathogen that requires a protein for infectivity yet is highly resistant to procedures that modify or destroy nucleic acids. Prions differ from bacteria, viruses, and viroids by their new structure and properties. Experiments designed to uncover participation of a nucleic acid in prion structure or infectivity consistently were given negative results. These approaches include: 1) infectivity measurements after ultraviolet and ionizing radiation or chemical treatments that modify or destroy nucleic acids, 2) purification studies aimed at physical detection of prion nucleic acid, and 3) a variety of molecular cloning schemes (2).

Human PrP^C is a glycoprotein of 253 amino acids before cellular processing. There is an 85-90% homology to prion proteins of other mammalian species. PrP^C is a membrane protein expressed mainly in neurons, but also in astrocytes and a number of other cells. It has an N-terminal signal sequence of 22 amino acids, which is cleaved off the translation product. Twenty-three terminal amino acids are removed when glycosylphosphatidylinositol (GPI) is attached to serine residue 230. Mature PrP^C is attached to the cell surface by this GPI anchor and undergoes endocytosis and recycling. There are two N-glycosylation sites that are glycosylated differently in different human CJD variants. The N-terminal moiety of the protein contains an octapeptide repeat, (PHGGGW_GQ)_{x4}, which has been suggested to function in copper binding. PrP^C purified from hamster brain consisted of 42% α -helical and only 3% β -sheet structure, whereas PrP purified from scrapie-infected hamster brain is composed of 30% α -helix and 43% β -sheet (6).

Progressive enrichment of brain homogenates for infectivity resulted in the isolation of a protease-resistant sialoglycoprotein, designated the prion protein (PrP) (48). This

protein was the major constituent of infective fractions and was found to accumulate in affected brains and sometimes to form amyloid deposits. The term Prion was proposed to distinguish the infectious pathogen from viruses or viroids (7). No differences in amino acid sequence between PrP^{Sc} and PrP^C have been identified. PrP^{Sc} is known to be derived from PrP^C by posttranslational process (7,25,28). Neither amino acid sequencing nor systematic studies of known covalent posttranslational modifications have shown any consistent differences between PrP^C and PrP^{Sc} (157).

The physiologic roles attributed to PrP^C are rather disparate and include: a) function as a membrane receptor; b) regulator of apoptosis; c) carrier or binding protein for copper ions; d) effectors in signal transduction mechanisms; e) regulator of synaptic transmission; and f) transcription factor. This redundancy reflects a complex lack of understanding regarding two crucial aspects, the topological organization and the subcellular localization of PrP (8). The normal function of PrP^C remains unknown, although its localization on the cell surface would be consistent with roles in cell adhesion and recognition, ligand uptake, or transmembrane signalling. Defining the physiological role of PrP^C may be relevant to understanding the disease state, since the protein may fail to perform its normal function when it is converted to the PrP^{Sc} isoform (9,11). The normal prion protein is widely expressed and bound to the cell surface by a glycosylphosphatidylinositol anchor. PrP has an unstructured domain of around 100 amino acids, and a structured C-terminal domain of similar size, which includes a single disulphide bond and two glycosylation sites (13).

The normal prion protein, PrP^C, is encoded by the prion protein gene (PRNP) on human chromosome 20, with equivalent prion genes in animals. The function is not known but it may have roles in anti-oxidant systems and cellular copper metabolism. In prion diseases, the normal host gene produces the normal host PrP^C but there is then an incompletely understood posttranslational conformational change to a disease-related form, PrP^{Sc}. PrP^{Sc} is relatively insoluble and relatively protease-resistant and accumulates in tissues forming amyloid structures. The precise pathogenesis of the neurological illness is not known, but PrP^{Sc} deposition is associated with the neurological changes of neuronal loss, astrocytic gliosis, and spongiform changes. In the acquired prion diseases, material from an affected host infects another. The infective agent (termed the "prion") has not been fully characterized, but PrP^{Sc} is associated with infectivity (15).

In a search for a posttranslational chemical modification that might explain the differences in the properties of these two PrP isoforms, PrP^{Sc} was analyzed by mass spectrometry (MS) and gas-phase sequencing (GPS). The amino acid sequence was the same as that deduced from the translated open reading frame (ORF) of the PrP gene, and no modifications that might differentiate PrP^C from PrP^{Sc} were found. These findings forced consideration of the possibility that conformation distinguishes the two PrP isoforms (17).

1.2. The Prion Diseases and Neurodegeneration

Prion diseases may present as genetic, infectious, or sporadic disorders, all of which involve modification of the prion protein (PrP), a constituent of normal mammalian cells. CJD generally present as progressive dementia, whereas scrapie of sheep and bovine spongiform encephalopathy (BSE) are generally manifest as ataxic illness (1,4,15,20). Although the brains of patients appear grossly normal up on postmortem examination, they usually show spongiform degeneration and astrocytic gliosis under the microscope (1,4,62,63). The hallmark of all prion diseases whether sporadic, dominantly inherited, or acquired by infection is that they involve the aberrant metabolism and resulting accumulation of the prion protein (1,3,4,80).

A group of infectious pathogens called prions cause transmissible neurodegenerative diseases in both human and animals. In humans, these diseases are kuru, Creutzfeldt-Jakob Disease (CJD), and Gerstmann-Sträussler-Scheinker Syndrome (GSS), whereas animal prion diseases include scrapie, bovine spongiform encephalopathy (BSE), and transmissible mink encephalopathy (TME). Gerstmann-Sträussler-Scheinker Syndrome (GSS) and familial CJD are unique in that they are inherited and transmissible, these diseases occur in families as an autosomal dominant trait with high penetrance, and extracts of brain tissue from the affected individual can transmit a scrapie-like disease to experimental animals (2,7,14,18). The inherited prion diseases include GSS, familial Creutzfeldt-Jakob Disease (fCJD), and Fatal Familial Insomnia (FFI). These patients present with characteristic clinical and neuropathological findings as early as their third or fourth decade of life and their family histories are compatible with an autosomal dominant pattern of inheritance. Molecular genetic studies argue that these diseases are caused by mutations in the prion protein (PrP) gene based on high LOD scores for 5 of the 20 known mutations (5,7,10).

Prion diseases are rapidly progressing, invariably fatal, neurodegenerative diseases associated with dementia and neurological deficits such as ataxia, visual disturbances, or myoclonus. Histologically, nerve cell loss, spongiform change, and various forms of prion protein deposits are found in the brain. They are a heterogenous group of diseases that can be acquired, hereditary, or idiopathic. All prion diseases are experimentally transmissible with a relatively long incubation time and a comparatively short clinical duration. The first possible person-to-person transmission of CJD was reported in a recipient of a corneal transplant from a donor with CJD in 1974. Other modes of accidental iatrogenic transmission were reported in the following years, including the use of contaminated EEG depth electrodes, neurosurgical instruments, cadaveric pituitary-derived gonadotrophins and human growth hormone (HGH), and dura matter grafts (6,10).

An increasing number of animal prion diseases are being recognized, scrapie, a naturally occurring disease of sheep and goat, has been recognized in Europe for over 200 years. Transmissible mink encephalopathy (TME) and chronic wasting disease (CWD) of mule deer and elk were described in captive animals from the 1940s. The appearance in UK cattle in 1986 of BSE, which rapidly evolved into a major epidemic, was widely attributed to transmission of sheep scrapie to cattle via contaminated feed prepared from rendered carcasses (7). Classical (sporadic) CJD is a rapidly progressive, multifocal dementia, usually with myoclonus. Onset usually occurs in the 45-to-75-years age group, manifested as fatigue, insomnia, depression, headaches, ill-defined pain sensation, mental deterioration and myoclonus. Kuru reached epidemic proportions among a defined population living in the Eastern Highlands of Papua New Guinea, onset of disease ranged from 5 to over 60 years (158). The central clinical feature is progressive ataxia; dementia is often absent (158). vCJD has a clinical presentation in which behavioural and psychiatric disturbances predominate, marked sensory phenomena (7,56,58).

GSS is an autosomal dominant disorder that present classically as a chronic cerebellar ataxia with pyramidal features, with dementia occurring later. The histologically hallmark is the presence of multicentric PrP-amyloid plaques (135). Although first associated with the P102L PRNP mutation (57), GSS is now known as a pathological syndrome associated with several different PRNP mutations and forms a part of the phenotypic spectrum of inherited prion diseases (7,57).

Sheep scrapie is the prototype of the growing group of TSEs. The typical symptoms of scrapie-sick sheep include hyperexcitability, pruritus, and myoclonus. The disease is characterized by rapid progression leading to tetraparesis and ultimately to the death of the affected animal. The clinical symptoms of BSE are insidious, and consist of behavioural changes (including aggressive behaviour, which is proverbially atypical in cows), and uncoordinated gait. A striking hallmark applying to all TSEs is that the brain is heavily affected in sharp contrast to the body that remains unharmed. The communal lesions are neuronal loss, spongiosis, and astrogliosis, accompanied by an accumulation microglia, and occasionally, the presence of amyloid plaques and various kinds of small deposits immunolabeled with anti-PrP antibodies (11,64).

Clinical findings vary in the different forms of acquired CJD. In kuru and in diseases caused by inoculation of contaminated growth hormone extracts, cerebellar ataxia is the primary sign. Dementia is less prominent and usually occurs late in the disease course. The incubation time is long ranging from 2 years to greater than 30 years. Interestingly, in diseases following corneal or dural transplants, or use of contaminated neurosurgical instruments (89), dementia is more prominent and the latency is shorter (1-2 years) (12).

1.3. Conversion and Aggregation of Prion Protein

The conversion of the PrP^C into PrP^{Sc} involves a conformation change, whereby the α -helical content diminishes and the amount of β -sheet increases. Understanding how PrP^C unfolds and refolds into PrP^{Sc} will be of paramount importance in transferring advances in the prion diseases to studies of other degenerative illnesses. The mechanism by which PrP^{Sc} is formed must involve a templating process whereby existing PrP^{Sc} directs the refolding of PrP^C into a nascent PrP^{Sc} with the same conformation (1,4,7).

A variety of experimental evidence indicates that PrP^{Sc} is formed during a posttranslational event from PrP^C or a precursor. The posttranslational conversion might involve a chemical modification, a stable conformational change, or tight binding to other cellular components. The nature of the difference between PrP^C and PrP^{Sc} that allows PrP^{Sc} to become a prion component is in the conformation. The enhanced resistance of PrP^{Sc} to protease digestion is a cardinal feature that distinguishes it from PrP^C, whereas PrP^C is completely degraded up on incubation with protease K, PrP^{Sc} loses an NH₂-terminal domain containing the octarepeats to

yield PrP²⁷⁻³⁰. Furthermore, PrP^C is soluble in the presence of various detergents whereas PrP^{Sc} forms insoluble aggregates. PrP²⁷⁻³⁰ polymerizes into rod-shaped structures in the presence of detergent. The prion rods behave like amyloid; they show green birefringence under polarized light upon staining with congo red (2,4,20). PrP^{Sc} serves as a nucleus for the formation of amyloid by recruiting molecules of PrP^C, and may be compared to amyloid-enhancing factors (AEF), which can dramatically accelerate the formation of AA type amyloid in mouse models (2). Models of PrP^{Sc} suggest that formation of the disease-causing isoform involves refolding of the region corresponding roughly to residues 108-144 into β -sheets (3). PrP^{Sc} acts as a template for the conversion of PrP^C into nascent PrP^{Sc}. Imparting the size of the protease-resistant fragment of PrP^{Sc} through conformational templating provides a mechanism for both the generation and propagation of prion strains (3). PrP^C exists in equilibrium with the second state, PrP^{*}, that is best viewed as a transient intermediate that participates in PrP^{Sc} formation either through an encounter with PrP^{Sc} or with another PrP^{*} molecule. Under normal circumstances, PrP^C dominates the conformational equilibrium. With infectious diseases, PrP^{Sc} specified here minimally as a PrP^{Sc}/PrP^{Sc} dimer is supplied exogenously. It can bind PrP^{*} to create a heteromultimer that can be converted into a homomultimer of PrP^{Sc}. Genetic evidence points to the existence of an auxiliary factor (Protein X) in this conversion. Protein X preferentially binds PrP^C and is liberated up on conversion of PrP^{*} to PrP^{Sc} (5,96). However, this hypothesis has been disputed by many.

In prion diseases, the normal protein undergoes a number of posttranslational modifications to accumulate within the neuropil of the central nervous system. This accumulation is accompanied by a change in the protein structure from a predominantly α -helix to a β -sheet structure. The N-terminus of the protein is highly flexible and undergoes profound conformational change during the conversion to abnormal PrP (81). The exact mechanism of conversion is poorly understood and may occur by protein dimerization or nucleated seeding. Prusiner has suggested that another protein (Protein X) might be responsible for this conversion as molecular chaperone. The conversion of PrP into β -pleated sheet will require high energy levels (82). Conversion of normal PrP to abnormal PrP can be achieved *in vitro* using a cell-free assay system, but the reaction requires a considerable excess of the abnormal form of the protein and is relatively inefficient (10,25,26,27,28,29,30,31,83).

In order to explain the mechanism by which a misfolded form of PrP could induce the refolding of “native”, normal PrP molecules into the abnormal conformation, two distinct models have been postulated: i) the template assistance or “refolding” model and ii) the nucleation-polymerization or “seeding” model. In the first model, the conformational change is kinetically controlled; a high activation energy barrier prevents spontaneous conversion at detectable rates. Interaction with exogenously introduced PrP^{Sc} causes PrP^C to undergo an induced conformational change to yield PrP^{Sc}. This reaction may involve extensive unfolding and refolding of the protein to explain the postulated high energy barrier and could be dependent on an enzyme or chaperone, provisionally designated as Protein X (66). In the second model, PrP^C and PrP^{Sc} are in equilibrium that strongly favouring PrP^C-PrP^{Sc}, is only stabilized when it adds on to a crystal-like aggregate of PrP^{Sc} acting as a seed in nucleation-dependent polymerization process (67). Consistent with the latter model, cell-free conversion studies indicate that PrP^{Sc} aggregates are able to convert PrP^C into a protease-resistant PrP isoform (11,68,69,70,71).

In scrapie-infected cells, PrP^C molecules destined to become PrP^{Sc} exit to the cell surface before conversion into PrP^{Sc} (25,28,46). Like other glycosylphosphatidylinositol (GPI)-anchored proteins, PrP^C appears to re-enter the cell through a subcellular compartment bounded by cholesterol-rich, detergent-insoluble membranes, which might be caveolae or early endosomes (101). Within this cholesterol-rich, non-acidic compartment, GPI-anchored PrP^C can be either converted into PrP^{Sc} or partially degraded (101). PrP^{Sc} is trimmed at the amino terminus in an acidic compartment in scrapie-infected cultured cells, to form PrP27-30. By contrast, amino-terminal trimming of PrP^{Sc} is minimal in brain, where little PrP27-30 is found (17,47,27,46).

1.4. Neuropathology of the Prion Protein

In addition to incubation times, neuropathologic profiles of spongiform changes have been used to characterize prion strains. However, recent studies with PrP transgenes argue that such profiles are not an intrinsic feature of strains. The mechanism by which prion strains modify the pattern of spongiform degeneration was perplexing since earlier investigations had shown that PrP^{Sc} deposition precedes neuronal vacuolation and reactive gliosis (3,4).

Neuropathology of the FFI discloses selective atrophy of the thalamus, the mediodorsal and anterior ventral group being especially affected. The inferior olive is also affected and isolated foci of spongiosis are found in the cortex. The affected areas show neuronal loss and astrocytic proliferation, but deposits of immunoreactive PrP are not always found as in other prionic diseases. When described, immunoreactive PrP appears in discrete zones and in small amounts (20,100).

1.5. Biochemical Analysis of the Prion Protein

The two types of PrP^{Sc} are distinguished by their different physicochemical properties, particularly their appearance on western transfer after digestion with proteinase K. The unglycosylated forms of PrP^{Sc} are seen as proteins of approximately 21 (type 1) and 19 kDa (type 2) relative molecular mass. Proteinase K has two preferential, if not exclusive, cleavage sites at codon 97 and 82 of PrP^{Sc}, most likely related to two different conformations of PrP^{Sc} (6).

Variant CJD is associated with PrP^{Sc} glycoform ratios that are distinct from those seen in classical CJD. Similar ratios are seen in BSE in cattle and BSE when transmitted to several other species (52). However, although such biochemical modifications of PrP are clearly candidates for the molecular substrate of prion strain diversity, it is necessary to be able to demonstrate that these properties fulfill the biological properties of strains, in particular that they are transmissible to the PrP in a host of both the same and different species. As PrP glycosylation occurs before conversion to PrP^{Sc}, the different glycoform ratios may represent selection of particular PrP glycoforms by PrP^{Sc} of different conformations. According to such a hypothesis, PrP conformation would be the primary determinant of strain type, with glycosylation being involved as a secondary process. However, because it is known that different cell types may glycosylate proteins differently, PrP^{Sc} glycosylation patterns provide a substrate for the neuropathological targeting that distinguishes different prion strains (7,24).

All cases of variant CJD are associated with type 2B PrP^{Sc}. Type 2B PrP^{Sc} has a high proportion of the diglycosylated form of PrP^{Sc} and is distinct from the PrP^{Sc} types seen in classical CJD (Types 1-2A), with differing fragment sizes following proteinase K digestion. Also types 1-2A are associated with a high proportion of monoglycosylated PrP^{Sc}. The glycoform ratios of proteinase K-digested PrP^{Sc} in vCJD were closely similar, however, to those seen in BSE passaged in a number of

mammalian species. Furthermore, when prions isolated from either bovine brain or human brain are transmitted to experimental mice, PrP^{Sc} isolated from the infected hosts is indistinguishable, either by the site of proteinase K or by glycoform ratio. In addition, vCJD and BSE show closely similar transmission properties in both transgenic and conventional mice, with indistinguishable neuropathology in both transgenic and a variety of inbred strains of mice (24).

The cellular prion protein PrP^C contains two N-linked complex-type oligosaccharides at positions 181 and 197. Accordingly, western blot analysis of PrP reveals three major bands, reflecting PrP that has two, one, or no glycosylation signals occupied. Glycosylation is important as a signal for correct intracellular trafficking of PrP^C and possibly also for selective targeting of PrP^{Sc} to specific brain regions (11,72).

1.6. Mutations and Polymorphisms of the PrP-Gene

More than 30 mutations of the PrP gene are now known to cause the inherited human prion diseases, and significant genetic linkage has been established for five of these mutations. The prion concept readily explains how a disease can be manifest as a heritable as well as infectious illness (1,4). The discovery that mutations of PRNP cause dominantly inherited prion diseases in humans linked the genetic and infectious forms of prion diseases (3,78). In fCJD, GSS, and FFI, mutations in PRNP located on the short arm of chromosome 20 are the cause of disease. Considerable evidence argues that the prion diseases are disorders of protein conformation (4,42,162).

A large number of different point mutations and insertion mutations of the prion protein gene have been identified in familial prion diseases. Insertion mutations represent additional repeats of the N-terminal Cu²⁺-binding octapeptide (50). Familial CJD is most often associated with the E200K mutation and less often with D178N-129 V, V180I, R208H, V210I, M232R, and insertion mutations, while GSS is found most often in families with the P102L mutation and less often with P105L, A117V, F198S, D202N, Q212P, Q217R and insertion mutations, FFI is caused by a D178N mutation of PRNP associated with methionine codon at position 129 of the same allele (6,42,161,162). Over 30 pathogenic mutations have been described in two groups: a) point mutations resulting in amino acid substitutions in PrP, or in one case production of a stop codon resulting in expression of a truncated PrP and b) insertions encoding additional integral copies of an octapeptide repeat present in a

tandem array of live copies in the normal protein (7). The identification of one of the pathogenic PRNP mutations in case with neurodegenerative disease allows diagnosis of an inherited prion disease and subclassification according to mutation (7,136).

Known or suspected genetic factors of phenotypic variability of inherited prion disease include the polymorphic codon 129 genotype of the mutant and wild-type alleles, the haplotype background of the mutation and unlinked genetic susceptibility loci. At the protein level, mutated PrP appears to be able to fold into a number of different pathogenic conforms (159). This diversity may be partly constrained by PrP primary structure, known as the conformation selection hypothesis (160). Diversity of PrP conformation within a single pedigree may account for phenotypic variability if different pathological conforms have differing toxicity or neuropathological targeting (13,97,159).

In humans with PrP point mutation, mutant PrP^C molecules might spontaneously convert into mutant PrP^{Sc}. While the initial stochastic event may be inefficient, once it happens, the process becomes autocatalytic. Whether all GSS and familial CJD patients contain infectious prions is unknown. If the former is found, mutant PrP^{Sc} molecules combine with the heterodimer (mutant PrP^{Sc}/wild PrP^C) and are subsequently transformed into heterodimer mutant PrP^{Sc}/wild PrP^{Sc}. This wild-type PrP^{Sc} produces the heterodimer (wild-type PrP^{Sc}/wild-type PrP^C) in an exponential process. If the latter is found, presumably, mutant PrP^{Sc} molecules alone can lead to the central nervous system dysfunction (14). In 1989 codon 102 and codon 117 point mutations of human PrP were reported to be linked to GSS (57). The results in codon 102 transgenic mice also strengthen the idea that this mutation is one of the essential events that cause GSS (59). Several polymorphisms and mutations were also reported in familial CJD and familial dementia (14,17,60,61,161,162).

1.7. Effect of the Codon 129 Polymorphism on Human Susceptibility

The common polymorphism at amino acid position 129 of the prion protein, where humans carry a methionine (M) or valine (V), clearly influences susceptibility to the sporadic and iatrogenic types of prion diseases and furthermore, determines in part the phenotype of the sporadic as well as of some inherited prion diseases. Several studies have revealed a marked over-representation of homozygotes (mainly for methionine) at this position in cases of sporadic CJD compared to the normal

population. CJD homozygotes at codon 129 also show a higher susceptibility to iatrogenic CJD and a shorter incubation times as well. There is also a strong correlation of codon 129 genotype and clinicopathological phenotype (6,7, 12,86,88,99,104,105).

Variant CJD demonstrate this effect most dramatically: all genetically tested cases have been homozygous for 129 M (56). A single codon 129 heterozygous patient, who had received blood from a donor subsequently diagnosed with vCJD, was found to have widespread prion protein deposition in the peripheral lymphoreticular system at autopsy, having died of an unrelated cause (13,98).

At codon 129 of PRNP, an individual may encode for methionine (M) or valine (V) and therefore, all humans are MM or VV homozygotes or MV heterozygotes. In the normal UK population, the distributions are approximately: MM 40%, VV10%, MV 50% (15). Two basic facts illustrate the potential importance of this polymorphism: approximately 80% of UK sporadic CJD cases and, to date, all cases of variant CJD are MM. Most notably, the D178N mutation gives rise to the clinical picture of genetic CJD when associated with 129 V on the mutant allele and yet results in FFI when associated with 129 M. In cases related to infection in or adjacent to the brain, for example, dura matter grafts-codon 129 MM is a risk factor, but with peripheral infection for example, pituitary hormone treatment (which was administered by infection). It is however, possible that cases within alternative codon 129 genotype may occur in the future as variations at this locus can influence incubation period. There is also the possibility that the clinical and pathological features in such cases might differ from variant CJD with an MM background (15).

The FFI disease is associated with a point mutation in the 178 codon of the prion protein (PrP) gene (PRNP) with a substitution of asparagine for aspartic acid (PrP 178 Asn) associated with methionine (Met) in the naturally polymorphic codon 129 of the mutated PRNP (163,164). Additionally the polymorphic codon 129 in the non-mutated allele conditions the severity type: 129 Met. In cases of fatal familial insomnia (FFI) methionine on the non-mutated allele is associated with short term disease and more thalamic damage with fewer cortical alterations, whereas heterozygosity Met/Val in the codon 129 is associated with a more prolonged disease and widespread neuropathological damage with cortical spongiosis (16).

1.8. Species Barriers and Strain Diversity of Prions

In contrast to pathogens with a nucleic acid genome that encode strain-specific properties in genes, prions presumably encipher these properties in the tertiary structures of PrP^{Sc}. Studies on transgenic animals argue that PrP^{Sc} acts as a template upon which PrP^C is refolded into a nascent PrP^{Sc} molecule through a process facilitated by another protein (1,94).

The passage of prions between species is almost always characterized by prolonged incubation times during the first passage in the new host. This prolongation is often referred to as the “species barrier”. Prions synthesized *de novo* reflect the sequence of the host PrP gene and not of the PrP^{Sc} molecules in the inoculum derived from the donor. On subsequent passage in a homologous host, the incubation times shorten to that recorded for all subsequent passages. From studies with transgenic mice, three factors have been identified that contribute to the species barrier: i) the difference in PrP sequences between the prion donor and recipient, ii) the strain of prion and iii) the species specificity of protein X, a factor defined by molecular genetic studies that bind to PrP^C and facilitates PrP^{Sc} formation. No further evidence has been found now of this hypothesis. The prion donor is the last mammal in which the prion was passaged and its PrP sequence represents the species of the prion. The strain of prion seems to be enciphered in the conformation of PrP^{Sc} (1,20,43,44,73).

The existence of prion strains raises the question of how heritable biological information can be enciphered in a molecule other than nucleic acid. Strains or varieties of prions have been defined by incubation times and the distribution of neuronal vacuolation. Subsequently, the patterns of PrP^{Sc} deposition were found to correlate with vacuolation profiles, and these patterns were also used to characterize strains of prions (1,3,20,35,38,39,40,74).

Studies of the drowsy (DY) and hyper (HY) prion strains isolated from mink by passage in Syrian Hamster showed that two strains produced PrP^{Sc} molecules with protease-resistant cores (PrP₂₇₋₃₀) of different molecular sizes as judged by gel electrophoresis (5,17,19,75,41). Following limited proteolysis, strain-specific migration patterns of PrP^{Sc} on polyacrylamide gels were seen that related to different N-terminal ends of HY and DY PrP^{Sc} following protease treatment and implying different conformations of HY and DY PrP^{Sc} (7,73). Multiple distinct strains of naturally occurring sheep scrapie were isolated in mice. Such strains are distinguished by their biological properties: They produce distinct incubation periods

and patterns of neuropathological targeting (so-called lesion profiles) (7,32,33,35,40,41).

Transmission of prion diseases between different mammalian species is restricted by a “species barrier”. On primary passage of prions from species A to species B, usually not all inoculated animals of species B develop disease. Those that do have much longer and more variable incubation periods than those that are seen with transmission of prions within the same species, where typically all inoculated animals would succumb within a relatively short and markedly consistent incubation period. On second passage of infectivity to further animals of species B, transmission parameters resemble within-species transmissions, with most, if not all, animals developing the disease with short and consistent incubation periods. Species barriers can therefore, be quantitated by measuring the fall in mean incubation period on primary and secondary passage or perhaps more rigorously, by a comparative titration study (7,11).

In the case of prion transmission from hamster to mice, this so-called species barrier was overcome by introducing hamster *PRNP* transgenes into recipient wild-type mice (45). Crucially, the properties of the prions produced were compatible with the prion species used for inoculation. Infection with hamster prions led to production of hamster prions, whereas infection with mouse prions gave rise to mouse prions. With respect to the protein-only hypothesis these findings can be interpreted as follows: hamster PrP^C but not murine PrP^C (the latter differing from the former by 10 amino acids) is an appropriate substrate for conversion to hamster PrP^C by hamster prions and vice versa (11,33,34,45,75).

Distinct isolates or strains of prions were first described in scrapie-diseased goats, where two dissimilar clinical manifestations (“scratching” and “drowsy”) were identified. These strains differ in their incubation times in various inbred mouse lines and by their lesion pattern in the brain. Strikingly, distinct strains of prions can be propagated in an inbred mouse strain that is homozygous with respect to *PRNP* (163). A perplexing finding with regard to the protein-only hypothesis meaning that an identical polypeptide chain is able to mediate different strain phenotypes. Both the “refolding” and the “seeding” model propose that each strain is associated with a distinct conformation of PrP^{Sc} and that each of these can convert PrP^C of its host into a likeness of itself. In deed, PrP^{Sc} species associated with two hamster-adapted scrapie strains, namely hyper (HY) and drowsy (DY), proved to display characteristic

clinical and histopathological properties as well as distinct biochemical patterns with respect to proteinase K digestion (73) readily explainable by the presence of different conformations of PrP^{Sc} (11,73).

In general, TSE diseases show a preference for transmission to the species of origin or a closely related species. Most noteworthy was the original demonstration of the transmissibility of CJD and kuru from human to chimpanzees (84,85). Transmission to a less closely related species is also possible and appears to involve a progressive adaptation during serial passage in the new host. For example, scrapie from sheep or goats and BSE from cattle have produced typical TSE disease in mice and mouse- and hamster-adapted agents from these and other sources have been used extensively for pathogenesis studies and characterization of the agent (12,35,36).

It is hypothesized that a range of abnormal PrP conformations and glycosylation states provide the basis for multiple prion “strains” with consistent clinicopathological correlates (13,37,38,39,40,49).

To test the hypothesis that differences in Prnp sequences might be responsible for the species barrier, transgenic mice synthesizing SHaPrP were constructed (75). The PrP genes of Syrian hamsters and mice encode proteins differing at 16 positions. Inoculation of Tg (SHaPrP) mice with SHa prions demonstrated abrogation of the species barrier, which resulted in abbreviated incubation times owing to a non-stochastic process. The length of the incubation time after inoculation with SHa prions was inversely proportional to the level of SHaPrPC in the brains of the Tg(SHaPrP) mice (17,75). Bioassays of brain extracts from clinically ill Tg(SHaPrP) mice inoculated with mouse prions revealed that only mouse prions, but no SHa prions, were produced. Conversely, inoculation of Tg(SHaPrP) mice with SHa prions led to only the synthesis of SHa prions (17).

1.9. Potential Abilities of Classical and Atypical Human TSE Strains to Propagate in Transgenic Mice

The species barrier between cattle BSE and human can not be directly measured, but it can be modeled in transgenic mice expressing human PrP^C, which produce human PrP^{Sc} when challenged with human prions (51). When such mice, expressing both human PrP valine 129 (at high levels) and mouse PrP, are challenged with BSE, three possibilities could be envisaged: these mice could produce human prions, murine prions or both. In fact only mouse prion replication could be detected.

Although there are caveats with respect to this model, particularly that human prion propagation in mouse cells may be less efficient than that of mouse prions; this result would be consistent with the bovine-to-human barrier being higher than the bovine-to-mouse barrier for this PRNP genotype. In the second phase of these experiments, mice expressing only human PrP were challenged with BSE. Although CJD isolates transmit efficiently to such mice at approximately 200 days, only infrequent transmissions over 500 days were seen with BSE, consistent with a substantial species barrier for this human PRNP genotype (7,55).

Susceptibility of mice to prions from other species is increased when the corresponding PrP transgene is introduced into a PrP knockout mouse, suggesting that the resident murine gene inhibits the propagation of the alien prions (11,65). In similar studies, transgenic mice expressing human PrP have been shown to have increased susceptibility to human TSE disease isolates (93,94). These results have broadened the possibilities for studying human isolates in less expensive and more rapid rodent models suitable for screening of possible therapeutic drugs. However, in spite of knowledge of PrP^{sen} (proteinase k-sensitive form of PrP) sequences and structures from a variety of species, the extent of species-specific resistance to TSE diseases remains impossible to predict solely by analysis of PrP sequences and structures (93,150). This is of critical importance in the matter of human susceptibility to BSE (12).

Transgenic mice overexpressing either the Leu102 PrP GSS mutant (59) or the extra amino acid octarepeat PrP mutant (95) develop a fatal neurological disease with neuropathology similar to TSE disease. However, in neither model is there generation of PrP^{res} (proteinase k-resistant form of PrP) with the high degree of protease-resistance found in the human counterparts of these models. GSS disease associated with Leu 102 PrP is in fact transmissible to monkeys and mice expressing only Pro102 PrP. These the questionable transmissibility and the lack of PrP^{res} suggests that this transgenic model may in fact be a diseased one due to overexpression of a mutant protein rather than a true TSE disease. These results suggest that mutant Leu102 PrP may alter susceptibility for TSE diseases rather than acting as a direct cause of GSS (12).

Human and mouse genetics have made major contributions to prion disease research. Perhaps most prominent among these was the linkage to chromosome 20 and mutation discovery in PRNP in families with dominantly inherited

neurodegenerative diseases (57). The fact that heterogenous diseases caused by mutations of PRNP were known to be transmissible to laboratory animals obviated the need to the search for a cryptic infectious organism (13).

Because initial transgenic studies had shown that the “species barrier” between mice and SHa for the transmission of prions can be abrogated by expression of SHaPrP transgene in mice, Tg mice synthesizing HuPrP were constructed. These Tg (HuPrP) FVB mice inoculated with the Hu prions failed to develop CNS dysfunction more frequently than non-Tg controls (91). Faced with apparent dichotomy, mice were constructed which expressing a chimeric Hu/Mo PrP transgene designated MHu2M (102). Hu PrP differs from mouse PrP at 28 of 254 positions while MHu2M differs at nine residues. It was found that mice expressing the MHu2M transgene are susceptible to human prions and exhibit abbreviated incubation times (91). When Tg(HuPrP) mice were crossed with PrP⁰ mice, they were rendered susceptible to the Hu prions. These findings suggested that Tg(HuPrP) FVB mice were resistant to Hu prions, because Mo PrP^C inhibited the conversion of Hu PrP^C into PrP^{Sc}; once Mo PrP^C was removed by gene ablation, then the inhibition was abolished (66). While earlier studies argued that PrP^C forms a complex with PrP^{Sc} during the formation of nascent PrP^{Sc} (75), these findings suggested that PrP^C also binds to another macromolecular (protein X) during the conversion process. As with the binding of PrP^C to PrP^{Sc}, which is most efficient when the two isoforms have the same sequence (75), the binding of PrP^C to protein X seems to exhibit the highest affinity when these two proteins are from the same species (17,20).

1.10. Alteration of Atypical TSE biological Properties after Transmission to Humanized Mice

Recently, several human PrP^{Sc} types have been identified that are associated with different phenotypes of CJD (151). This has been demonstrated in studies with CJD isolates, with both PrP^{Sc} fragment-sizes and the ratios of the three PrP glycoforms (diglycosylated, monoglycosylated and unglycosylated PrP) maintained on passage in transgenic mice expressing human PrP (52). Furthermore, transmission of human prions and bovine prions to wild-type mice results in murine PrP^{Sc} with fragment sizes and glycoform ratios that correspond to the original inoculum (7,52,53).

1.11. Potential Similarities and Links between Atypical TSE Cases and other Known Prion Protein

The appearance of a novel human prion disease, variant CJD, and the clear experimental evidence that it is caused by exposure to BSE has highlighted the need to understand the molecular basis of prion propagation, pathogenesis and the barriers limiting the intermammalian transmission (7). The inherited prion diseases can be diagnosed by PRNP analysis, and the use of these definitive genetic diagnostic markers has allowed the recognition of a wider phenotypic spectrum of human prion diseases to include atypical dementias and fatal familial insomnia (7,54).

The unusually young age range of vCJD patients and their distinctive pathology suggested that they represented a new clinical TSE disease and the initial occurrence of these patients in the UK suggested an association with BSE in cattle. Subsequent laboratory experiments indicated a strong similarity between BSE and vCJD based on patterns of infectable mouse strains; lesion distribution in mouse brain; PrP gel banding patterns and neuropathology after transmission to cynomolgous macaques (49,90). Based on these data, most observers agree that vCJD represents spread of BSE from cattle to humans (12).

Macaque monkeys and marmosets both developed neurologic disease several years after inoculation with bovine prions, but only the macaques exhibit numerous PrP plaques similar to those found in vCJD (20,89).

1.12. Aim of the Work

In this work we studied the pathogenesis and evaluate the strain characteristics of prion diseases by using transgenic mice. This work consists of two main parts:

In the first part, we studied the pathogenesis of prion diseases by using EGFP-PrP transgenic mice expressing EGFP-PrP protein (fluorescent protein). EGFP-PrP transgenic mice represent a unique system for examining the pathogenesis and progression of prion diseases *in vivo* and *in vitro*. It may be possible to visualize PrP^{Sc} deposition in the brains or other organs of these animals before and after infection with prion strains. Also, EGFP-PrP could help us to follow up the localization, colocalization, distribution and trafficking of PrP^{Sc} intra- and extracellularly to know the sites of formation, conversion and accumulation of PrP^{Sc}

inside the neurons. Moreover, EGFP-PrP is considered as a protein-marker and affinity reagent for the isolation of proteins involved in prion replication. Establishment of EGFP-PrP transgenic mice considered a useful model for studying several other aspects of prion biology.

In the second part, we studied the transmission characteristics and biological properties of different human prion strains, also an assessment of the effect of codon-129 polymorphism of the PRNP on the human susceptibility. We used humanized mice expressing human PrP by direct replacement of the mouse PrP gene. Two inbred lines with an identical genetic background were produced to express human PrP with the codon-129 MM and VV genotypes. Mice were inoculated intracerebrally with brain homogenates from cases of human prion diseases such as sporadic CJD (MM1 and MM2) and vCJD strains and assessed for incubation times, biochemical features as well as clinical and pathological signs of the disease.

2. Material and Methods

2.1. Materials

All the chemical reagents, biological reagents, buffers, utensils (plastic & glass wares) are of high-quality analytical grade and were purchased from specialized and trusted sources.

Table 1: Chemicals

Chemicals	Company
-Acetic acid 100%	-Sigma Aldrich (Steinheim, Germany)
-Acrylamide-bis 30%	-Merck (Darmstadt, Germany)
-Agarose gel	-Karl Roth, Karlsruhe, Germany
-APS (Ammonium persulfate 10%)	-Sigma Aldrich (Steinheim, Germany)
-Bromophenol Blue	-Merck (Darmstadt, Germany)
-CDP-Star (Chemiluminescence system)	-Tropix (Bedford, USA)
-EDTA (Ethelendiamine tetraacetic acid)	-Roth (Karlsruhe, Germany)
-Eosin	-Merck (Darmstadt, Germany)
-Glycerine	-Merck (Darmstadt, Germany)
-Glycine	-Sigma Aldrich (Steinheim, Germany)
-HCl	-Roth (Karlsruhe, Germany)
-Haematoxyline	-Merck (Darmstadt, Germany)
-I-Block	-Tropix (Bedford, USA)
-K ₂ HPO ₄	-Merck (Darmstadt, Germany)
-KH ₂ PO ₄	-Merck (Darmstadt, Germany)
-Methanol 100%	-Merck (Darmstadt, Germany)
-MgCl ₂	-Merck (Darmstadt, Germany)
-Milk Powder (Blotting Grade)	-Roth (Karlsruhe, Germany)
-NaCl	-Roth (Karlsruhe, Germany)

-Na ₂ HPO ₄	-Merck (Darmstadt, Germany)
-NaH ₂ PO ₄	-Merck (Darmstadt, Germany)
-NaOH	-Merck (Darmstadt, Germany)
-NBT (4-Nitroblue tetrazolium chloride)	-Roche diagnostic (Mannheim, Germany)
-Nonidet P40	-Roth (Karlsruhe, Germany)
-PMSF (Phenylmethylsulphonylfluoride)	-Sigma Aldrich (Steinheim, Germany)
-PFA (Paraformaldehyde 4%)	-Merck (Darmstadt, Germany)
-Sarkosyl (N-Lauryl-Sarkosin sodium salt)	-Merck (Darmstadt, Germany)
-SDS (Sodiumdodecylsulfate)	-Roth (Karlsruhe, Germany)
-TEMED (N,N,N,N-Tetramethylethylenediamine)	-Sigma Aldrich (Steinheim, Germany)
-Tris-base	-Sigma Aldrich (Steinheim, Germany)
-Tris-HCl	-Sigma Aldrich (Steinheim, Germany)
-Tween-20	-Roth (Karlsruhe, Germany)
-β-Mercaptoethanol	-Sigma Aldrich (Steinheim, Germany)
-SOC (Sodium deoxycholate)	-Sigma Aldrich (Steinheim, Germany)
-Developer & Fixer	-Sigma Aldrich (Steinheim, Germany)

Table 2: Biologicals

Biologicals	Company
-Monoclonal Mouse Anti-Prion Protein Ab, clone 3F4	-DakoCytomation, Glostrup, Denmark
-Monoclonal Mouse Anti-Prion Protein Ab, clone 4H11	-Center for Neuropathology, Munich
-Monoclonal Anti-Prion Protein Ab, clone L42	-Biopharm, Darmstadt, Germany

-Anti-prion protein Ab, CDC1	-Novus Biologicals
-Monoclonal Anti-Prion Protein Ab, anti – GFP	-MoBiTec, Göttingen, Germany
-ECL Anti-mouse IgG, horseradish peroxidase linked whole antibody (from sheep)	-GE Healthcare, UK
-Prestained Protein Marker (PeqGold)	-PeqLab,Biotechnology, Erlangen, Germany

Table 3: Buffers for Sample Preparation

Buffer	Composition
-PBS Buffer 10X: (1Litre)	-Na ₂ HPO ₄ 12.7 g NaH ₂ PO ₄ 3.9 g NaCl 85 g
-PBS Buffer 1X :(1Litre)	-100 ml 10X PBS + 900 ml d.water, adjust PH 7.3
-PBS-Tween 20:(1litre)	-1Litre 1XPBS 1ml Tween 20
-Lysis Buffer: (200ml)	-100 mM Tris 2.42 g 100 mM NaCl 1.17 g 10 mM EDTA 0.76 g 0.5% Nonidet P40 1 ml 0.5% Sodium deoxycholate (SOC) 1 g PH 6.9 at 37°C
-Proteinase K: (Roche diagnostic,Indianapolis,USA)	-33 mg/ml d.water (2 µl PK/20 µl Homogenate)

Table 4: Buffers for SDS-PAGE and Western Blot analysis

Buffer	Composition
-Lämmli Sample Buffer 2X:(10ml) (Also, 4X LSB with double amounts)	-125 mM Tris 0.15 g 4 mM EDTA 0.015 g 20% Glycerine 2 ml 8% β-Mercaptoethanol 800 μl 6% SDS 0.6 g PH 6.8
- I-Block:	-2 g I-Block 1litre 1X PBS-Tween 20, mix with heating at 60°C for 0.5-1 hour
-PBS & PBS-Tween 20	-As previous
-Separating gel: 13% Acrylamide	-13% Acrylamide + 0.375 MTris.HCl PH 8.8 + 0.1% SDS + 0.05% APS + 0.035% TEMED
-Stacking gel: 5% Acrylamide	-5% Acrylamide + 0.125 MTris.HCl, PH 6.8 + 0.1% SDS,+ 0.05% APS + 0.035% TEMED
-Running Buffer: (10X) (Tris-glcine SDS-PAGE)	-Tris base 30,3 g Glycine 144 g SDS 10 g ddH ₂ O to 1 litre Total volume 1 litre
-Blotting Buffer:	-100ml 1XRunning buffer (Tris-glycine) 900ml ddH ₂ O 20% 100%Methanol
-SDS: 10%	-50 g SDS +400ml ddH ₂ O, heat to

-Methanol: 70%	68°C, adjust PH to 7.2, adjust volume to 500ml with ddH ₂ O
-Water:	-70ml 100%Methanol + 30ml ddH ₂ O
-ECL Western blotting detection reagents (reagent 1 & 2)	-Sterile, bidistilled Millipore water
	-GE Healthcare, UK

Table 5: Buffers for FACS analysis

Buffer	Composition
- Flow Cytometry Staining Buffer	-1x PBS, ≤ 5% FBS, 0.1% sodium azide, 4°C (eBioscience, Cat. No. 00-4222)
- RBC Lysis Buffer	-155mM NH ₄ Cl, 10mM KHCO ₃ , 100mM EDTA, 37°C (eBioscience, Cat. No.00-4333)

Table 6: DNA Isolation Kits and PCR-Reagents

Reagent	Description
-DNA Extraction Kits	-DNeasy Blood & Tissue Kit, QIAGEN
-Taq-Polymerase (Hot-Star Taq-Mastermix)	-Eppendorf, Hamburg, Germany
-Primers: HuM_for: 5`-CTA CCC ACC TCA GGG CGG TGG TGG-3` HuM_rev: 5`-TGG TGG CTG TAC TCA TCC ATG-3` LL_for: 5`-ATG GCG AAC CTT GGC TAC TGG CTG-3`	-MVG Oligo Synthese, Ebersberg

<p>LL_rev: 5`-TCA TCC CAC GAT CAG GAA GAT GAG-3`</p> <p>-Restriction Enzymes: Nspl & Ddel</p> <p>-10X NEBuffer 2</p> <p>-10X NEBuffer 3</p> <p>-BSA (Bovine Serum Albumin)</p> <p>-SYBR Gold Nucleic Acid Gel Stain (0.7µl /50ml agarose gel)</p> <p>-DNA-Ladder (PageRuler Prestained Protein Ladder) (50 & 100 bp)</p> <p>-6X DNA Loading Dye</p> <p>-Running buffer: (TAE-buffer) 500ml TAE (50X)</p>	<p>-New England BioLabs, Frankfurt</p> <p>- New England BioLabs, Frankfurt</p> <p>- New England BioLabs, Frankfurt,</p> <p>- New England BioLabs, Frankfurt,</p> <p>-Invitrogen, Molecular Probes</p> <p>- New England BioLabs, Frankfurt, Germany</p> <p>-Fermentas</p> <p>-121 g Tris-base 28.5 ml Acetic acid 100% 9.31 g Na-EDTA 500 ml dd.water</p>
--	--

Table 7: Consumables

Consumables	Company
-Microcentrifuge Tubes 0.2,1.5, 2 ml	-Eppendorf, Hamburg, Germany
-Plastic Tubes 15,50 ml	-Sarstedt, Nümbrecht, Germany
-Gel Blotting Paper GB005	-VWR,Whatman,Schleicher&Schuel, Dassel, Germany
-Serological pipet 5,10,25 ml	-VWR, Dassel, Germany
-Micropipet Tips	-ART, Molecular Bioproduct

-Hyperfilm ECL (X-ray film)	-Amersham Pharmacia, Piscataway, USA
-Nitrocellulose membrane PVDF pore size:0.45 µm	-Millipore, Eschborn, Germany
-Transparent Sheet	-Soennecken, Prospekthüllen, Overath, Germany
-Needles	-TerumoEurope, Leuven, Belgium
-Fluorescent Mounting Medium	-Biomeda, Foster City, CA

Table 8: Equipments

Equipment	Company
-Confocal Laser Scanning Microscope	-Leica DM LFSA, TCS sp2 TMC
-Vibratome Microtome	-Vibratome company, St. Louis, MO
-Microcentrifuge 5415R	-Eppendorf, Hamburg, Germany
-Thermocycler, Mastercycler personal	-Eppendorf, Hamburg, Germany
-Vortex	-Vortex Gene
-Shaker	-Rocky
-Thermomixer Comfort	-Eppendorf, Hamburg, Germany
-Heater	-HLC
-Balance	-Sartorius Max.400 g, 0.000 g Sensitivity
-Electrophoresis Power Supply	-Consort, 3000V—300mA E833
-Hamilton Syringe	-Hamilton, Bonaduz, Germany
-Gel-pouring apparatus	-BioRad, München, Germany
-Gel electrophoresis apparatus	-VWR, Ismaning, Germany
-Semiphor Transphor Blot-machine (Semi-dry transfer)	-Amersham Bioscience, Freiburg, Germany
-Gel combs, spacer,...etc	-PeqLab, Erlangen, Germany
-Microwave	-Moulinex, Samou, Radolfzell
-Developing machine	-Optimax TypTR, MS laborgerät, Wieslack
-Micropipette 10,20,200,1000 µl	-Eppendorf, Hamburg, Germany
-Flow cytometer	-BD Bioscience

2.2. Methods

3.1.1. Construction of EGFP-PrP Transgene

Fischer et al. (1996) developed a PrP-encoding vector based on the murine PrP gene from which the large intron had been deleted and that contained 6 kb of 5' and 2.2 kb of 3' flanking sequence, named as „half-genomic construct“ or pPrPHG (Figure 1)(21). This vector, which contains the wild-type PrP sequence, restored susceptibility to scrapie in a dose-dependent manner when introduced into PrP⁰ mice. The transgenic construct was created to express EGFP-PrP under PrP regulatory elements (phgEGFP-PrP). The EGFP-PrP coding sequence was cloned into the murine half-genomic PrP locus (Figure 2). The appropriate constructs were injected into the pronuclei of PrP⁰ zygotes and transgene-carrying animals were identified and bred to PrP⁰ mice (These mice were a gift from Dr. Marko Maringer).



Figure 1: The phgGFP-PrP Fusion Protein Transgene Construct

New phgEGFP-PrP transgene construct showing inclusion of EGFP-transgene in the open reading frame (ORF) and deletion of the large intron with fusion of exon 2 and exon 3

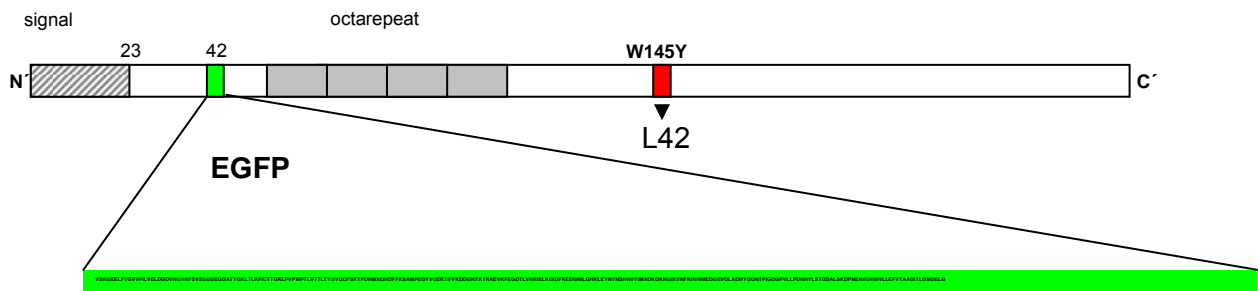


Figure 2: EGFP-PrP L42 transgene construct

The EGFP-PrP transgene showing the site of insertion of the transgene in the prion protein gene and also showing the site of insertion of the human prion protein epitope L42 which recognizes the EGFP-PrP and not recognize mice PrP.



Pronucleus-injection



Figure 3: Pronucleus injection of EGFP-PrP in nuclei of Oocytes

2.2.2. Generation of Transgenic Mice

EGFP-PrP transgenic mice: Five independent lines of transgenic mice expressing a chimeric EGFP-PrP fusion protein under regulatory elements of the half-genomic mouse PrP locus were produced by using pronuclear micro-injection of fertilized

mouse oocytes (Figure 3). By using these mice we were able to visualize the localization EGFP-PrP in brains and in various organs in histological sections (76).

Humanized transgenic mice: Mice were produced to express human prion protein (PrP) by direct replacement of the mouse PrP gene. Since the human PrP gene has variation at codon 129, with MM, VV and MV genotypes, two inbred lines with an identical genetic background were produced to express human PrP with the codon-129 MM and VV genotypes. Mice were inoculated with sCJD and vCJD and assessed for incubation times, biochemical analysis, clinical and pathological signs of the disease (23) (These mice were a gift from Prof. Jean Manson, University of Edinburg, UK).

LL-mutant mice: Transgenic mice were generated with point mutation, which expressing mouse prion protein with proline 101 to leucine (P101L) exchange. With this mutation, these mice being susceptible to human Gestmann-Sträussler-Scheinker Syndrome (GSS). We infect these mice with GSS strain of human case to study the transmission efficiency of the disease (144).

2.2.3. Infection of Transgenic Mice

EGFP-PrP transgenic mice: These mice were infected with scrapie strain RML intracerebrally under anaesthesia (isofluran). Inocula were prepared from brains of terminally ill mice. Twenty-five percent (25%) (w/v) brain homogenates were prepared in sterile PBS using a motorized tissue grinder. Homogenates were clarified by centrifugation for 5 minutes at 900xg. Brain homogenates were diluted to 1% using sterile PBS and 25 µl were injected intracerebrally into the right parietal lobe of 4-6 weeks old recipient mice using a 25 gauge needle (77).

Humanized transgenic mice: These mice were divided into six groups of HuM and another six groups of HuV, each group included eight animals. These groups were infected with different cases of sCJD and vCJD obtained from human cases that had died with prion diseases. The mice were infected intracerebrally according to the previous method (Table 9).

HuM-mice		HuV-mice	
Group 1	sCJD (129 MM1)	Group 1	sCJD (129 MM1)
Group 2	sCJD (129 MM1)	Group 2	sCJD (129 MM1)
Group 3	sCJD (129 MM2)	Group 3	sCJD (129 MM2)
Group 4	sCJD (129 MM2)	Group 4	sCJD (129 MM2)
Group 5	vCJD	Group 5	vCJD
Group 6	vCJD	Group 6	vCJD

Table 9: Groups of human transgenic mice, HuMM and HuVV inoculated with different TSE strains of human prions

LL-mutant mice: These mice consist of two groups with eight mice and infected intracerebrally with human GSS cases as previously discussed.

2.2.4. Determination of Incubation Times

The incubation time is defined as the time elapsed between infection of mice and appearance of clinical signs. Animals were monitored regularly for the appearance of clinical symptoms, including ataxia, weight loss, kyphosis, hyperexcitability and hind limb paralysis. Ataxia was assessed by observing the mice walking on a metal grid apparatus. Mice were scored as ill if they exhibited two or more clinical symptoms (38,95).

2.2.5. SDS-PAGE and Western Blot analysis of Infected Animals

We followed the method described by “abcam” company (www.abcam.com/technical) and by others (154,155,156).

Sample preparation:

Brain tissue was weighed and 1:10 homogenate (w/v) was prepared by using Lysis buffer and Daunce homogenizer and needles of different sizes. Homogenates were collected, aliquoted in small tubes and stored at -80°C until use.

Protease K digestion:

To 10 µl brain homogenate, 1 µl PK was added (1:10 from 33mg/ml water) and was incubated at 37°C for 1 hour, then the reaction was stopped with 1.4 µl PMSF 80 mM.

Preparation of samples for loading into gel:

To 5 µl PK-digested sample, 15 µl Lysis buffer and 7 µl 4X LSB were added, mixed and boiled at 95-100°C for 10 minutes. Samples were spun down shortly to remove condensates from the tube wall.

Preparation of SDS-PAGE gel:

Separating acrylamide gels were prepared and poured in the size-required gel-casting apparatus until two thirds height, then the surface was covered with a small amount of isopropanol and the gels were allowed to polymerize 30-60 minutes at room temperature or until interface appeared. The isopropanol was poured off and rinsed with ddH₂O and then the stacking gel was poured on top of the separating gel. Comb was inserted into the stacking gel, taking care to avoid forming bubbles on the ends of the teeth, the gel was allowed to polymerize 30-60 minutes

Electrophoresis:

Gel was clamped onto electrophoresis tank, binding clips were removed carefully and the comb from gel. The gel was placed against electrophoresis tank with the cut out plate facing the tank and clamped into place. Upper and lower reservoir were filled with running buffer, wells were striatened out with Hamilton syringe, wells and bottom of gel were rinsed out with buffer using bent-needle syringe.

Loading samples:

Samples were prepared as described together with positive control, molecular weight marker and loading control, samples were loaded into wells using a Hamilton syringe. Electrodes were attached so that proteins migrated towards the anode and the gel was run at 100-200 V until dye front reached the bottom of the gel. Electrodes were disconnected and the gel sandwich was extracted for blotting.

Western blotting: (Semi-dry conditions)

The transfer box, blotting papers (wetted in blotting buffer) and PVDF membrane (activated in methanol 100% for 3 minutes and then in blotting buffer) were prepared. The paper was put, then the PVDF membrane, then the gel and again the paper and the box was covered (use 1kg weight), the electrodes were attached at suitable mA

(0.8 mA/cm² surface area of gel) for 2 hours. After that the electrodes were disconnected and the membrane was taken for blocking (107,153).

Blocking the membrane:

The membrane was blocked with I.Block for 1 hour at 37°C with shaking to prevent non-specific background binding of the primary and/or secondary antibodies.

Incubation with antibodies:

The membrane was incubated with the primary antibody (e.g. 3F4, 4H11,..etc) at 4°C over night with shaking. Then washing with PBS-Tween four times, 10 minutes for each, then incubation of the membrane in secondary antibody (e.g. sheep anti-mouse IgG, horseradish peroxidase) at 37°C for 1 hour and then washing again four times, 10 minutes each.

Developing the membrane:

The membrane was incubated in ECL chemiluminescence reagent for 1-2 minutes and then was put between two-layer transparent plastic sheets. The membrane then was exposed to x-ray film for different periods and the film then was developed in developing machine. The detection of protein bands on the film was carried out, imaging and analysis of pictures was then made by using digital camera or scanner and then the results were evaluated.

2.2.6. Histology and Immunohistochemistry

After fixation in 10% buffered formalin, brains were treated for 1.5 hour in 98% formic acid (to reduce the titre of infectivity for safety reasons), cut transversely into four sections and embedded in paraffin. Paraffin sections were made, stained with H&E for normal histological examination and stained also for immunohistochemistry for detection of disease-associated prion protein deposits (PrP^{Sc}) in the brain. Sections of immunohistochemistry were processed by using monoclonal anti-prion protein antibodies; 3F4 for HuM & HuV mice and 4H11 for LL mice (1:2000 dilution) and over night incubation of primary antibody. We used the Vectastain Elite ABC kit (Vector labs,UK). Identification of antibody binding was through deposition of 3,3'-diaminobenzidine chromogen via a horseradish peroxidase reaction (23,24).

2.2.7. Determination of Lesion Profiles “Scoring”

Scoring of the abundance and location of TSE-associated vacuolation, spongiosis, cell loss and astrogliosis in grey and white matter of the brain is routinely used for strain classification in transgenic mice (17,19) and was used to assess all the mice in this study (23). PrP deposits were classified as 1) reticular or “synaptic”, 2) coarse or perivascular and 3) plaque-like or focal (22,24,30).

2.2.8. FACS analysis of EGFP-PrP transgenic mice

To analyze the distribution of EGFP-PrP in peripheral blood, thymus, bone marrow and spleen, we used FACS analysis to detect EGFP-PrP on single cell preparations from EGFP-PrP transgenic tissues. Immunofluorescent Staining of Cell Surface Antigens for Flow Cytometric Analysis (FACS Analysis) ([www.eBioscience.com/BestProtocols/Immunofluorescent Staining of Cell Surface Antigens for Flow Cytometric Analysis \(FACS Analysis\).htm](http://www.eBioscience.com/BestProtocols/Immunofluorescent%20Staining%20of%20Cell%20Surface%20Antigens%20for%20Flow%20Cytometric%20Analysis%20(FACS%20Analysis).htm)).

Steps:

- 1-Making a single cell suspension from peripheral blood, lymphoid tissues or cultured cell lines
- 2-Staining cells with antibodies (either as a directly fluorochrome-conjugated antibody or in successive steps of unlabelled antibody and fluorochrome-conjugated secondary reagents)
- 3-Washing steps to remove all unbound reagents
- 4-Running and analyzing on a flow cytometer

Method:

A-For Cell Suspensions of Mouse Lymphoid Tissue

Cell Preparation:

- 1-Tissue (spleen, lymph nodes, thymus) were harvested and teased it apart into single cell suspension by pressing with plunger of a syringe or by mashing between two frosted microscope slides using 10 ml of Staining Buffer.
- 2-Tissues were Transferred into a 50ml conical tube and allowed the big clumps and debris to settle to the bottom or run the suspension through nylon meshes (Falcon Cat. No. 2350) to get single cell suspension.
- 3-Cell suspensions were centrifuged 4-5 min (300-400xg) at 4°C, and discard supernatant.

- 4-If using spleen, RBC lysis was performed; otherwise, go to the next step.
- 5-The samples were resuspended in 50ml of Staining Buffer and a cell count was performed and viability analysis (e.g. Trypan Blue).
- 6-Cells were spun again, supernatant discarded, and cells resuspended in Staining Buffer at 2×10^7 /ml. If using labeled primary antibodies, pre-incubate the cells with 0.5-1 μ g of anti-CD16/CD32 per million cells for 5-10 minutes on ice prior to staining.

Antibody Preparation and Incubation:

- 1-Diluted to previously-determined optimal concentration of primary antibody was prepared in 50 μ l of Staining Buffer and dispensed to each test tube or well of a microtiter plate. Dispense 50 μ l of Staining Buffer were dispensed into the unstained or negative control tube. For titration studies, as a general rule, titrations in the range of 2-0.03 μ g/million cells should be performed.
- 2-50 μ l of cell suspension (equal to 10^6 cells) were added to each tube or well; mixed gently.
- 3-The mix was incubated for 20 minutes in the dark on an ice bath or in a refrigerator.
Note: Some antibodies may require longer incubation times. Determine these conditions in your preliminary experiments.
- 4-After the incubation period, add Staining Buffer (2ml for tubes or 200 μ l for microtiter plates).
- 5-Cells were centrifuged for 5 minutes (300-400xg) at 4°C. Aspirate supernatant.
- 6-2 times for a total of 3 washes were repeated.
- 7-Stained cell pellet were resuspended and analyzed samples on a flow cytometer.
 - a-If using fluorochrome-labeled antibodies, resuspend stained cell pellet in 500 μ l of Staining Buffer and run on a flow cytometer.
 - b-If using purified- or biotin-labeled antibodies, add the proper second step (a fluorochrome-conjugated secondary antibody or -Avidin) in 50-100 μ l of Staining Buffer to each sample. Incubate in the dark for 15-30 minutes on an ice bath or in a refrigerator. Wash 2 times as above (Steps 4 and 5). Resuspend stained cell pellet in 500 μ l of Staining Buffer and run on a flow cytometer.
- 8-For discrimination of viable and dead cells, stained with a viability dye.
Note: If performing multiple color staining, add fluorochrome-labeled antibodies simultaneously and follow incubations and washing steps as mentioned above. Keep

all steps in the cold and keep samples protected from light when working with fluorescent antibodies.

B- For Cell Suspensions of Erythrocytes

- 1-To previously-determined optimal concentration of purified or biotin-conjugated antibody was diluted in 50µl of Staining Buffer and dispense to each test tube. 50µl of Staining Buffer were dispensed into the unstained or negative control tube. Fluorochrome-conjugated anti-human antibodies were pretitrated for optimal performance and should be used at 20µl per sample.
- 2-100µl of whole blood was added to each tube, mixed gently.
- 3-It was incubated for 15-30 minutes at room temperature in the dark. Note: Some Antibodies with low affinity binding may require longer incubation times. These conditions were determined in preliminary experiments.
- 4-2ml of 1X RBC Lysis Buffer (pre-warmed to room temperature) were added per tube, mixed gently.
- 5-Samples were incubated in the dark at room temperature for 10 minutes. Do not exceed 15 minutes of incubation with the RBC Lysis Buffer.
- 6-Samples were spun (300-400xg) at room temperature, supernatant aspirated and washed 1 time with 2ml of Staining Buffer.
- 7-Stained cell pellet was resuspended and analyzed samples on a flow cytometer.

2.2.9. *In Vitro* Conversion Assay of EGFP-PrP

Analysis of EGFP-PrP localization pre- and post-infection of cell culture (RK13 cells), which expressing EGFP-PrP protein, was carried out by using scrapie strains 22L and ME7. Transfected cells were then examined for intracellular PrP aggregations and with western blot.

2.2.10. Confocal Laser Scanning Microscopy Leica "LSM"

Brains of EGFP-PrP mice were fixed in 4% paraformaldehyde for 48 hours at 4°C, transferred to 0.1M phosphate buffer, pH 7.2 and stored at 4°C. Sagittal sections (50-100 µm thickness) were cut using a Vibratome and placed in sterile PBS containing 0.02% sodium azide. For visualization of intrinsic EGFP-PrP fluorescence, sections were mounted on glass slides using Fluorescent mounting medium, covered and sealed with silicon and sterilized in 2M NaOH for 30 minutes. Sections were viewed

with a Leica LSM Confocal laser scanning microscope with wet objective (10&40x). Processing of digital images was accomplished using Leica LSM software and Adobe Photoshop (Adobe system, San Jose, CA).

2.2.11. Rescue Studies on transgenic F35 Mice

F35-mice are mice with truncated prion protein gene, with deletion from codon 32 to 135 (These mice were a gift from Prof. Charles Weissmann, Zurich). This deletion causes ataxia and specific degeneration of the granular layer of the cerebellum within 3-4 months after birth. The defect was completely abrogated if one or more copies of a wild-type murine PrP gene were introduced into mice carrying multiple copies of the truncated gene (Figure 8) (22). In this experiment, we introduced EGFP-PrP allele into F35-mice to see if this PrP-construct can rescue the deleterious effect of the truncated gene or not.

2.2.12. Genotyping of HuM, HuV and LL mice:

Genotyping of HuM, HuV and LL mice was carried out before starting the experiment to be sure that all the genetic background of the mice was correct. At first DNA was isolated, then amplified through PCR, then restricted by restriction enzymes (Table 10&11), lastly, separated on agarose gel electrophoresis and the gel was photographed by a digital camera on a U.V. lamp, the images were analyzed and evaluated (108,152).

DNA Isolation:

DNA was isolated from tails of tested mice by using DNeasy blood & Tissue Kit (Qiagen) according to the protocol of Qiagen Company.

Analysis of HuM, HuV and HuMV mice :

PCR-mix : (25µl) 9 µl ddH₂O
2.5 µl HuM_fwd
2.5 µl HuM_rev
10 µl Hot star Taq-mix
1 µl genomic DNA

Table 10: PCR-programme for genotyping of HuM, HuV and HuMV mice

Step	Temperature	Time	
1	95°C	15 minutes	Hot Start
2	95°C	1 minute	
3	64°C	30 seconds	
4	72°C	1 minute	
5	Go to Step 2 34X		
6	72°C	10 minutes	
7	4°C	Hold	

-expected product size: 371 bp

Nspl-Restriction:(50µl) 34 µl ddH₂O

5 µl 10X NEBuffer 2 (1X)

0.5 µl 10mg/ml BSA(100 yg/ml)

0.5 µl 20U/µl Nspl (10 U/µl)

10 µl PCR-product

The mix was incubated 2 hours at 37°C and then heated to inactivate Nspl by incubating for 20 minutes at 65°C. 8.5 µl 6x loading dye was added and analyzed on 2% agarose gel (use 50 bp Ladder as standard). Expected fragments are 244 + 127 bp for HuM, 371 bp for HuV and 371 + 244 + 127 bp for HuMV.

Analysis of LL mice:

PCR-mix: (25 µl) 9 µl ddH₂O

2.5 µl LL_fwd

2.5 µl LL_rev

10 µl Hot star Taq-mix

1 µl genomic DNA

Table 11: PCR-programme for genotyping of LL mice

Step	Temperature	Time	
1	95°C	15 minutes	Hot Start
2	95°C	1 minute	
3	62°C	30 seconds	
4	72°C	1 minute	
5	Go to Step 2 34X		
6	72°C	10 minutes	
7	4°C	Hold	

-expected product size: 764 bp

Ddel-Restriction: (50µl) 34.5 µl ddH₂O

5 µl 10X NEBuffer 3 (1X)

0.5 µl 20U/yl Ddel (10 U/µl)

10 µl PCR-product

The mix was incubated 2 hour at 37°C and then heated to inactivate Ddel by incubating for 20 minutes at 65°C. 8.5 µl 6x loading dye was added and analyzed on 1.8% agarose gel. Expected fragments are 464 + 151 + 149 bp for LL, 613 + 464 + 151 + 149 bp for heterozygous and 613 +151 bp for wild-type mice.

3. Results

3.1. Investigation of Pathogenic Mechanisms of Prion Diseases using Transgenic Mice expressing EGFP-PrP

3.1.1. Expression of EGFP-PrP in EGFP-PrP Transgenic Mice

Five independent lines of transgenic mice carrying a chimeric EGFP-PrP fusion protein were generated and visualized for the localization of EGFP-PrP in various organs in histological sections. Analyses of these mice were carried out *in vivo* before infection. Histological sections from paraformaldehyde fixed tissues from EGFP-PrP transgenic mice were analyzed using confocal laser scanning microscopy. Images of whole-brain sections showed expression of EGFP-PrP in all of the five transgenic lines (Figure 4 for EGFP-PrP-6 as example). Three of the five transgenic lines showed similar expression patterns, only varying in intensity of EGFP fluorescence while two lines showed slightly different patterns of EGFP distribution in brain (figure 4 right part for lines EGFP-PrP-13 and EGFP-PrP-17), probably due to integration effects of the transgene. These lines are analyzed in detail with respect to their expression patterns of EGFP-PrP and are subject to infection with the RML scrapie strain.

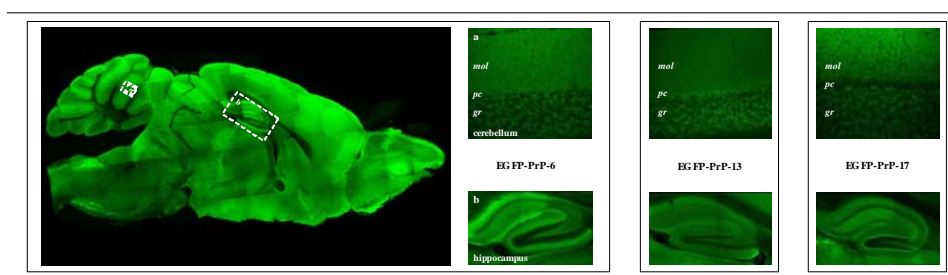


Figure 4: Confocal laser scanning microscopy of EGFP-PrP transgenic mice showing different expression patterns of EGFP-PrP.

In histological sections from EGFP-PrP transgenic mice we were able to detect EGFP fluorescence in five independent lines. Left part: EGFP-PrP-6 brain (with enlargement of: a: cerebellum, b:

hippocampus). Right part: lines EGFP-PrP-13 and -17 show slightly different expression patterns of EGFP-PrP compared to EGFP-PrP-6 (for example, cerebellum and hippocampus). *mol*, molecular layer; *pc*, Purkinje cells; *gr*, granule cell layer.

3.1.2. FACS analysis of EGFP-PrP Transgenic Mice

To analyze the distribution of EGFP-PrP in peripheral blood, thymus, bone marrow and spleen, we used FACS analysis to detect EGFP on single cell preparations from EGFP-PrP transgenic tissues. Positive cells were detected in bone marrow and peripheral blood of transgenic mice (Figure 5 for bone marrow). Histograms show two gated regions of samples from EGFP-PrP positive transgenic mouse compared to non-transgenic littermate (both EGFP-PrP-24).

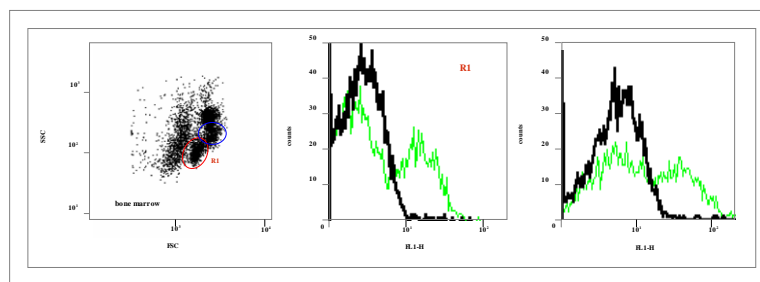


Figure 5: FACS analysis of EGFP-PrP-24 mice showing positive cells in transgenic samples

Bone marrow was flushed from femur of transgenic and non-transgenic EGFP-PrP-24 mice. Dot plot on the left shows typical distribution of cell populations discriminated by forward (FSC) and side scatter (SSC). FACS analysis and gating of distinct populations showed EGFP (as seen in FL1-H) positive cells in transgenic sample (green line) while non-transgenic samples were negative (black line) in two gated regions (R1 and R2) from dot plot.

3.1.3. *In vitro* Conversion Assay and Susceptibility of EGFP-PrP to Scrapie infection

To analyze EGFP-PrP localization pre and post infection, RK13 cells were transfected with EGFP-PrP and suitable hygromycin resistance vector. Western blot analysis of EGFP-PrP cell extract digested with proteinase k (PK) showed no sign of PK resistant PrP four, eight and eleven passages after incubation with 22L scrapie

prions (Figure 6). To address the question whether chimeric EGFP-PrP is convertible to a PK resistant form we used an *in vitro* conversion assay where we incubated ^{35}S labeled EGFP-PrP as well as wild-type mouse PrP with PrP^{Sc} from a mouse infected with scrapie strain ME7. No detectable PK resistant PrP derived from EGFP-PrP was found, while wild-type mouse PrP was effectively converted to a PK resistant form (Figure 7). The *In vitro* conversion assay using a mixture of labeled EGFP-PrP and unlabeled wild-type PrP did not result in conversion of EGFP-PrP. Our results show that EGFP-PrP^C was not susceptible for Scrapie infection and not converted into EGFP-PrP^{Sc} form.

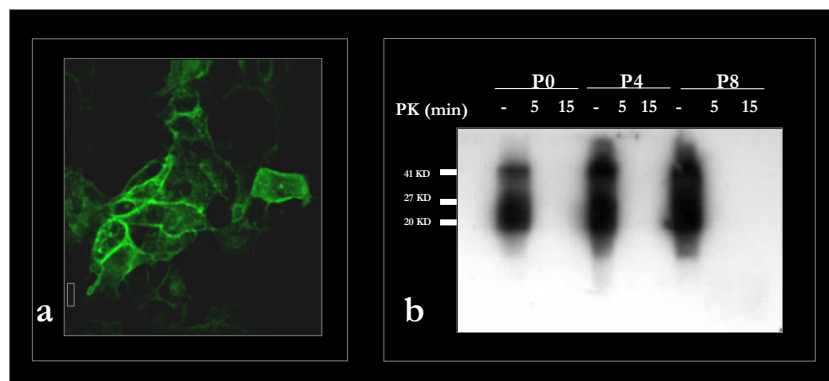


Figure 6: Analysis of stable clones of RK13 cells transfected with phgEGFP-PrPL42 construct.

a. Confocal laser scanning microscopy image of EGFP-PrP positive RK13 cells.

b. Western blot analysis of RK13 EGFP-PrP before (P0) and at different time-points (four (P4) or eight (P8) passages) after incubation with 22L scrapie. Cell extracts were digested with proteinase k (PK) to analyze for PK resistant PrP^{Sc}.

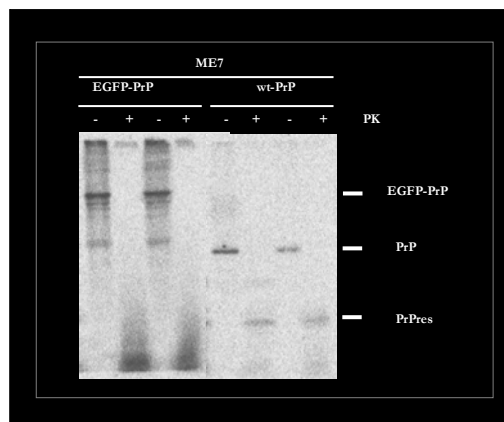


Figure 7: *In vitro* conversion assay of EGFP-PrP.

In an *in vitro* conversion assay PrPSc from ME7 infected mice was used to analyze conversion of EGFP-PrP and wt-PrP to PrP^{res}.

3.1.4. Rescue Studies using F35 Mice

F35-mice are mice with truncated PrP gene, with deletion from codon 32 to 134 (Figure 8) and this deletion causing ataxia and specific degeneration of the granular layer of the cerebellum within 3-4 months after birth (Figure 9). PrP in F35 was expressed in all layers of the cerebellum except for the Purkinje cells. The defect was completely abrogated if one or more copies of a wild-type murine PrP gene were introduced into mice carrying multiple copies of the truncated gene. Introduction of EGFP-PrP alleles into F35-mice cannot rescue the deleterious effect of the truncated gene. Massive pathological changes in the cerebellum: degeneration of the granular cell layer with dramatic reduction in the width, coarse vacuolation of the white matter. The Purkinje cells appeared normal and the molecular layer was only reduced in width. The remainder of the brain showed no obvious changes except for patchy astrocytosis and there were no PrP deposits (Figure 9).

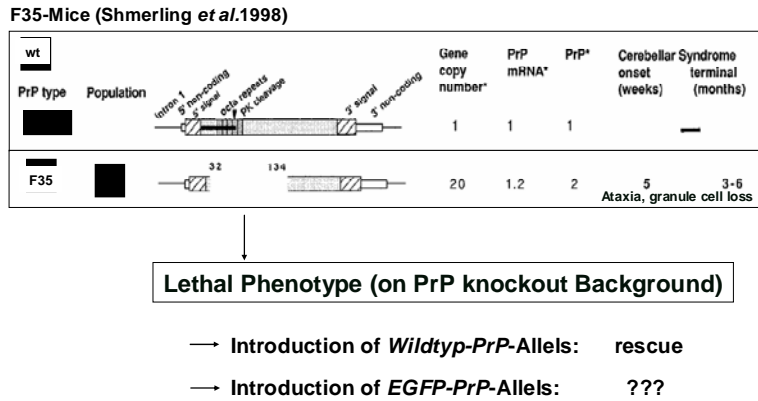


Figure 8: Illustration showing structure of F35-PrP truncated gene with deletion of 32-234 residues (Shmerling et al. 1998)

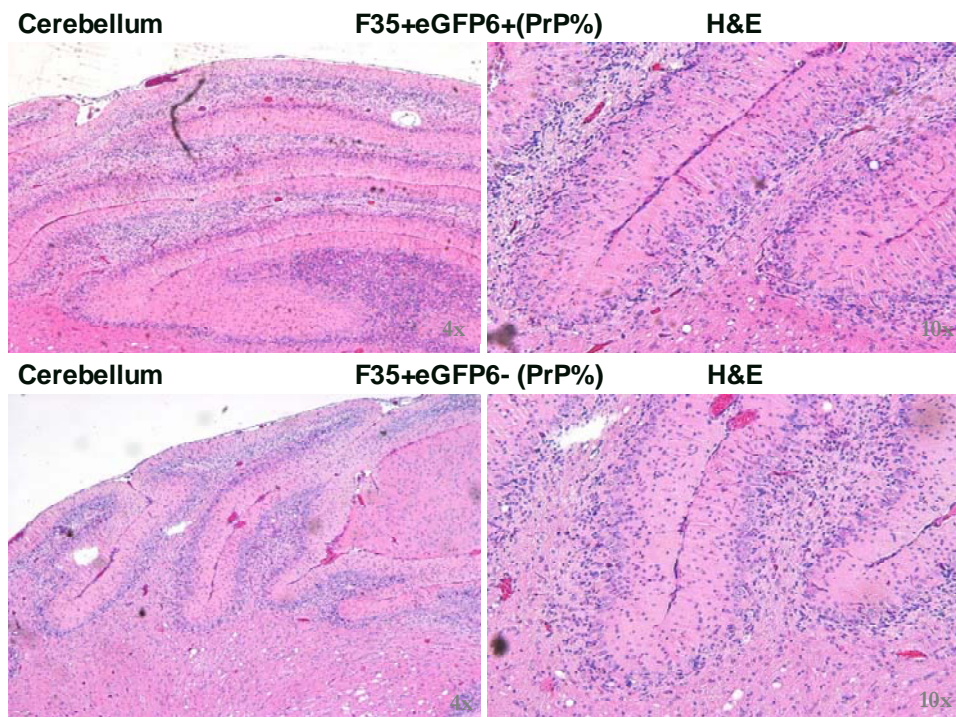


Figure 9: Histopathological effects of F35-PrP truncated gene on mice

Massive pathological changes in the cerebellum: degeneration of the granular cell layer with dramatic reduction in the width, coarse vacuolation of the white matter. The purkinje cells appeared normal and the molecular layer was only reduced in width. The remainder of the brain showed no obvious

changes except for patchy astrocytosis and there were no PrP deposits. There was no difference between F35-mice with and without EGFP-PrP allele.

3.1.5. Incubation Times of Infected EGFP-PrP Mice

Survival data revealed similar incubation periods of EGFP-mice and wt-mice, which about 150 days post infection with means; 148 ± 8 d.p.i. (line 24) and 150 ± 8 d.p.i. So that our results revealed that introduction of EGFP-PrP transgene into wild-type murine prion protein gene did not have any prolonging or shortening effect on incubation times of the disease in transgenic mice after intracerebral infection with RML scrapie prion (Figure 10).

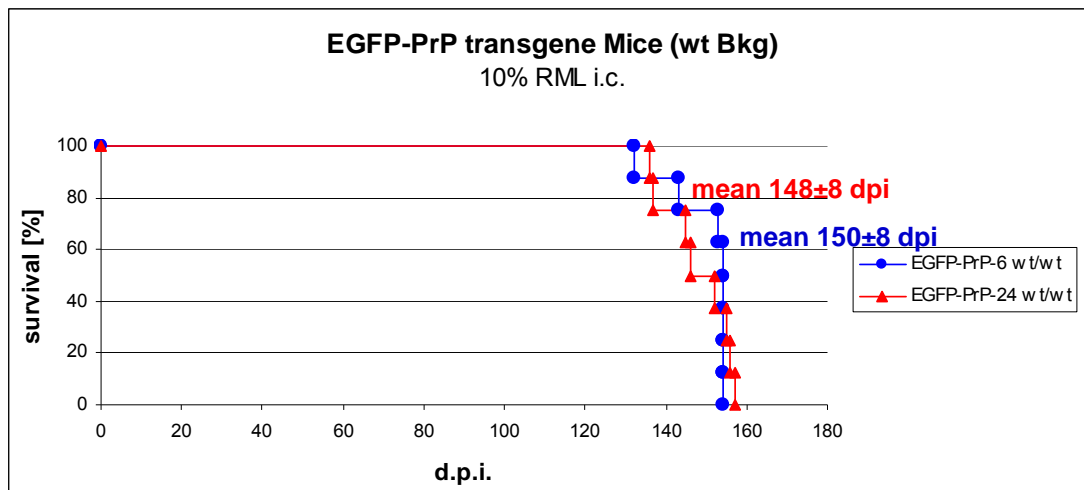


Figure 10: Survival data of scrapie infected EGFP-PrP/wt-PrP-mice

3.1.6. Biochemical Analysis of Infected EGFP-PrP Mice

Western blot showed that EGFP-PrPC was not converted *in vivo* into EGFP-PrP^{Sc} after proteinase k digestion by using L42 antibody which specific for detection of EGFP-PrP only, but when we used 4H11 antibody, we found that wild-type PrP and EGFP-PrP appeared to be converted into resistant form of PrP which giving bands after proteinase k digestion (Figure 11).

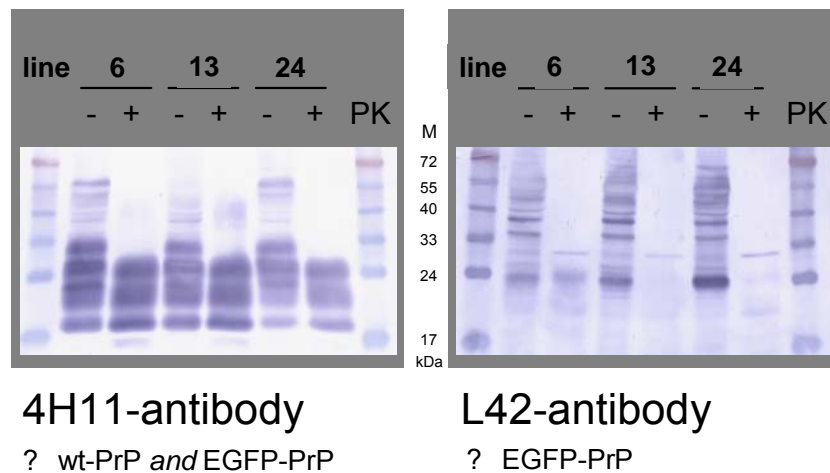


Figure 11: Western Blot of scrapie infected EGFP-PrP/wt-PrP mice

3.1.7. Histology and Immunohistochemistry of Infected Brain Tissue

We cut brains of mice infected intracerebrally with RML scrapie and terminally killed for histological and immunocytochemical examination. Histological examination showed that all sections of infected brains exhibit all neuropathological features of prion diseases such as: spongiform changes, neuronal cell loss and neuronal degeneration. IHC with CDC1 and L42 showed the presence of PrP deposits of the two proteins; wild-type PrP and EGFP-PrP protein bound together (by using CDC1 anti-prion protein antibody which recognizes the two types of prion protein; wild-type PrP and EGFP-PrP) and also PrP deposits of EGFP-PrP alone in the same locations of the wild-type PrP, but with low concentrations (by using L42 anti-prion protein which recognizes only the EGFP-PrP transgene and can not recognize the wild-type of murine PrP) which means that EGFP-PrP^C binds physically to the protease-resistant form EGFP-PrP^{Sc} *in vivo* and EGFP-PrP can not convert into the disease-form EGFP-PrP^{Sc} by itself (Figures 12&13).

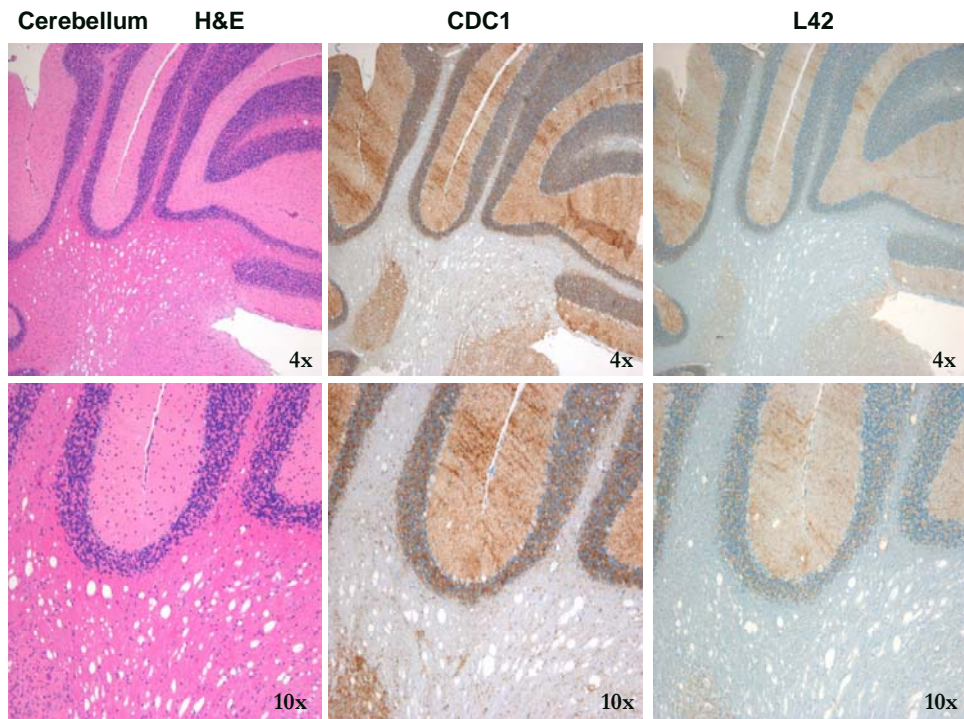


Figure 12: Histology by H&E and Immunohistochemistry by CDC1 & L42

Cerebellum sections stained with H&E showing spongiosis and neuronal degeneration in all layers. Also, immunohistochemistry revealed the presence of strong immunopositivity for PrP^{Sc} deposits in the Molecular and granular cell layers only with CDC1 antibody and weak signal with L42 which detects only EGFP-PrP.

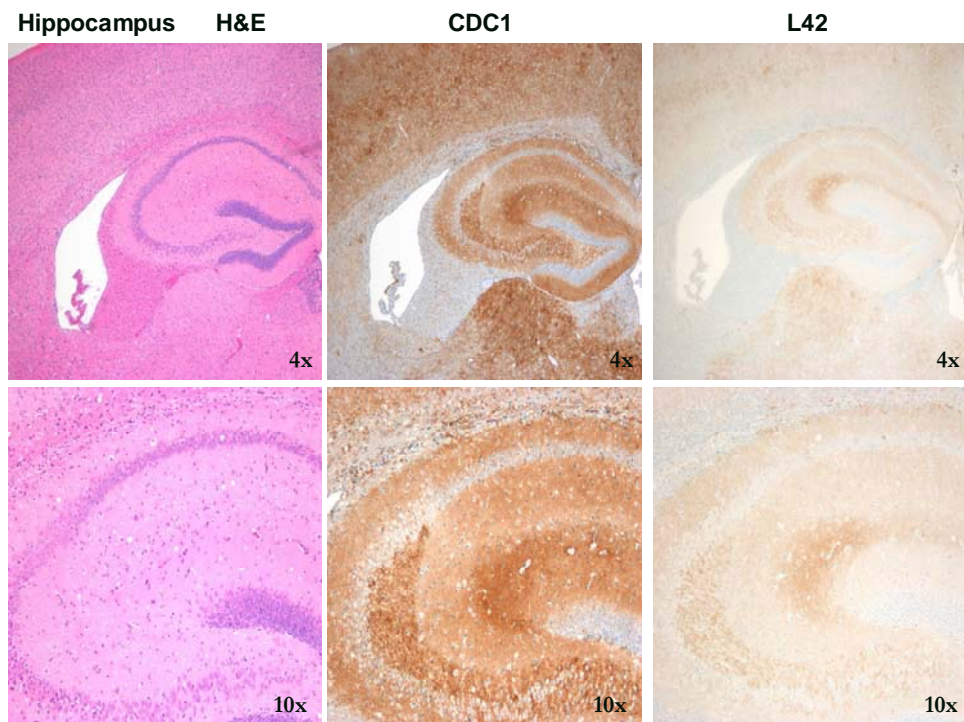


Figure 13: Histology by H&E and Immunohistochemistry by CDC1 & L42

Hippocampus sections stained with H&E showing spongiosis and neuronal degeneration. Also, immunohistochemistry revealed the presence of strong immunopositivity for PrP^{Sc} deposits in hippocampus with CDC1 antibody and a weak signal with L42 which detect only EGFP-PrP.

3.1.8. Confocal Laser Scanning Microscopy of Infected Brain Tissue

In our experiment on EGFP-PrP transgenic mice, we cut brains of mice infected intracerebrally with RML scrapie and terminally killed with control mock mice; these samples were cut by vibratome dissection (100 µm thick). These samples were examined by Confocal Laser Scanning Microscopy for the presence or absence of pathological prion protein aggregates. Different parts of the CNS were examined including cerebral cortex, hippocampus, thalamus, basal ganglia, corpus callosum, cerebellum and medulla oblongata (Figures 14-16). The results revealed the presence of pathological PrP-aggregates distributed throughout the CNS and these aggregates were highly fluorescent. Also our results confirmed that localizations of the pathological EGFP-PrP aggregates are similar to the localization of wild-type PrP-aggregates.

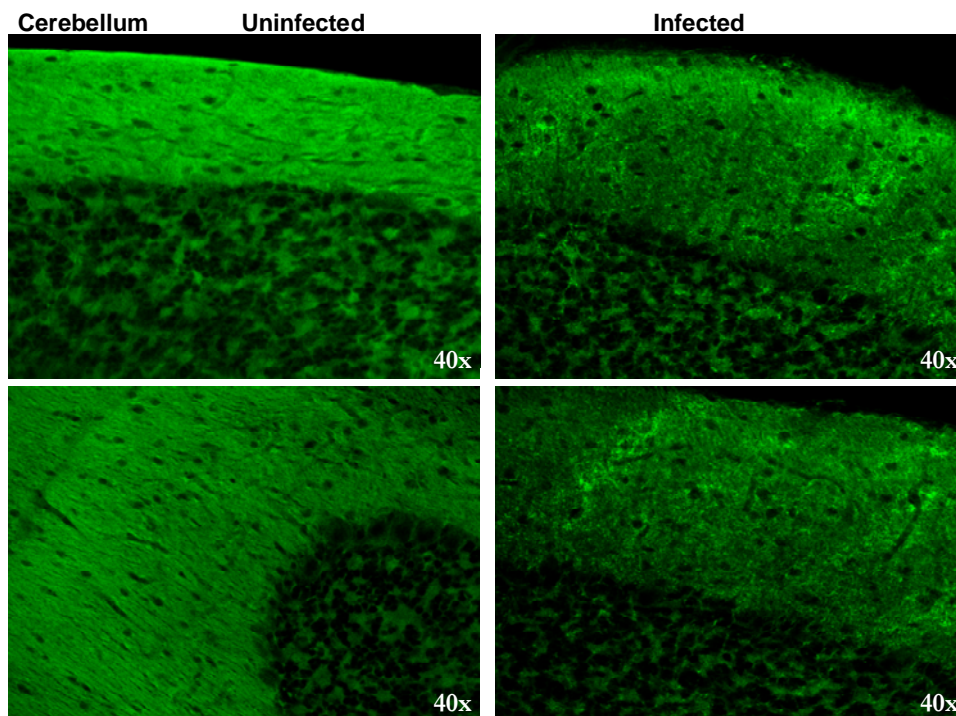


Figure 14: Cerebellum of infected mice showing strongly fluorescent aggregates distributed throughout the molecular and granular cell layers in comparison with non-infected mice, which were negative for aggregates.

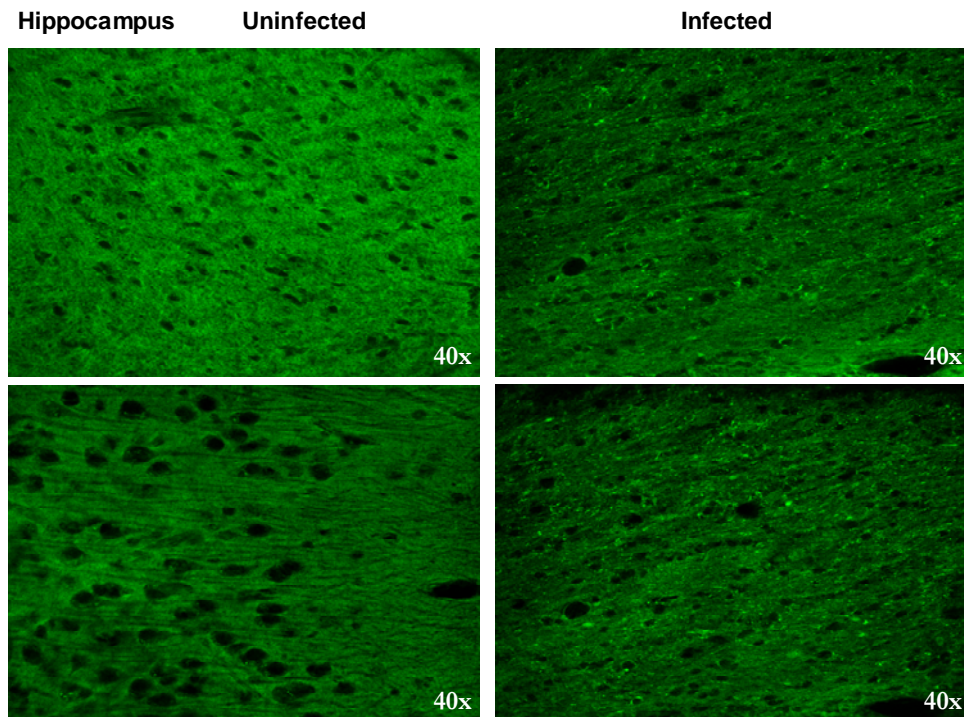


Figure 15: Hippocampus of infected mice showing strongly fluorescent aggregates in comparison with non-infected mice, which were negative for aggregates.

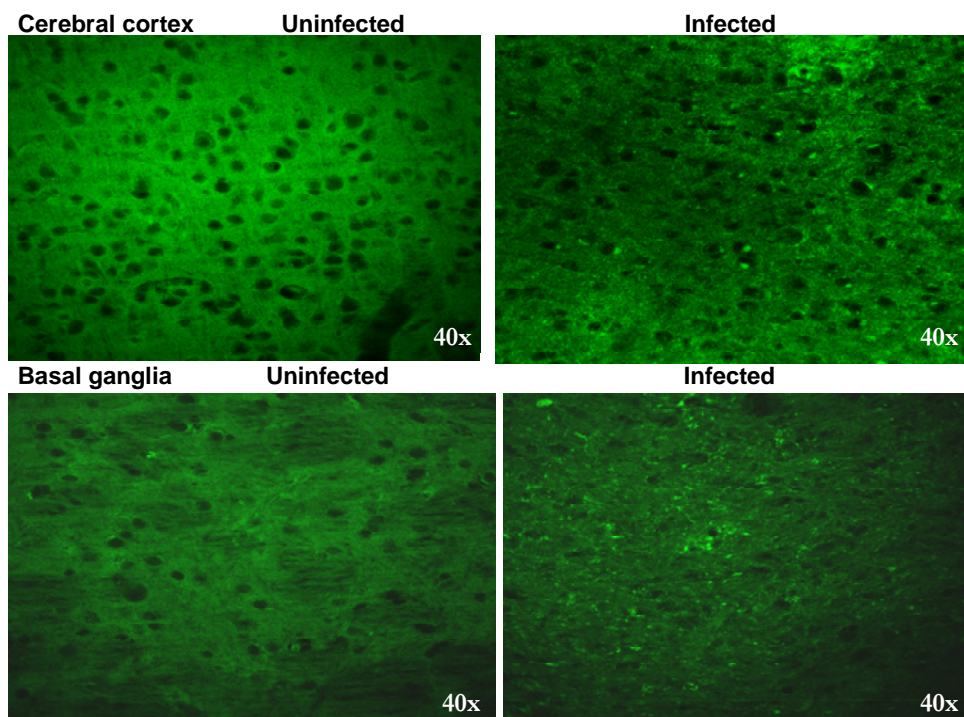


Figure 16: Cerebral cortex and basal ganglia of infected mice showing a lot of fluorescent aggregates distributed widely in nervous tissue in comparison with non-infected mice, which were negative for aggregates.

3.2. Evaluation of Prion Strain Properties using Transgenic Mice Expressing Human PrP and LL-mice

3.2.1. Susceptibility and Incubation Times of Humanized and LL Mice intracerebrally infected with Human TSE Strains

In general, all the humanized transgenic mice including HuMM and HuVV are susceptible to various TSE strains. Sporadic CJD and variant CJD strains from human cases were transmitted to all humanized transgenic mice either with HuMM or HuVV codon-129 polymorphism with different pathological characteristics for each genotype and a gradation of transmission efficiency from HuMM to HuVV mice. Two different materials of sCJD from two different human cases were used for infection, types of inoculated materials are 129-MM1 (a & b) and 129-MM2 (a & b), also, we used two different materials of vCJD obtained from two different human cases died from vCJD, designated vCJD (a & b).

For the HuMM mice inoculated with sCJD 129-MM1-a and 129-MM1-b cases, our results showed that all the mice were susceptible (8/8 & 8/8) with different incubation times with means of 481.4 ± 61.7 days and 484.3 ± 37.6 days respectively. Also, all the HuMM mice inoculated with 129-MM2-a and 129-MM2-b cases were susceptible (7/7 & 8/8) with incubation times with means of 514.3 ± 79.1 days and 507.1 ± 51.8 days respectively (Figures 18&19). All HuVV mice infected with 129-MM1-a and 129-MM1-b cases were susceptible (8/8 & 8/8) with incubation times with means of 585.2 ± 66.5 days and 627.6 ± 66.1 days respectively, while all HuVV mice infected with 129-MM2-a and 129-MM2-b cases were susceptible (7/7 & 8/8) with incubation times with means of 677.5 ± 54.3 days and 578.9 ± 71.2 days respectively (Figures 18&19) (Tables 12&13).

Our results reveal that all HuMM mice inoculated with vCJD-a and vCJD-b cases were susceptible (7/7 & 4/4) with incubation times with mean of 611.4 ± 112.7 days and 551.8 ± 204.3 days respectively. Also, all HuVV mice inoculated with vCJD-a and vCJD-b cases were susceptible to infection (7/7 & 7/7) with incubation times with means of 673.6 ± 116 and 689.2 ± 72.2 days respectively (Figures 18&19).

We examined also the transmission properties of Gerstmann-Sträussler-Scheinker Syndrome (GSS) to transgenic mice with the 101LL mutation, designated LL-mice which equivalent to the P102L mutation in the human PRNP gene. We used two different GSS cases (a & b) and our results show that all LL-mice were susceptible to

infection with human GSS-a and GSS-b cases (8/8 & 8/8) with incubation times with means 279.9 ± 18 days and 474.3 ± 172.1 days respectively (Figure 21).

Time range	HuMM-mice					
	sCJD MM1-a	sCJD MM1-b	sCJD MM2-a	sCJD MM2-b	vCJD-a	vCJD-b
0-400	1	1	0	1	0	2
401-500	4	5	3	2	2	0
501-600	3	2	3	5	0	0
>600	0	0	1	0	5	2
Time range	HuVV-mice					
	sCJD MM1-a	sCJD MM1-b	sCJD MM2-a	sCJD MM2-b	vCJD-a	vCJD-b
0-400	1	1	2	1	0	2
401-500	1	0	0	0	2	0
501-600	4	3	0	5	1	1
>600	2	4	5	2	4	4

Table 12: Time Scoring of Incubation Times of HuMM and HuVV mice after infection with sCJD MM1 (a&b), sCJD MM2 (a&b) and vCJD (a&b).

Strain	HuMM-mice		HuVV-mice	
	Incubation Time (Mean \pm SD)	Glycoform Type	Incubation Time (Mean \pm SD)	Glycoform Type
sCJD MM1-a	481.4 \pm 61.7	1	585.2 \pm 66.5	1
sCJD MM1-b	484.3 \pm 37	1	627.6 \pm 66.1	1
sCJD MM2-a	514.3 \pm 79.1	2	677.5 \pm 54.3	1
sCJD MM2-b	507.1 \pm 51.8	1	578.9 \pm 71.2	1
vCJD-a	611.4 \pm 112.7	2	673.6 \pm 116	2
vCJD-b	551.8 \pm 204	2	689.2 \pm 72.2	2

Table 13: Incubation Times and Glycoform Types of HuMM and HuVV mice after infection with sCJD MM1 (a&b), sCJD MM2 (a&b) and vCJD (a&b).

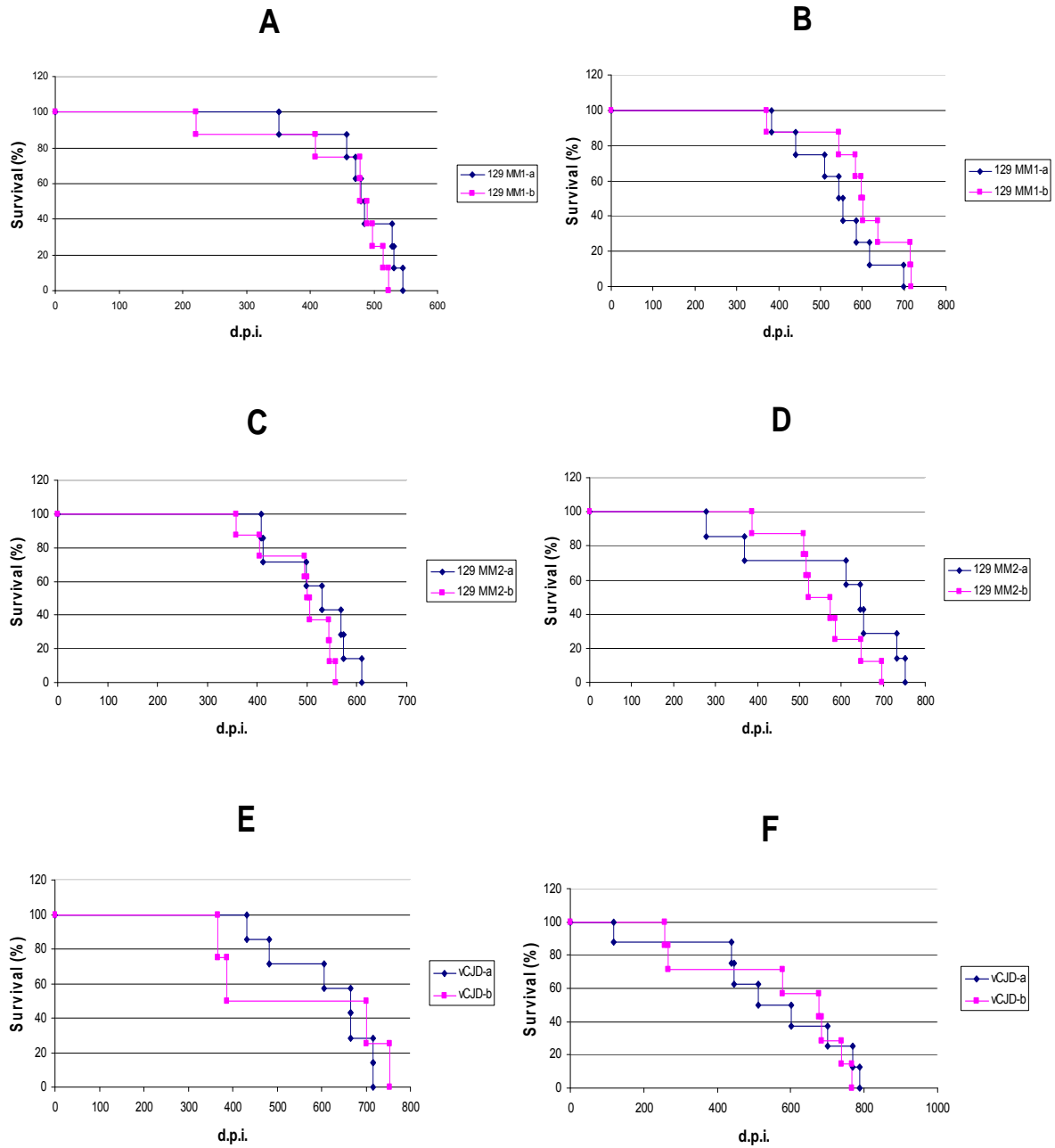


Figure 17: Incubation Times of Humanized Mice infected with TSE Strains

(A) HuMM mice infected with 129 MM1 (a & b) sCJD (B) HuVV mice infected with 129 MM1 (a & b) sCJD (C) HuMM mice infected with 129 MM2 (a & b) sCJD (D) HuVV mice infected with 129 MM2 (a & b) sCJD (E) HuMM mice infected with vCJD (a & b) (F) HuVV mice infected with vCJD (a & b).

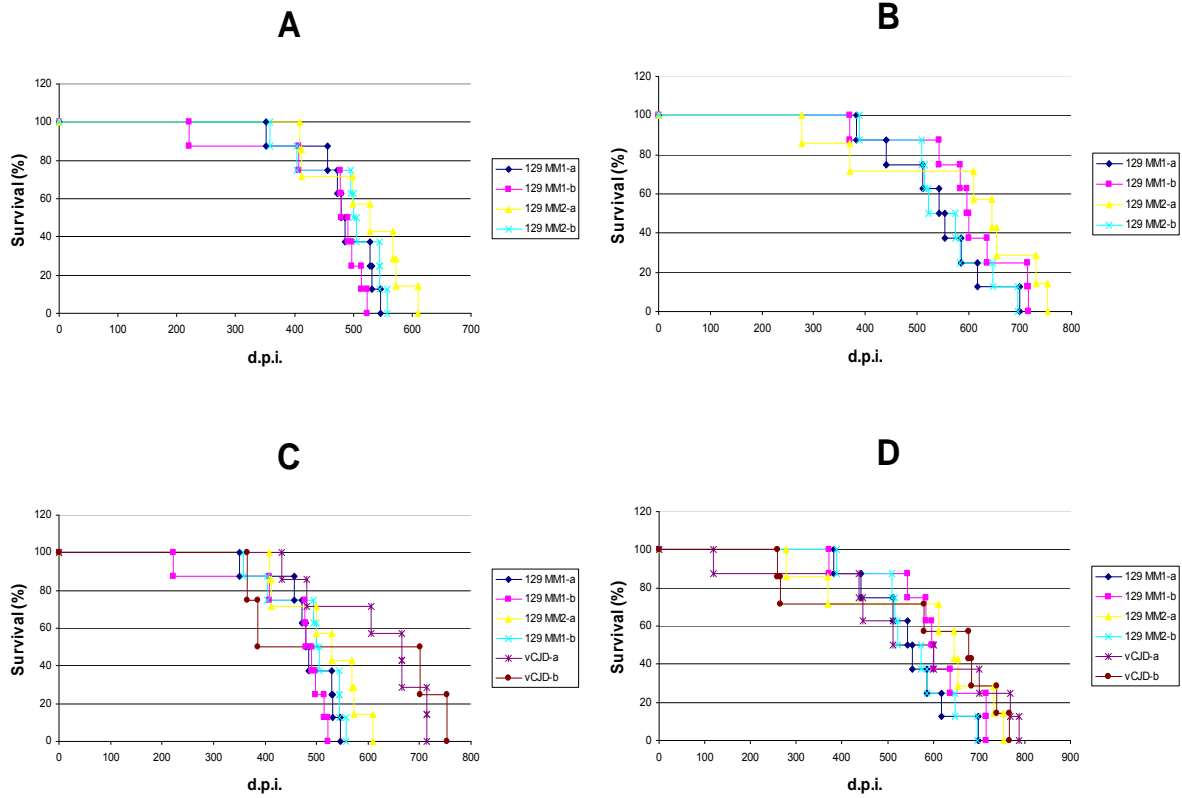
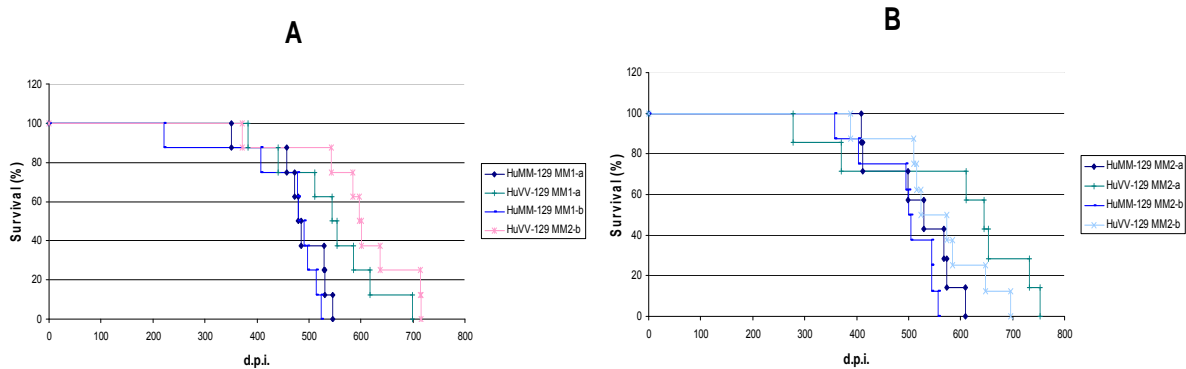


Figure 18: Comparison of Incubation Times Between Different TSE Strains

(A) Between 129 MM1 (a & b) sCJD and 129 MM2 (a & b) sCJD in HuMM mice (B) Between 129 MM1 (a & b) sCJD and 129 MM2 (a & b) sCJD in HuVV mice (C) Between 129 MM1 (a & b) sCJD and 129 MM2 (a & b) sCJD and vCJD (a & b) in HuMM mice (D) Between 129 MM1 (a & b) sCJD and 129 MM2 (a & b) sCJD and vCJD (a & b) in HuVV mice.



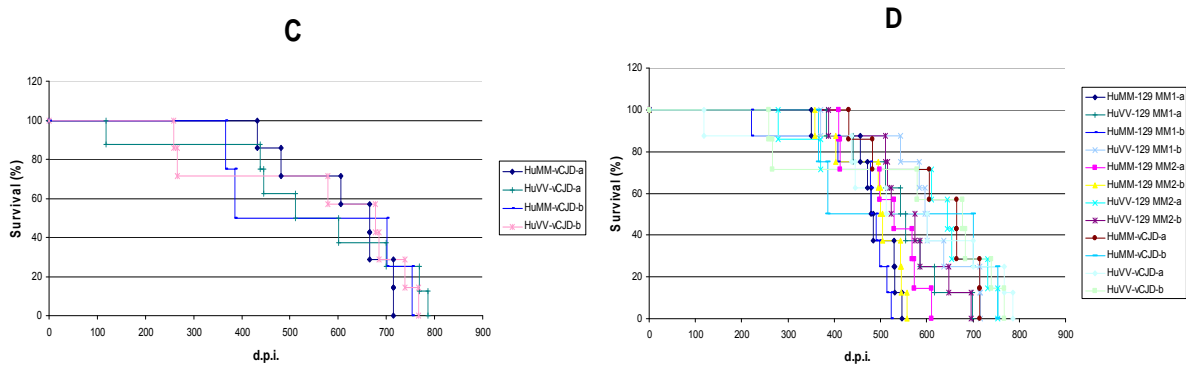


Figure 19: Comparison of Incubation Times Between HuMM and HuVV Mice Infected With Different TSE Strains

(A) HuMM and HuVV infected with 129 MM1 (a & b) sCJD (B) HuMM and HuVV infected with 129 MM2 (a & b) sCJD (C) HuMM and HuVV infected with vCJD (a & b) (D) HuMM and HuVV infected with 129 MM1 (a & b) sCJD, 129 MM2 (a & b) sCJD and vCJD (a & b).

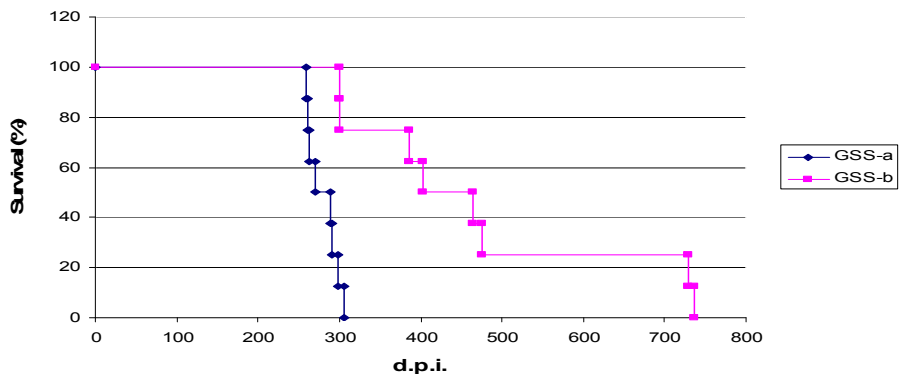


Figure 20: Incubation Times of LL Mice Infected With Two Different GSS Strains (a & b)

3.2.2. Neuropathology and Lesion Profiling

Our results revealed the presence of CJD pathological signs of spongiosis, neuronal cell loss, astrogliosis and different patterns of PrP deposition, the severity and time of appearance of these lesions differs greatly according to the strain of the prion used for inoculation and to the genotype and codon-129 polymorphism of the transgenic mice. Lesions were more rapid and more aggressive in HuMM mice than in HuVV mice and by sCJD MM1 than with MM2. Some cases showed massive vacuolation and neuronal death, while others showed extensive PrP deposition with different patterns from synaptic until large kuru plaques (Figures 22-27).

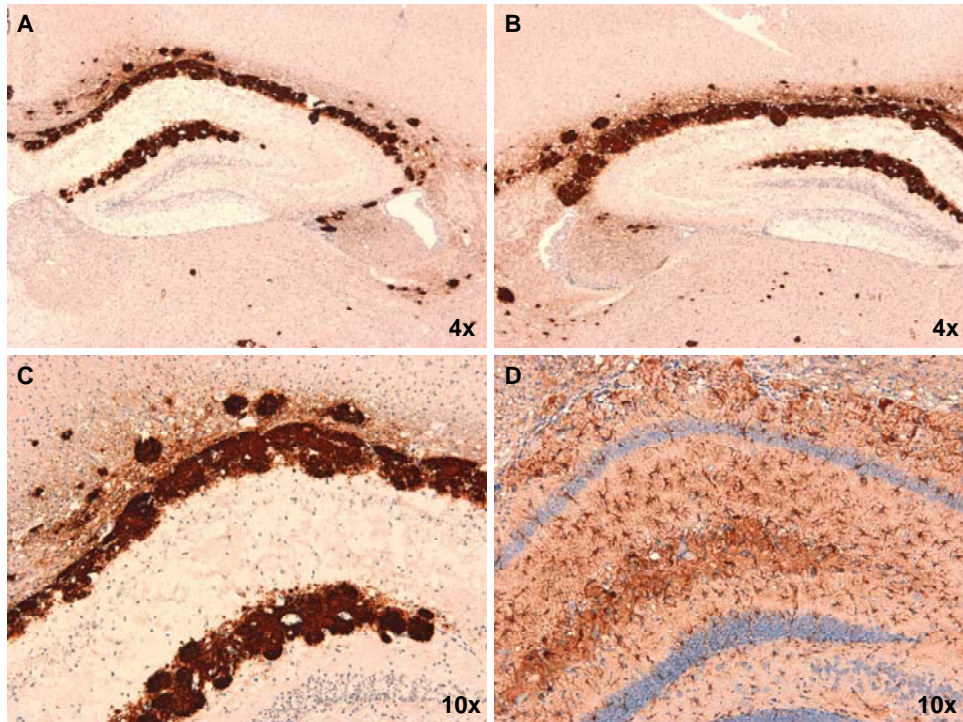


Figure 21: Immunohistochemical pattern of PrP deposition (A-C) and astrogliosis (D) in the hippocampus of LL mice inoculated with GSS-b 729 days post inoculation

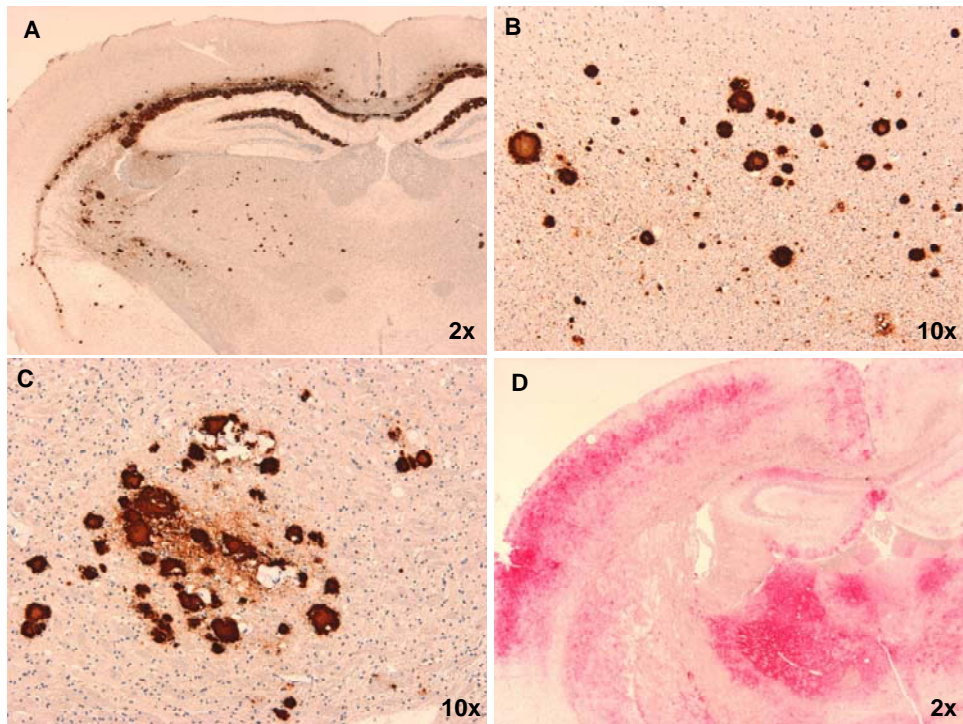


Figure 22: Immunohistochemical patterns of PrP deposition in LL mice

A-C: LL mice inoculated with GSS-b, 729 days post inoculation, A: plaques in the cortex, corpus callosum, hippocampus and thalamus, B&C: cortex and thalamus showing large kuru plaques, D: LL mice inoculated with GSS-a, 260 days post inoculation showing synaptic distribution of PrP in the cortex, hippocampus and thalamus

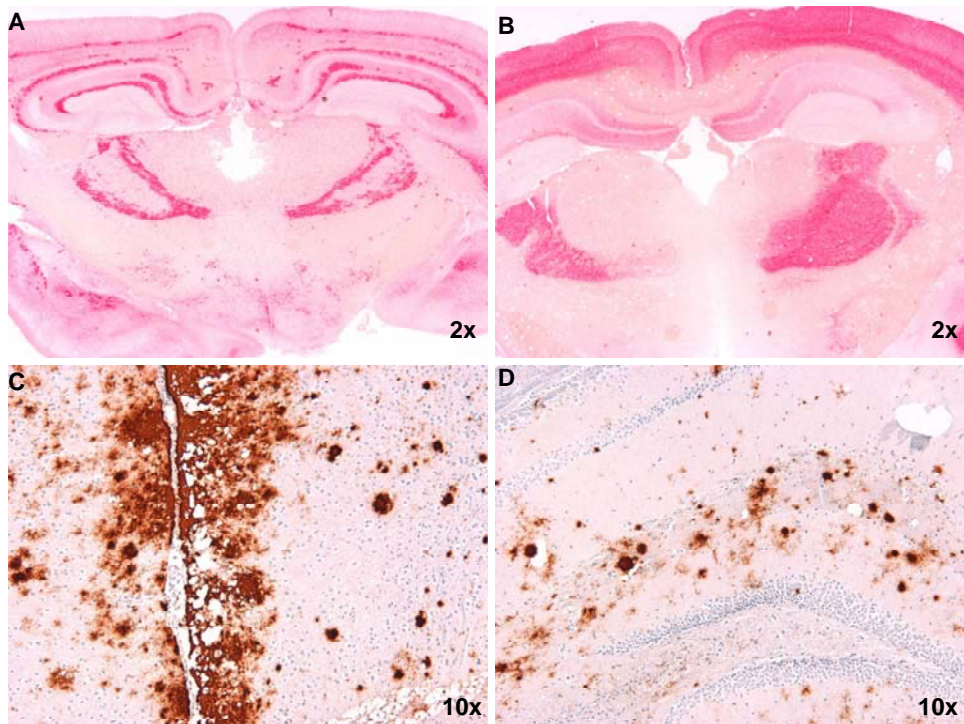


Figure 23: Immunohistochemistry showing patterns of PrP deposition in transgenic mice express human PrP

A: HuMM mice inoculated with sCJD MM1-b, 523 days post inoculation showing synaptic pattern of PrP deposition in different brain regions, B: HuVV mice inoculated with vCJD-a, 438 days post inoculation showing extensive synaptic pattern of PrP with spongiosis, C&D: HuMM mice inoculated with vCJD-a, 665 days post inoculation showing coarse deposition of PrP with presence of some large plaques in the cortex and hippocampus

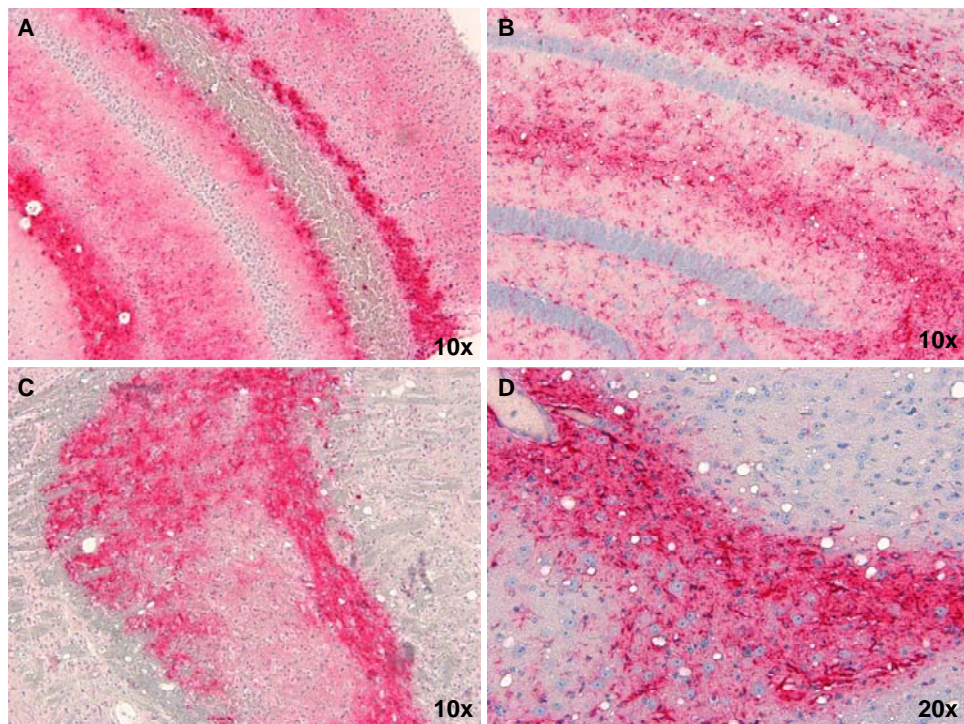


Figure 24: Immunohistochemistry showing patterns of PrP deposition (A&C) and astrogliosis (B&D) in the hippocampus and thalamus of HuVV mice inoculated with sCJD MM1, 601 days post inoculation

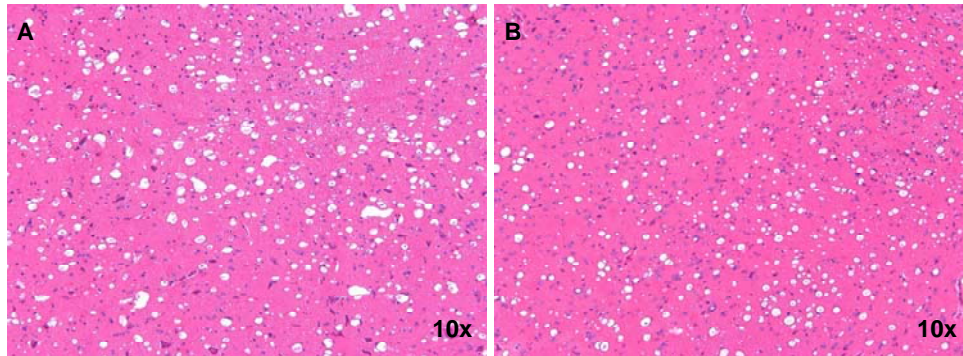
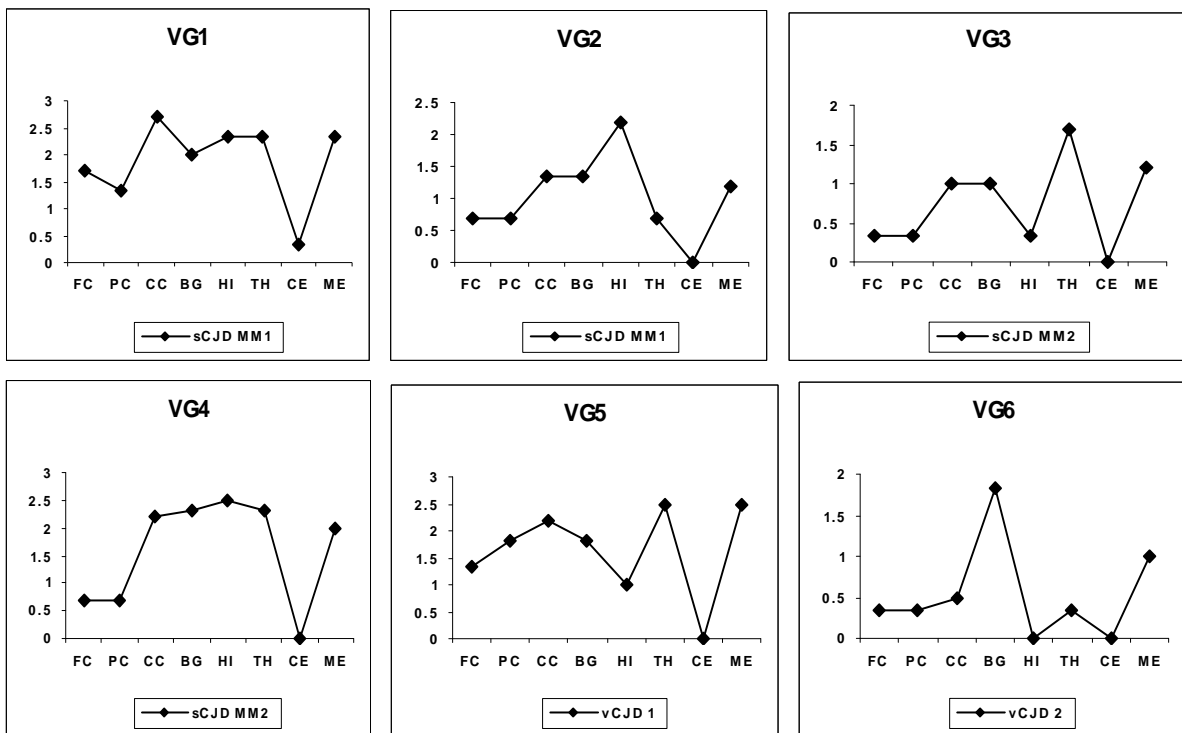


Figure 25: Histological sections (H&E) showing extensive spongiosis in the medulla (A) and thalamus (B) in HuVV mice inoculated with sCJD MM1, 586 days post inoculation



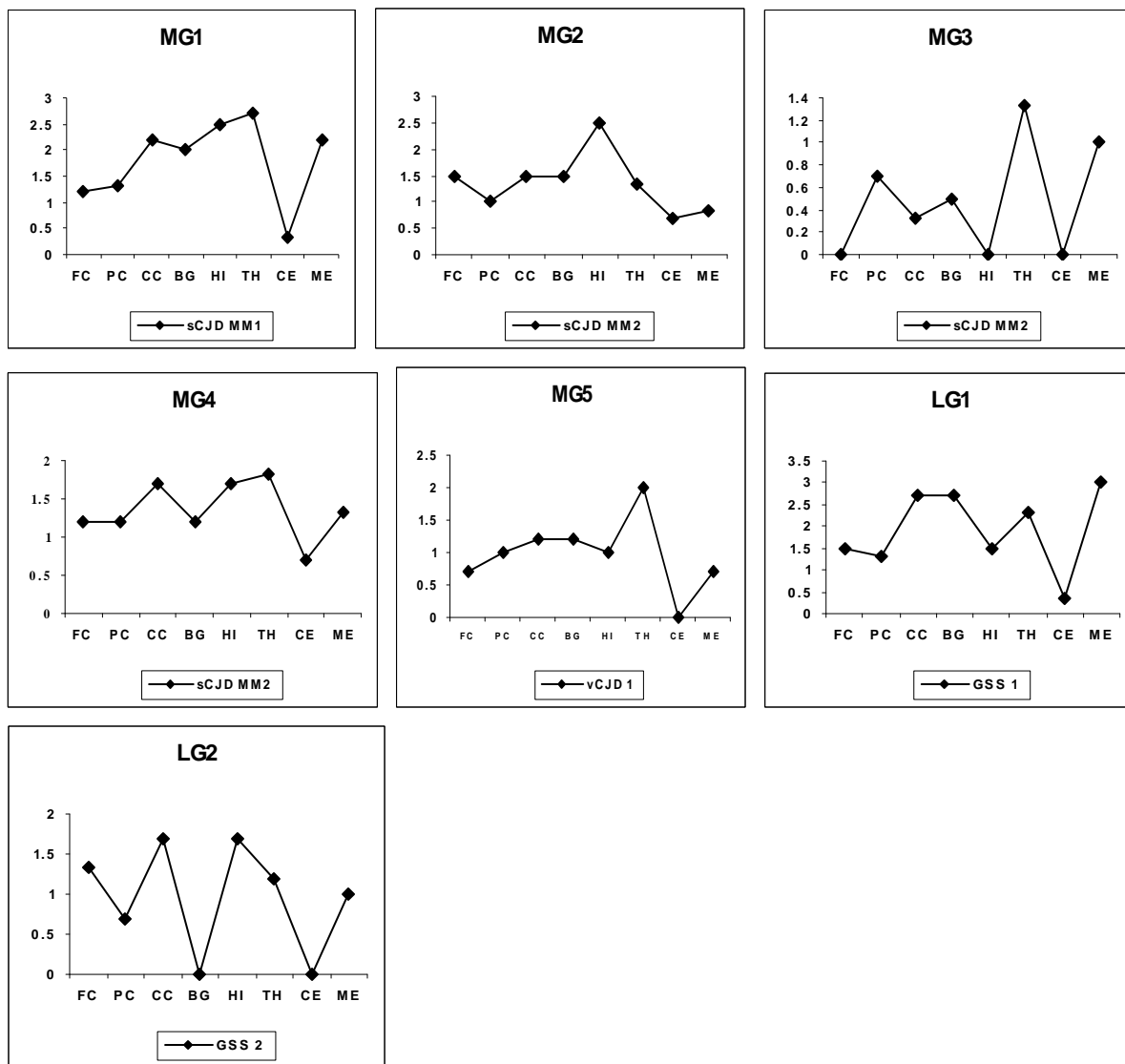


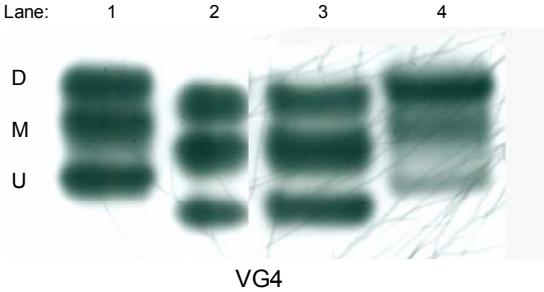
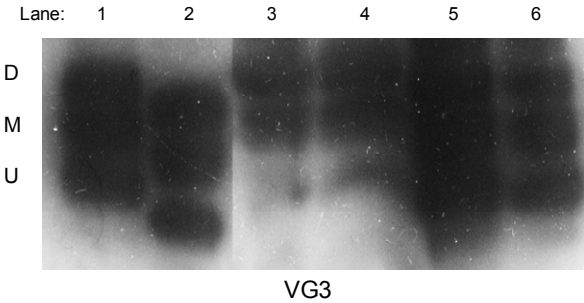
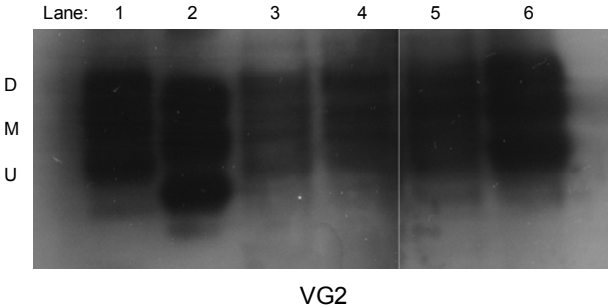
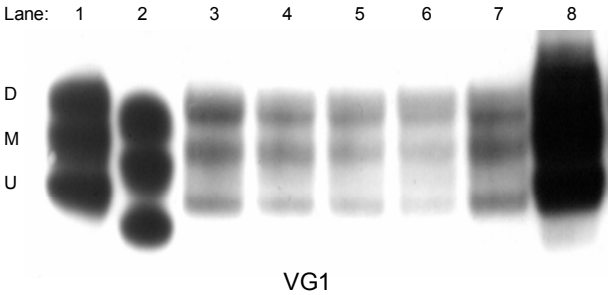
Figure 26: Lesion Profiles for the different sCJD, vCJD and GSS Strains

Groups were classified according to the codon 129 genotype and the protease-resistant prion protein (PrPSc) type. MM1 means MM genotype and type 1 PrPSc, MM2 means MM genotype and type 2 PrPSc. VG1&MG1:HuVV&HuMM mice infected with case-a sCJD MM1, VG2&MG2: HuVV&HuMM mice infected with case-b sCJD MM1, VG3&MG3: infected with case-a sCJD MM2, VG4&MG4: infected with case-b sCJD MM2, VG5&MG5: infected with case-a vCJD, VG6: infected with case-b vCJD, LG1&LG2: infected with case-a &-b of GSS respectively. The following gray matter regions were assessed: frontal cortex (FC), parietal cortex (PC), corpus callosum (CC), basal ganglia (BG), hippocampus (HI), thalamus (TH), cerebellum (CE) and medulla oblongata (ME). Spongiosis was scored on a 0 to 4 scale (not detectable, mild, moderate, severe and status spongiosus), neuronal loss and astrogliosis on 0 to 3 scale (not detectable, mild, moderate and severe). Lesion profiles were obtained by averaging the three scores for each brain region examined.

3.2.3. Biochemical Analysis of Infected Humanized Mice

Brain extract 10% from all terminally-ill human transgenic mice, either HuMM or HuVV were analyzed biochemically by western blot analysis by using anti-prion protein antibodies as 3H4 for HuMM & HuVV mice and 4H11 for LL mice, using semi-

dry blotting method to investigate the type of the PrP glycoform. The type 1 and 2 PrP were used in every blot as a positive control (Table 13) (Figures 28-30).



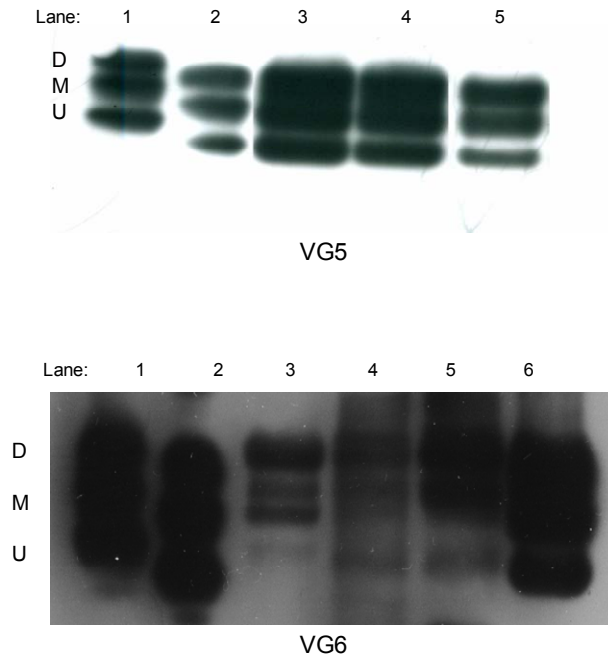
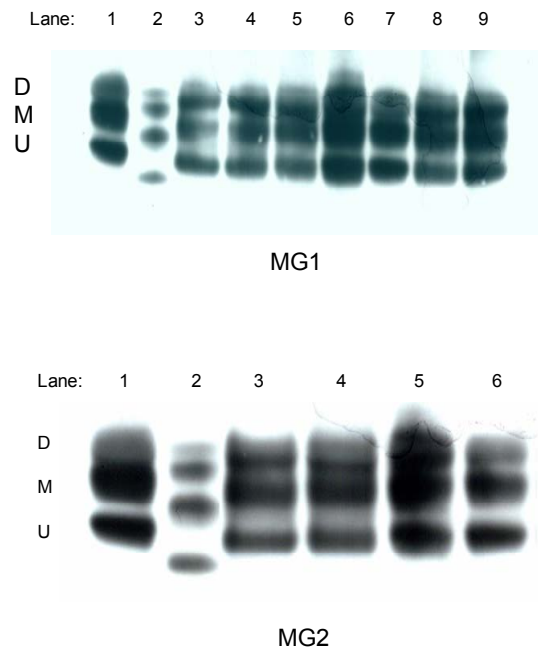


Figure 27: Western Blot of HuVV Groups Infected with different TSE Strains

VG1&VG2: HuVV mice infected with sCJD MM1 (a&b); VG3&VG4: HuVV mice infected with sCJD MM2 (a&b); VG5&VG6: HuVV mice infected with vCJD (a&b); Lane 1&2 in every blot refers to positive control type 1&2.



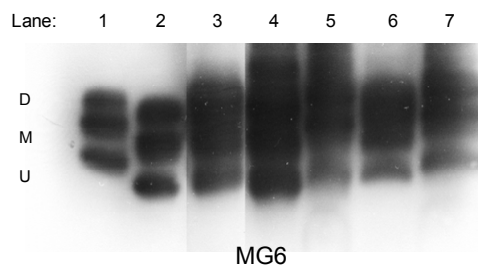
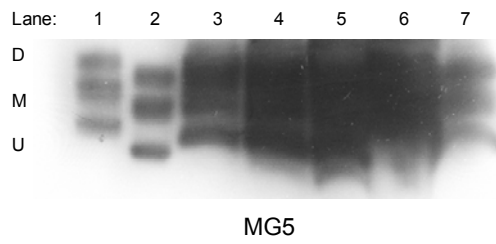
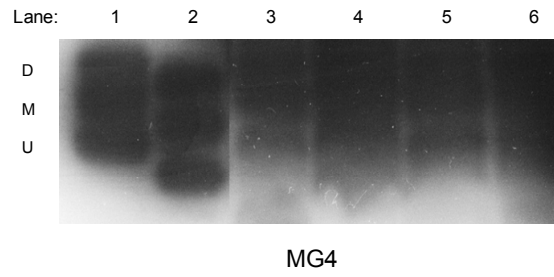
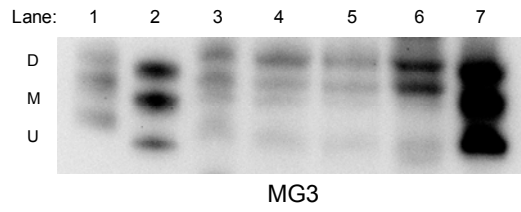


Figure 28: Western Blot of HuMM Groups Infected with different TSE Strains

MG1&MG2: HuMM mice infected with sCJD MM1 (a&b); MG3&MG4: HuMM mice infected with sCJD MM2 (a&b);
MG5&MG6: HuMM mice infected with vCJD (a&b); Lane 1&2 in every blot refers to positive control 1&2.

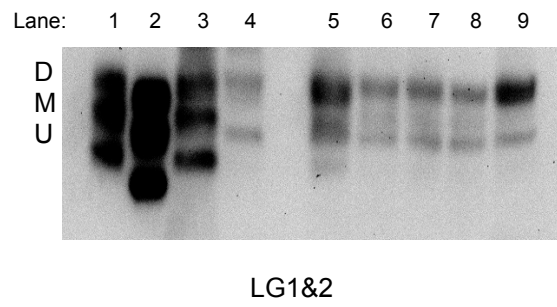


Figure 29: Western Blot of LL Groups Infected with different GSS Cases

Lane 1&2: positive control type 1&2; Lane3&5: LG1, mice infected with GSS-a case; Lane 4,6,7,8,9: LG2, mice infected with GSS-b case

4. Discussion

4.1. Investigation of Pathogenic Mechanisms of Prion Diseases using Transgenic Mice expressing EGFP-PrP

In this experiment, Maringer and our group generate a five independent lines of transgenic mice that express a chimeric EGFP-PrP fusion protein under the regulatory elements of the half-genomic mouse PrP locus (Figure 2). Using these mice we were found that it is possible to visualize the localization of EGFP-PrP in various organs in histological sections. We find that EGFP-PrP behaves similarly to wild-type PrP in its posttranslational processing, cellular trafficking and anatomical localization in the brain (109,134). Histological sections from paraformaldehyde fixed tissues from EGFP-PrP transgenic mice were analyzed using confocal laser scanning microscopy. Images of all brain sections showed expression of EGFP-PrP in all transgenic lines. Three of the five transgenic lines showed similar expression patterns, only varying in intensity of EGFP-PrP fluorescence, while two lines showed slightly different patterns of EGFP-PrP distribution in the brain, probably due to integration effects of the transgene (Figure 4).

The results reported here extend previous studies of EGFP-PrP fusion proteins expressed cell lines. When the same construct used here, in which EGFP-PrP is inserted in the open reading frame (ORF) of the PrP-coding gene, was expressed in transfected BHK and CHO cells, the fusion protein was found to be glycosylated, GPI-anchored and localized intracellularly and to the cell surface. These characteristics are similar to those of PrP without the EGFP-PrP moiety. In a similar construct, EGFP-PrP molecules carrying PrP mutations were partially retained in the ER of cultured cells and were present at reduced levels on the cell surface, analogous to their untagged PrP counterparts (118). Similar results have been reported by others using alternative EGFP-PrP fusion proteins (121,125,131).

We are in general agreement with other studies that showed that EGFP-PrP expressed in neurons is also processed and trafficked along the secretory pathway in a normal fashion. The fusion protein is glycosylated, GPI-anchored and localized to the cell surface and the Golgi apparatus of neurons in brain tissues and in culture (76,130,138,140). At high expression levels of PrP, a fraction of PrP molecules is inefficiently translocated into the ER, and these unprocessed forms remain in the cytoplasm where they are normally degraded by the proteasome (141).

Our results revealed that EGFP-PrP fusion proteins were expressed in the all brain tissues and very clear in the hippocampus and cerebellum especially in molecular, granular and Purkinje cell layers (Figure 4). Several previous studies have utilized immunohistochemistry to study the localization and distribution of PrP in the normal brain at the light or electron microscopic levels. There is general agreement that PrP is concentrated in neuropil layers that are rich in synapses, such as the strata oriens, radiatum and lacunosum-moleculare of the hippocampus, the stratum moleculare of the dentate gyrus and the molecular layer of the cerebellum (76). However, there is disagreement on several specific points such as preferential localization of the PrP in synaptic vesicles and/or pre-synaptic plasma membrane (117), while others suggest that PrP is present on both presynaptic and postsynaptic membranes (119,129,132). Also others reported the presence of PrP on axonal fiber tracts (128,142) and distinct intracellular accumulation of PrP within a subset of neurons (128). It has been argued that cytoplasmic PrP arises by retrotranslocation of PrP from the lumen of the ER (122,123,124,133). Neurons that accumulate cytoplasmic PrP are those that overexpress the protein compared to their neighbours, or that have lower activities of translocation factors or the proteasome (76).

Several technical problems implicate interpretations of these immunocytochemical studies and may account for some of the discrepancies in the results reported (76). These include different effects of processing steps used in immunohistochemistry for preparation of tissue sections such as antibody-induced redistribution of GPI-anchored PrP in paraformaldehyde-fixed sections (127), fixation-induced changes in PrP antigenicity (143), extraction and relocation of membrane-bound PrP by the detergent used to improve antibody accessibility (126), differential reactivity of antibodies with different PrP glycoforms and cleavage products (120,137), and diffusion of enzymatic reaction product used to visualize antibody localization (139). The use of an EGFP-PrP fusion protein to visualize the localization of PrP in brain tissue avoids all difficulties faced with immunohistochemical techniques because it allows antibody-independent visualization of the protein through its fluorescence.

Our results are in agreement with results of the previous immunohistochemical studies and EGFP-PrP studies on transgenic mice which demonstrate preferential localization of the PrP in synaptic regions of the neocortex, hippocampus, dentate gyrus and cerebellum. Although the signal was considerably weaker; we could also visualize fluorescence on surface of neuronal cell bodies, including pyramidal cells in

the hippocampus and granular cells in the dentate gyrus and in the cerebellum. Our results indicate that EGFP-PrP is localized primarily along myelinated and unmyelinated axons and in presynaptic terminals (76).

We conducted FACS analysis of EGFP-PrP transgenic mice to analyze the distribution of EGFP-PrP in peripheral blood, thymus, bone marrow, spleen. We used FACS analysis to detect EGFP-PrP on single cell preparations from EGFP-PrP transgenic tissues. Positive cells were detected in bone marrow and peripheral blood of transgenic mice (Figure 5). Positive results of FACS analysis revealed that EGFP-PrP was expressed in tissues other than nervous tissues and this finding confirmed that EGFP-PrP behave in similar manner like wild-type PrP, which expressed in tissues other than nervous tissues like blood cells, bone marrow, thymus and spleen, also confirmed correct transgenesis of EGFP-PrP fusion protein transgene in transgenic mice and expression pattern and distribution of EGFP-PrP similar to wild PrP (134).

We found that introduction of EGFP-PrP transgene in F35-mice can not rescue them from neurodegeneration induced by expression of PrP Δ 32-134. Expression of EGFP-PrP in Tg (F35)/PrP% mice can not prevent the progression and severity of clinical symptoms and can not abrogate the pathological phenotype of F35-mice (Figure 9). This attachment of the EGFP-PrP moiety abolishes the physiological function of the PrP necessary for the rescue phenomenon. My results concerning rescue studies were in disagreement with other results using similar EGFP-PrP construct which revealed that introduction of EGFP-PrP transgene into the F35-mice can abrogate the pathological phenotype of F35-mice and stop the progression and severity of the adverse effects like ataxia and cerebellar degeneration after 3-5 months (76). It has been speculated that PrP supplies a trophic function by binding to a receptor whose activity is blocked by binding of PrP Δ 32-134. Wild-type PrP is postulated to bind the receptor with a higher affinity than PrP Δ 32-134 and thereby way titrate out the inhibitory effect of the defect protein (22).

To analyze EGFP-PrP localization pre and post-infectional, we transfected RK13 cells with EGFP-PrP and a suitable hygromycin resistance vector. Western blot analysis of EGFP-PrP cell extract digested with proteinase k (PK) showed no signs of PK-resistant PrP four, eight and eleven passages after incubation with 22L scrapie prions (Figure 6). To address the question of whether chimeric EGFP-PrP is convertible to PK-resistant form, we used an *in vitro* conversion assay where we

incubated ³⁵S-labeled EGFP-PrP as well as wild-type mouse PrP with PrP^{Sc} from a mouse infected with scrapie strain ME7. No detectable PK-resistant PrP derived from EGFP-PrP was found, while wild-type mouse PrP was effectively converted to a PK-resistant form (Figure 7). The *in vitro* conversion assay using a mixture of labeled EGFP-PrP and unlabeled wild-type PrP did not result in conversion of EGFP-PrP.

In this study, we describe experiments in which EGFP-PrP transgenic mice were inoculated intracerebrally with RML scrapie prions. We found that although EGFP-PrP^C was not itself converted into EGFP-PrP^{Sc}, the fusion protein served as a highly specific marker that bound to PrP^{Sc} generated from endogenous PrP^C (Figure 11). This feature allowed us to visualize the accumulation of PrP^{Sc} *in situ* by fluorescence microscopy without the need for immunohistochemical staining and the application of antigen retrieval techniques.

Also, our results are in agreement with other results that revealed that EGFP-PrP can not be converted into EGFP-PrP^{Sc} by itself but binds to PrP^{Sc} of endogenous origin (77). We hypothesized that EGFP-PrP binds to PrP^{Sc} but that the presence of the bulky EGFP moiety prevents the subsequent conversion step that would generate EGFP-PrP^{Sc}. Additionally, we propose that EGFP-PrP competes with endogenous PrP^C for access to binding sites on PrP^{Sc}, thereby slowing prion propagation in mice expressing both proteins. Because of the specific affinity between EGFP-PrP and PrP^{Sc}, we envision that the fusion protein is incorporated into growing aggregates of PrP^{Sc}, thus marking the location of PrP^{Sc} and permitting its detection by fluorescence microscopy. Consistent with this proposal, we observed a striking and progressive accumulation of fluorescent aggregates in the brains of scrapie-inoculated Tg (EGFP-PrP⁺⁰)/PrP^{+/+} mice during the course of infection. EGFP-PrP aggregates were observed in many brain areas and took several forms, including granular and plaque-like deposits in the neuropil as well as intracellular accumulations in neuronal somata and axon tracts. These aggregates were absent from uninoculated control mice (Figures 14-16). The redistribution of EGFP-PrP in infected animals preceded by ~50 days the onset of clinical symptoms, the appearance of astrocytosis and the detection of PrP^{Sc} on western blots (77).

Visualization of PrP^{Sc} in EGFP-PrP mice by fluorescence microscopy represents a significant advance over conventional immunohistochemical techniques because of the improved ability to detect natural *in situ* localization of the PrP^{Sc} extra- and intracellularly after scrapie infection without possible effects which can be generated

from processing steps of immunohistochemistry. Immunohistochemical studies on light microscopy typically describe several different patterns of PrP^{Sc} deposition in the brain, depending on the prion strain and host, including dense plaques, diffuse plaques, granular deposits within the neuropil (synaptic form) and perineuronal aggregates (110,111,113). Most of these deposits appear to be extracellular, a conclusion that is confirmed by electron microscopic studies that have identified both fibrillar and non-aggregated forms of PrP^{Sc} in spaces surrounding neurons and their processes (111,112). Published images showing intracellular accumulation of PrP^{Sc} in brain are rare (114,115,116).

We do not believe that the novel features of PrP^{Sc} localization reported here are artifacts resulting from the expression of a foreign protein transgene. First, EGFP-PrP⁺⁰/PrP^{+/+} transgenic mice eventually show the same symptoms and neuropathological features as the non-transgenic ones and they accumulate similar levels of PrP^{Sc}. Second, after immunohistochemical staining of formic acid-treated sections, the distribution of PrP^{Sc} in the neuropil was very similar in EGFP-PrP⁺⁰/PrP^{+/+} and non-transgenic animals. This observation suggests that the expression of EGFP-PrP does not cause a major redistribution of PrP^{Sc}. However, visualization of PrP^{Sc} in EGFP-PrP⁺⁰/PrP^{+/+} mice is indirect, because it relies on binding of EGFP-PrP to PrP^{Sc}. Thus, it is possible that some deposits of PrP^{Sc} may not be evident by fluorescence microscopy because of the dissociation of PrP^{Sc} and EGFP-PrP. Conversely, some EGFP-PrP aggregates could form independently of PrP^{Sc} (77).

Concerning incubation times of EGFP-PrP transgenic mice intracerebrally infected with RML scrapie strain, we found that these are comparable and similar to incubation times of wild mice (Figure 10). Our interpretation that this similarity in incubation times between EGFP-PrP⁺⁰/PrP^{+/+} and wild-type PrP is partly due to the presence of wild PrP allele in these transgenic mice which express normal PrP and partly due to EGFP-PrP^C which is not converted into EGFP-PrP^{Sc} by itself, so that has no effect on the incubation times.

EGFP-PrP transgenic mice represent a unique system for examining the pathogenesis and progression of prion disease *in vivo*. It may be possible to visualize PrP^{Sc} deposition in the brains or other organs of these animals while they are alive and to assess the effects of therapeutic agents. Also, EGFP-PrP can help us to follow

up the trafficking of PrP^{Sc} intracellularly to know the sites of formation, conversion and accumulation of PrP^{Sc} inside the neurons.

4.2. Evaluation of Prion Strains Properties using Transgenic Mice Expressing Human PrP and LL mice

In these experiments, we investigated the different strain properties and transmission efficiencies of different human TSE strains including biological, genetic, pathological and biochemical features of these strains. We used for these studies transgenic mice producing human PrP and infected them with various TSE strains from brains of human cases died from prion diseases. Several properties were investigated including: susceptibility, incubation time, biochemistry, neuropathology and lesion profiles of transgenic mice infected with human prion strains. Also, the effect of the codon-129 polymorphism on human-to-human transmission of different TSE strains by using gene-targeted inbred mice developed by direct replacement of the murine PrP gene for the human gene was investigated. These mice produce human PrP under the control of the normal regulatory elements of murine PrP and these express physiological concentrations of PrP with the correct tissue distribution. Two inbred lines with an identical genetic background were used to express human PrP with the codon-129 MM and VV genotypes, named HuMM and HuVV respectively. Each line differs by only a single codon in *PRNP* and in all other respects the mice were genetically identical.

In general, all the humanized transgenic mice including HuMM and HuVV are susceptible to various TSE strains. Sporadic CJD and variant CJD materials from human cases were transmitted to the humanized transgenic mice either with the MM or VV codon-129 polymorphism with different pathological characteristics for each genotype and a gradation of transmission efficiency from the HuMM to HuVV mice. Two different materials of sCJD from two different human cases were used for infection, types of inoculated materials are sCJD MM1 (a&b) and sCJD MM2 (a&b), also, we used two different materials of vCJD obtained from two different human cases died from vCJD, designated vCJD (a&b).

Higher susceptibility of transgenic humanized mice to different human prion strains of sCJD and vCJD may be attributed to the presence of human PrP transgene in these mice which express human PrP (75,92).

Our results reveal that the incubation times of all HuVV mice are longer than that of HuMM mice infected with human TSE cases either sCJD MM1 or sCJD MM2 or vCJD. The mean incubation times of HuMM mice infected with sCJD MM1 (a&b) are 481.4 ± 61.7 (Mean \pm SD) and 484.3 ± 37 days while the corresponding mean incubation times of HuVV mice infected with the same cases are 585.2 ± 66.5 and 627.6 ± 66.1 days with difference of 103.8 and 143.3 days, respectively (Figures 20) (Tables 12&13).

Similarly, the mean incubation times of HuMM mice infected with sCJD MM2 (a&b) are 514.3 ± 79.1 and 507.1 ± 51.8 days while the corresponding mean incubation times of HuVV mice infected with the same cases are 677.5 ± 54.3 and 578.9 ± 71.2 days, with differences of 163.2 and 71.8 days, respectively. Also, the mean incubation times of HuMM mice infected with vCJD (a&b) are 611.4 ± 112.7 and 551.8 ± 204 days while the corresponding mean incubation times for HuVV mice infected with the same cases are 673.6 ± 116 and 689.2 ± 72.2 days with differences of 62.2 and 137.4 days, respectively (Figures 18-20).

These higher incubation times of prion strains in HuVV mice than in HuMM mice could be attributed to the genetic effect of the codon-129 polymorphism of PrP gene, the genetic background with methionine homozygosity at codon-129 may support the infection to prion strains and conversion of PrP^C into PrP^{Sc}, while the presence of genetic background with valine residue at codon-129 may not support or hinder the infection and conversion of PrP^C into PrP^{Sc}, also, incubation times can vary for other reasons, such as the genotype of the recipient animal, whether or not the recipient is of the same species as that from which the agent come, the route of inoculation and the particular strain of the prion which is involved (106).

Also, our results show that the general mean incubation times of sCJD MM2 are higher than that of sCJD MM1 either in the HuMM or HuVV mice, while these mean incubation times are 510.7 ± 65.5 and 628.2 ± 62.8 days for sCJD MM2 in HuMM and HuVV mice, the corresponding mean incubation times for sCJD MM1 are 482.9 ± 49.4 and 606.4 ± 66.3 days in HuMM and HuVV, respectively (Figures 18&19). We found that the type of the glycoform pattern of PrP has a significant effect on the incubation times of prion diseases even between the TSE strains having the same genetic structure at codon-129 of prion protein gene and we found that type 2 of prion protein glycoform has a prolongation effect on the incubation time when infecting mice (host) either with similar genetic background and codon-129 residue such as HuMM mice or

with different genetic background and codon-129 residue such as HuVV mice. We can say that the prion protein with type 1 glycoform pattern may support the pathogenesis of prion infection and conversion of PrP^C into PrP^{Sc} more than type 2 glycoform (80,106).

In similar manner, our results revealed that the general mean incubation times of vCJD are higher than that of sCJD MM1 and MM2 in either HuMM or HuVV mice, while these mean incubation times are 581.6±158.4 and 681.4±94.1 days for HuMM and HuVV mice infected with vCJD, the mean incubation times are 510.7±65.5, 482.9±49.4 and 628.2±62.8, 606.4±66.3 days for HuMM and HuVV mice infected with sCJD MM2 and sCJD MM1, respectively (Figures 19).

Our interpretation for these higher incubation times of vCJD than that of sCJD MM1 and MM2 in HuMM and HuVV mice is due to relative species barriers which may be stored or still present in newly emerging prion disease vCJD which is thought to originate from bovine prion disease, BSE, and these barriers are completely not present in original human prion strains such as sCJD either MM1 or MM2. We argue that these species barriers are not absolute barriers but relative when we compare between vCJD and sCJD and this in turn could explain the low number of vCJD cases in human population in comparison with sCJD. Prion strain type may affect transmission barriers via an effect on PrP^{Sc} tertiary structure and state of aggregation (12,23,55).

In cerebral cortex there were band-like deposits of synaptic pattern of PrP with presence of some plaque-like aggregates intermixed in layer 3 and more less in layer 6 of neocortex, also, plaque-like deposits were present in linear distribution in the hippocampus especially in oriens, stratum radiatum, stratum lacunosum-molecular and sometimes in granular and polymorphic cell layers of dentate gyrus. Synaptic and coarse deposits were found in the lateral area of the thalamus in the shape triangle, synaptic pattern of PrP distribution were found in molecular and granular layer of cerebellum, scanty or no plaque-like deposits were found in the corpus callosum, basal ganglia and brain stem regions (Figures 24&25). These results are in agreement with other authors who reported the presence of spongiosis, cell death, astrogliosis and synaptic pattern of PrP deposition in the same regions of gray matter in transgenic mice and in human beings affected with the same TSE strains (23,24,146).

Lesion profiles in HuMM mice were more severe and more rapid than in HuVV mice infected with vCJD (a&b) especially with HuMM mice infected with vCJD-a strain (Figure 27). Vacuolation, cell loss and astrogliosis were present in all mice which were more extensive in corpus callosum, basal ganglia, thalamus and medulla and to less extent in cortex and hippocampus. Extensive distribution of synaptic pattern of PrP deposition in all layers of the neocortex, thalamus (in lateral triangle) and hippocampus (stratum oriens, stratum radiatum, stratum lacunosum-moleculare), with little synaptic deposits in basal ganglia, corpus callosum and medulla (Figures 24-26). HuMM mice infected with vCJD-a case showed more severe pathological lesions in the form of kuru plaques which were more extensive in the central raphe of the neocortex, corpus callosum, hippocampus, thalamus and little in basal ganglia and medulla and this distribution of PrP deposits may be because these regions are rich in synapses (76). These kuru plaques consist of pale centers and dark peripheries and are not surrounded by vacuoles (Figure 24). These results are in disagreement with results of others who reported that vCJD strains in HuMM mice result in florid plaques in the hippocampus with eosinophilic core with paler halo and is surrounded by a ring of vacuolation (23).

Biochemical analysis of brain extracts of our mice revealed that PrP of HuMM and HuVV mice infected with sCJD MM1 (a&b) are type 1 glycoform pattern with predominance of diglycosylated form and equal monoglycosylated and unglycosylated forms (Figures 28&29) and these results are consistent with glycoform type of the infecting strain sCJD MM1 and in agreement with other results (6,24,52).

Western blot of brain homogenates of HuMM and HuVV mice infected with sCJD MM2 (a&b) revealed that PrP of HuMM mice infected with sCJD MM2-a is type 2 glycoform with predominance of diglycosylated and monoglycosylated form and weak unglycosylated form, while PrP of HuMM mice infected with sCJD MM2-b and PrP of HuVV mice infected with sCJD MM2 (a&b) are glycoform type 1 with predominance of diglycosylated and monoglycosylated form and weak unglycosylated form. Also, we observed that glycoform percentage of PrP in HuMM mice infected with sCJD MM2-b and PrP in HuVV mice infected with sCJD MM2 (a&b) are similar to glycoform percentage of type 2 PrP in HuMM mice infected with sCJD MM2-a and similar to type 1 in electrophoretic velocity of protein (Figures 28&29) and we can explain this change due to alteration of strain properties in TSE strains upon transmission and

passage from species to another as a type of adaptation or due to the effect of the host on certain new TSE strains (7,11, 52,53,73).

Western blot results of PrP in HuMM and HuVV mice infected with vCJD (a&b) reveal that PrP were type 2 glycoform with predominance of diglycosylated form and equal monoglycosylated and unglycosylated forms in mice infected with vCJD-a case and predominance of diglycosylated and monoglycosylated forms more than unglycosylated form for PrP of mice infected with vCJD-b case and these differences are small and may be due to strain variability of vCJD (6,23,55,92,148,149).

Our results reveal that vCJD can be transmitted to MM and VV individuals and these results are in disagreement with other published data suggesting that VV individuals can not propagate the vCJD biochemical phenotype (149). All PRNP codon-129 MM and VV genotypes are susceptible to vCJD infection: however, aggressive development of pathological lesions of vacuolation and PrP deposition were more rapid in the MM genotype mice. An explanation for this finding might be provided by *in vitro* conversion of recombinant human PrP by BSE and vCJD agents, which has shown that PrP with methionine at position 129 is more efficiently converted than PrP with valine, and that conversion by vCJD is significantly more efficient than by BSE (83). A long incubation time during which PrP^{Sc} is deposited predicts that in human beings infection could be present in all genotypes for a significant period before clinical onset. Incubation periods of more than 30 years have been reported in the human TSE disease kuru (147).

A mutation equivalent to P102L in the human PrP gene, associated with Gerstmann-Sträussler-Scheinker syndrome (GSS) (57), has been introduced into the murine PrP gene by gene targeting. Inbred mice homozygous for this mutation (101LL) were inoculated with brain homogenate from patients who died of Gerstmann-Sträussler-Scheinker syndrome (GSS). All LL mice infected with LL GSS (a&b) cases were susceptible to the disease and developed clinical signs with different incubation times of GSS-a and GSS-b. The mean incubation times for LL mice infected with GSS-a case is 279.9 ± 18 days and for GSS-b strain is 474.3 ± 172 days; incubation times of GSS-b case are longer than that of GSS-a case (Figure 21). Similarly, histopathological examination of these mice reveal that the presence of vacuolation, cell loss and astrogliosis are more abundant in corpus callosum, basal ganglia, thalamus and medulla and less in the neocortex and hippocampus, with no lesions in the cerebellum. Extensive synaptic pattern of PrP deposition in layer 2, 3 and 5 of the

neocortex, basal ganglia, thalamus and medulla with presence of little plaque-like deposits in corpus callosum and medulla, all these lesions are present in LL mice infected with GSS-a case, while lesions in LL mice infected with GSS-b case were different which showed presence of large kuru plaques with pale center and dark periphery in the neocortex, along the entire length of the corpus callosum, basal ganglia, hippocampus and thalamus (Figures 22&23), with the exception of the cerebellum and medulla, spongiosis and astrogliosis are low in all regions (78,79). Biochemical analysis of PrP from brain extracts of LL mice infected with GSS (a&b) cases revealed that PrP are type 1 glycoform with predominance of diglycosylated form and very weak signal of unglycosylated form (Figure 30).

Our findings are in agreement with others who reported higher susceptibility and pathological lesions of vacuolation in thalamus, corpus callosum and medulla, with diffuse PrP deposits in the thalamus, cortical layers and corpus callosum (144). Differences in incubation times and in pathology can be attributed to the different cases of the GSS (a&b) used for infection. The differences between prions may due to different conformations or sequences of PrP^{Sc} which is specified by the recipient to determine the tertiary structure of nascent PrP (1,43,44,73).

The existence of prion strains raises the question of how heritable biological information can be enciphered in a molecule other than nucleic acid. Strains or varieties of prions have been defined by incubation times and the distribution of neuronal vacuolation. Subsequently, the pattern of PrP^{Sc} deposition were found to correlate with vacuolation profiles and these patterns were used also to characterize strains of prions (1,3,20,35,38,39,40).

On the basis of a number of family studies, GSS, linked to the 102L mutation in human PrP, has been described as a genetic disease with an autosomal dominant mode of inheritance and high penetrance (57,145). Introduction of this mutation in situ into one or both of the endogenous murine PrP genes has not resulted in an inheritable spontaneous TSE in mice. Perhaps differences in other amino acids between the mouse and human PrP block the specific effects of the human 102L appearing as a disease in mice (144).

5. Summary

Prions are unprecedented infectious pathogens that cause a group of invariably fatal neurodegenerative diseases mediated by an entirely novel mechanism. Prions are devoid of nucleic acids and seen to be composed exclusively of a modified isoform of PrP designated PrP^{Sc}. The normal, cellular PrP, denoted PrP^C, is converted into PrP^{Sc} through a process whereby a portion of its α -helical and coil structure is refolded into β -sheet. This structural transition is accompanied by profound changes in the physicochemical properties of the PrP and by appearance of pathological lesions.

In the first part of this work, we studied the pathogenesis of prion diseases by using EGFP-PrP transgenic mice expressing a tagged prion protein, EGFP-PrP (Fluorescent protein). By using this fluorescent tagged protein, we could study the pathogenesis and progression of the different prion diseases *in vivo* and *in vitro*; it was possible to visualize the PrP^{Sc} deposition in the brains and other organs of these animals before and after infection with prion strains. Also, EGFP-PrP may help to follow up the localization, colocalization, distribution and trafficking of PrP^{Sc} intra- and extra cellular to know the sites of formation, conversion and accumulation of PrP^{Sc} inside the neurons. Different techniques were used in this study including inoculation of transgenic mice, cell culture, FACS analysis, western blot, histological, immunohistochemical analysis, vibratome microtomy and confocal laser scanning microscopy for imaging of fluorescent prion protein.

Five independent lines of transgenic mice carrying a chimeric EGFP-PrP fusion protein were generated and visualized for the localization of EGFP-PrP in various organs in histological sections. Analysis of these mice was carried out *in vivo* before and after infection. The results showed that three of the five transgenic lines showed similar expression patterns, only varying in intensity of EGFP fluorescence while two lines showed slightly different patterns of EGFP distribution in the brain.

In vitro conversion assay using a mixture of labeled EGFP-PrP and unlabeled wild-type PrP did not result in conversion of EGFP-PrP and results showed that EGFP-PrP was not susceptible to scrapie infection and not converted into EGFP-PrP^{Sc} form. Also, introduction of EGFP-PrP alleles into F-35 mice, could not rescue the deleterious effect of the truncated gene while this defect was completely abrogated with introduction of wild-type murine PrP gene. Analysis of EGFP-PrP mice after

intracerebral infection with scrapie prion RML showed that these mice were susceptible for infection, survival data revealed similar incubation times of EGFP-PrP mice and wild-type mice, with about 150 days, so that the introduction of the EGFP-PrP transgene into wild-type mice had no prolonging or shortening effect on incubation times. Western blot results confirmed that EGFP-PrP can not be converted into a resistant form EGFP-PrP^{Sc}, but it binds physically to the wild-type originated PrP^{Sc}. Histological examination of terminally killed EGFP-PrP mice showed all neuropathological features of prion diseases such as spongiform changes, neuronal loss and neurodegeneration. Immunohistochemistry showed the presence of PrP deposits of the two proteins; wild-type PrP and EGFP-PrP protein bound together and also PrP deposits of EGFP-PrP alone in the same locations of the wild-type PrP, but with low concentrations. Confocal laser scanning microscopy revealed the presence of pathological PrP aggregates distributed throughout the CNS and these aggregates were highly fluorescent with similar localization as wild-type PrP aggregates.

In the second part of this work we studied the strain properties and transmission efficiencies of different human prions such as sporadic CJD, variant CJD and GSS from human cases died from prion diseases, using transgenic mice expressing human PrP and mice with the 101LL mutation, also, we investigated the effect of the codon-129 polymorphism of the PrP gene on susceptibility. Two inbred humanized mouse lines with identical genetic background to express human PrP with the codon-129 MM and VV genotype and one inbred line of LL mice were made. Mice were inoculated intracerebrally with human material of sporadic CJD (MM1&MM2), variant CJD and GSS (only LL mice) and examined for susceptibility, incubation times, western blot, clinical and pathological signs of the disease.

Our results revealed that all mice were susceptible for infection by all human TSE strains with different pathological characteristics for each genotype and gradation of transmission efficiency from HuMM to HuVV mice, also, higher incubation times and extensive pathological lesions in HuVV mice than in HuMM and this may be due to the effect of codon-129 on the incubation times and pathogenesis. There are also alterations in the type of glycoform pattern of some strains.

6. Zusammenfassung

Prionen sind neuartige Krankheitserreger, die zu einer Gruppe von stets tödlichen neurodegenerativen Krankheiten führen. Sie sind nach unserem derzeitigen Wissen frei von Nukleinsäuren und scheinen ausschließlich aus einer modifizierten Isoform des Prionproteins (PrP), PrP^{Sc}, zu bestehen. Die normale physiologische Form des PrP, allgemein als PrP^C bezeichnet, wird durch einen Prozess, bei dem ein Teil der α -helikalen Struktur in ein β -Faltblatt umgeformt wird, in PrP^{Sc} umgewandelt. Dieser strukturelle Übergang wird begleitet von tiefgreifenden Veränderungen in den physikalisch-chemischen Eigenschaften des PrP.

Der erste Teil dieser Arbeit beschäftigt sich mit der Pathogenese der Prionerkrankungen in transgenen Mäusen, die ein mit Enhanced Green Fluorescent Protein (EGFP) markiertes PrP exprimieren (EGFP-PrP). Es sollte damit möglich sein, die Progression der verschiedenen Prionablagerungen im Gehirn und anderen Organen darzustellen, ebenso wie die Kolo-kalisation mit anderen Proteinen zu verfolgen. Für diese Analyse wurden verschiedene Techniken wie die Inokulation von transgenen Mäusen, Zellkultur, FACS und Western Blot Analyse, histologische und immunhistochemische Gewebsanalyse, Vibratome Microtomy und konfokale Laserscanning-Mikroskopie verwendet.

Fünf unabhängige transgene Linien mit chimärem EGFP-PrP Fusionsprotein wurden untersucht. Eine vor Infektion durchgeführte Analyse dieser Mäuse zeigte, dass drei der fünf Linien ein ähnliches Expressionsmuster aufwiesen und sich nur in der Intensität der EGFP Fluoreszenz unterschieden, während zwei Linien ein abweichendes Muster der EGFP Verteilung im Gehirn erkennen ließen.

In vitro Umwandlungsversuche mit Hilfe einer Mischung von markiertem EGFP-PrP und unmarkiertem Wildtyp-PrP zeigten, dass EGFP-PrP nicht in die EGFP-PrP^{Sc} Form umfaltbar ist. Auch die Einführung eines EGFP-PrP Allels in F-35 Mäuse, die ein partiell deletiertes PrP exprimieren und nicht lange überlebensfähig sind, kann den klinischen Phänotyp nicht konvertieren, während dieser Mangel durch die transgene Einführung eines Wildtyp-PrP-Gens aufgehoben wurde. Eine Analyse der EGFP-PrP Mäuse nach intrazerebraler Inokulation mit RML-Scrapie-Prionen zeigte, dass diese Mäuse in der Tat mit Scrapie infizierbar waren; Überlebens-Daten zeigten ähnliche Inkubationszeiten von EGFP-PrP Mäusen und Wildtyp-Mäusen von über 150 Tagen. Western Blot Ergebnisse ergaben, dass das EGFP-PrP auch *in vivo* nicht in die postulierte resistente Form EGFP-PrP^{Sc} konvertiert werden kann; EGFP-PrP

scheint sich an Wildtyp-PrP^{Sc} lediglich anzulagern. Histologische Untersuchungen terminal getöter EGFP-PrP Mäuse zeigten alle neuropathologischen Merkmale von Prion-Erkrankungen wie spongiforme Veränderungen, Verlust von Neuronen und Neurodegeneration. Die immunhistochemische Untersuchung zeigte PrP-Ablagerungen der beiden Proteine. Die Konfokale Laser Scanning Mikroskopie zeigte das Vorhandensein von pathologischen PrP-Aggregaten verteilt im gesamten ZNS; diese Aggregate waren hoch fluoreszierend mit ähnlicher Lokalisation wie Wildtyp PrP^{Sc}-Aggregate.

Im zweiten Teil dieser Arbeit untersuchten wir die Inkubationszeit und Pathogenese der Übertragung verschiedener Formen humaner Prionkrankheiten, nämlich der sporadischen CJD, der varianten CJD und GSS, bei der Übertragung auf transgene Mäusen, die humanes wildtyp-PrP bzw. humanes PrP mit einer 101LL Mutation exprimieren. Dabei wurde der Einfluss des Codon-129 Polymorphismus auf die Übertragbarkeit und das pathologische Ausprägungsmuster beschrieben. Mäuse wurden intrazerebral mit menschlichem Material von Fällen von sporadischer CJD (MM1&MM2), varianter CJD und GSS (nur LL Mäuse) inokuliert.

Unsere Ergebnisse bestätigen, dass alle transgenen Mäuse anfällig für Infektionen durch alle untersuchten menschlichen TSE-Stämme sind. Dabei zeigten sich unterschiedliche pathologische Charakteristika für jeden Codon 129-Genotyp und unterschiedliche Effizienz der Transmission auf HuMM bzw. HuVV Mäuse. Die hier mit Standardfällen herausgearbeiteten bzw. bestätigten Muster stellen jetzt die Grundlage für die Beurteilung atypischer humaner CJD oder GSS Fälle, die für die Beurteilung der schwierigen Frage, ob sich neue humane Prionstämme entwickeln oder entwickelt haben, von großer Bedeutung sein wird.

7. References

- (1) Prusiner, S.B. (1998) Prions. *Proceeding of the National Academy of Science USA* 95, 13363-13383
- (2) Stahl, N. and Prusiner, A.B. (1991) Prions and Prion Proteins. *The Federation of American Societies for Experimental Biology Journal* 5, 2799-2807
- (3) Prusiner, A.B., Scott, M.R., DeArmond, S.J. and Cohen, F.E. (1998) Prion Protein Biology. *Cell* 93, 337-348
- (4) Prusiner, S.B. (1998) The Prion Diseases. *Brain Pathology* 8, 499-513
- (5) Cohen, F.E., Prusiner, S.B. (1998) Pathologic Conformations of Prion Proteins. *Annual Review of Biochemistry* 67, 793-819
- (6) Kretzschmar, H.A. (2002) Prion Diseases. *Encyclopedia of the Human Brain* 5, 47-60
- (7) Collinge, J. (2001) Prion Diseases of Human and Animals: Their Causes and Molecular Basis. *Annual Review of Neuroscience* 24, 519-550
- (8) Griffoni, C., Toni, M., Spisni, E., Bianco, Maria C., Santi, S., Riccio, M. and Tomasi, V. (2003) The Cellular Prion Protein. *Cell Biochemistry and Biophysics* 38, 287-304
- (9) Harris, D.A. (1999) Cellular Biology of Prion Diseases. *Clinical Microbiology Reviews* 12 (3), 429-444
- (10) Ironside, J.W. (1998) Prion Diseases in Man. *Journal of Pathology* 186, 227-234
- (11) Aguzzi, A. and Heppner, F.L. (2000) Pathogenesis of Prion Diseases: a progress report. *Cell Death and Differentiation* 7, 889-902
- (12) Chesebro, B. (2003) Introduction to the transmissible spongiform encephalopathies or prion diseases. *British Medical Bulletin* 66, 1-20
- (13) Mead, S. (2006) Prion Disease Genetics. *European Journal of Human Genetics* 14, 273-281
- (14) Kitamoto, T. and Tateishi, J. (1996) Human Prion Disease and Human Prion Protein Disease. *Current Topics in Microbiology and Immunology* 207 (166p), 27-34
- (15) Knight, R.S.G. and Will, R.G. (2007) Prion Diseases. *Journal of Neurology, Neurosurgery and Psychiatry* 75 (Suppl I), i36-i42
- (16) Taberner, C., Polo, J.M., Sevillano, M.D., Munoz, R., Berciano, J, Cabello, A., Baez, B, Ricoy, J.R., Carpizo, R., Figols, J., Cuadrado, N., Claveria, L.E.

- (2000) Fatal familial insomnia: Clinical, neuropathological, and genetic description of a Spanish family. *Journal of Neurology, Neurosurgery and Psychiatry* 68, 774-777
- (17) Prusiner, S.B. (1996) Molecular biology and pathogenesis of prion diseases. *Trends In Biochemical Sciences* 21, 482-487
- (18) Prusiner, S.B. (1994) Biology and Genetics of Prion Diseases. *Annual Reviews of Microbiology* 48, 655-686
- (19) Prusiner, S.B. and DeArmond, S.J. (1994) Prion Diseases and Neurodegeneration. *Annual of Review of Neurosciences* 17, 311-339
- (20) Prusiner, S.B. (1997) Prion Diseases and The BSE Crisis. *Science* 278 (5336), 245-251
- (21) Fisher, M, Rüllicke, T., Raeber, A., Sailer, A., Moser, M., Oesch, B., Brandner, S., Aguzzi, A. and Weissmann, C. (1996) Prion protein (PrP) with amino-proximal deletions restoring susceptibility of PrP knockout mice to scrapie. *The European Molecular Biology Organization Journal* 15(6), 1255-1264
- (22) Shmerling, D., Hegyi, I., Fisher, M., Blätter, T., Brandner, S., Götz, J., Rüllicke, T., Flechsig, E., Cozzio, A., Mering, C., Hangartner, C., Aguzzi, A., Weissmann, C. (1998) Expression of Amino-Terminally Truncated PrP in the Mouse Leading to Ataxia and Specific Cerebellar Lesions. *Cell* 93, 203-214
- (23) Bishop, M.T., Hart, P., Aitchison, L., Baybutt, H.N., Plinston, C., Thomson, V., Tuzi, N.L., Head, M.W., Ironside, J.W., Will, R.G. and Manson, J.C. (2006) Predicting susceptibility and incubation time of human-to-human transmission of vCJD. *Lancet Neurology* 5, 393-398
- (24) Parchi, P., Giese, A., Capellari, S., Brown, P., Schulz-Schaeffer, W., Windl, O., Zerr, I., Budka, H., Kopp, N., Piccardo, P., Poser, S., Rojiani, A., Streichemberger, N., Julien, J., Vital, C., Ghetti, B., Gambetti, P., Kretzschmar, H.A. (1999) Classification of Sporadic Creutzfeldt-Jacob Disease Based On Molecular and Phenotypic Analysis of 300 Subjects. *Annals of Neurology* 46 (2), 224-233
- (25) Borchelt, D.R., Scottt, M., Taraboulos, A., Stahl, N., Prusiner, S.B. (1990) Scrapie and Cellular Prion Proteins Differ in Their Kinetics of Synthesis and Topology in Cultured Cells. *The Journal of Cell Biology* 110, 743-752
- (26) Borchelt, D.R., Taraboulos, A., Prusiner, S.B. (1992) Evidence for Synthesis of Scrapie Prion Proteins in the Endocytic Pathway. *The Journal of Biological Chemistry* 267 (23), 16188-16199
- (27) Cauphey, B., Race, R.E., Ernst, D., Buchmeier, M.J. and Chesebro, B. (1989) Prion Protein Biosynthesis in Scrapie-Infected and Uninfected Neuroblastoma Cells. *Journal of Virology* 63 (1), 175-181

- (28) Cauphey, B. and Raymond, G.J. (1991) The Scrapie-associated Form of PrP Is Made from a Cell Surface Precursor That Is Both Protease- and Phospholipase-sensitive. *The Journal of Biological Chemistry* 266 (27), 18217-18223
- (29) Cauphey, B.H., Dong, A., Bhat, K.S., Ernst, D., Hayes, S.F. and Cauphey, W.S. (1991) Secondary Structure Analysis of the Scrapie-Associated Protein PrP 27-30 in Water by Infrared Spectroscopy. *Biochemistry* 30, 7672-7680
- (30) Gasset, M., Baldwin, M.A., Fletterick, R.J. and Prusiner, S.A. (1993) Perturbation of the secondary structure of the scrapie prion protein under conditions that alter infectivity. *Proceedings of the National Academy of Science USA* 90, 1-5
- (31) Pan, K-M, Baldwin, M., Nguyen, J., Gasset, M., Serban, A., Groth, D., Mehlhorn, I., Huang, Z., Fletterick, R.J., Cohen, F.E. (1993) Conversion of α -helices into β -sheets features in the formation of the scrapie prion proteins. *Proceedings of the National Academy of Science USA* 90, 10962-10966
- (32) Bruce, M.E. and Dickinson, A.G. (1987) Biological Evidence that Scrapie agent Has an Independent Genome. *Journal of General Virology* 68, 79-89
- (33) Kimberlin, R.H., Cole, S., Walker, C. (1987) Temporary and Permanent Modifications to a Single Strain of Mouse Scrapie on Transmission to Rats and Hamsters. *Journal General Virology* 68, 1875-1881
- (34) Kimberlin, R.H., Walker, C. A., Fraser, H. (1989) The genomic Identity of Different Strains of Mouse Scrapie Is Expressed in Hamsters and Preserved on Reisolation in Mice. *Journal General Virology* 70, 2017-2025
- (35) DeArmond, S.J., Yang, S-L, Lee, A., Bowler, R., Taraboulos, A., Groth, D., Prusiner, S.B. (1993) Three scrapie prion isolates exhibit different accumulation patterns of the prion protein scrapie isoform. *Proceedings of the National Academy of Science USA* 90, 6449-6453
- (36) Prusiner, S.B., Groth, D., Serban, A., Koehler, R., Foster, D., Torchia, M., Burton, D., Yang, S-L, DeArmond, S.J. (1993) Ablation of the prion protein (PrP) gene in mice prevents scrapie and facilitates production of anti-PrP antibodies. *Proceedings of the National Academy of Science USA* 90, 10608-10612
- (37) Bruce, M.E., McBride, P.A., Farquhar, C.F. (1989) Precise targeting of the pathology of the sialoglycoprotein, PrP, and vacuolar degeneration in mouse scrapie. *Neuroscience Letters* 102, 1-6
- (38) Dickinson, A.G., Meikle, V.M.H., Fraser, H. (1968) Identification Of A Gene Which Controls The Incubation Period of some Strains of Scrapie Agent In Mice. *Journal of Comparative Pathology* 78, 293-299

- (39) Fraser, H., Dickinson, A.G. (1973) Scrapie In Mice: Agent-Strain Differences In The Distribution And Intensity Of Grey Matter Vacuolation. *Journal of Comparative Pathology* 83, 29- 40
- (40) Hecker, R., Taraboulos, A., Scott, M., Pan, K-M, Yang, S-L, Torchia, M., DeArmond, S.J., Prusiner, S.B. (1992) Replication of distinct scrapie prion isolates is region specific in brains of transgenic mice and hamsters. *Genes & Development* 6, 1213-1228
- (41) Bessen, R.A., Marsh, R.F. (1992) Biochemical and Physical Properties of the Prion Protein from two Strains of the Transmissible Mink Encephalopathy Agent. *Journal of Virology* 66 (4), 2096-2101
- (42) Goldfarb, L.G., Peterson, R.B., Tabaton, M., Brown, P., LeBlanc, A.C., Montagna, P., Cortelli, P., Wills, P.R., Hauw, J.J., McKeever, P.E., Monari, L., Schrank, B., Swergold, G.D., Autilio-Gambetti, L., Gajdusek, D.C., Lugaresi, E., Gambetti, P. (1992) Fatal Familial Insomnia and Familial Creutzfeldt-Jakop Disease: Disease Phenotype Determined by a DNA Polymorphism. *Science* 258, 806-808
- (43) Prusiner, S.B. (1992) Chemistry and Biology of Prions. *Biochemistry* 31 (49),
- (44) Prusiner, S.B. (1991) Molecular Biology of Prion Diseases. *Science* 252, 1515-1522
- (45) Scott, M., Foster, D., Miranda, C., Serban, D., Coufal, F., Wälchli, M., Torchia, M., Groth, D., Carlson, G., DeArmond, S.J., Westaway, D., Prusiner, S.B. (1989) Transgenic Mice Expressing Hamster Prion Protein Produce Species-Specific Scrapie Infectivity and Amyloid Plaques. *Cell* 59, 847-857
- (46) Stahl, N., Borchelt, D.R., Hsiao, K., Prusiner, S.B. (1987) Scrapie Prion Protein Contains a Phosphatidylinositol Glycolipid. *Cell* 51, 229-240
- (47) Taraboulos, A., Rogers, M., Borchelt, D.R., McKinley, M.P., Scott, M., Serban, D., Prusiner, S.B. (1990) Acquisition of protease resistance by prion proteins in a scrapie-infected cell does not require asparagine-linked glycosylation. *Proceedings of the National Academy of Science USA* 87, 8262-8266
- (48) Bolton, D.C., McKinley, M.P., Prusiner, S.B. (1982) Identification of a Protein That Purifies with the Scrapie Prion. *Science* 218, 1309-1311
- (49) Bruce, M.E., Will, R.G., Ironside, J.W., McConnell, I., Drummond, D., Suttie, A., McCardle, L., Chree, A., Hope, J., Birkett, C., Cousens, S., Fraser, H., Bostock, C.J. (1997) Transmissions to mice indicate that 'new variant' CJD is caused by the BSE agent. *Nature* 389, 498-501
- (50) Poulter, M., Baker, H.F., Frith, C.D., Leach, M., Lofthouse, R., Ridley, R.M., Shah, T., Owen, F., Collinge, J., Brown, J., Hardy, J., Mullan, M.J., Harding, A.E., Bennett, C., Doshi, R., Crow, T.J. (1992) Inherited Prion Disease With

- 144 Base Pair Gene Insertion: 1. Genealogical and Molecular Studies. *Brain* 115, 675-685
- (51) Collinge, J., Palmer, M.S., Sidle, K.C.L., Hill, A.F., Gowland, I., Meads, J., Asante, E., Bradley, R., Doey, L.J and Lantos, P.L. (1995) Unaltered susceptibility to BSE in transgenic mice expressing human prion protein. *Nature* 378, 779-783
- (52) Collinge, J, Sidle, K.C.L., Meads, J., Ironside, J., Hill, A.F. (1996) Molecular analysis of prion strain variation and the etiology of 'new variant' CJD. *Nature* 383, 685-690
- (53) Collinge, S.B., Collinge, J, Jefferys, J.G.R. (1996) Hippocampal slices from prion protein null mice: disrupted Ca^{2+} -activated K^+ currents. *Neuroscience Letters* 209, 49-52
- (54) Collinge, J., Owen, F., Poulter, M., Leach, M., Crow, T.J., Rossor, M.N., Hardy, J., Mullan, M.J., Janota, I, Lantos, P.L. (1990) Prion dementia without characteristic pathology. *The Lancet* 336, 7-9
- (55) Hill, A.F., Disbruslais, M., Joiner, S., Sidle, K.C.L., Gowland, I., Collinge, J. (1997) The same prion strain causes vCJD and BSE. *Nature* 389, 448-450
- (56) Hill, A.F., Butterworth, R.J., Joiner, S., Jackson, G., Rossor, M.N., Thomas, D.J., Frosh, A., Tolley, N., Bell, J.E., Spencer, M., King, A., Al-Sarraj, S., Ironside, J.W., Lantos, P.L., Collinge, J. (1999) Investigation of variant Creutzfeldt-Jakob disease and other human prion diseases with tonsil biopsy samples. *The Lancet* 353, 183-189
- (57) Hsiao, K., Baker, H.F., Crow, T.J., Poulter, M., Owen, F., Terwilliger, J.P., Westaway, D., Ott, J., Prusiner, S.B. (1989) Linkage of a prion protein missense variant to Gerstmann-Sträussler Syndrome. *Nature* 338, 342-345
- (58) Zeidler, M., Stewart, G.E., Barraclough, C.R., Bateman, D.E., Bates, D., Burn, D.J., Colchester, A.C., Durward, W., Fletcher, N.A., Hawkins, S.A., Mackenzie, J.M., Will, R.G. (1997) New variant Creutzfeldt-Jakob disease: neurological features and diagnostic tests. *The Lancet* 350, 903-907
- (59) Hsiao, K.K., Scott, M., Foster, D., Groth, D.F., DeArmond, S.J., Prusiner, S.B. (1990) Spontaneous Neurodegeneration in Transgenic Mice with Mutant Prion Protein. *Science* 250, 1587-1590
- (60) Kitamoto, T., Lizuka, R., Tateishi, J. (1993) An Amber Mutation of Prion Protein In Gerstmann-Sträussler Syndrome with Mutant PrP Plaques. *Biochemical and Biophysical Research Communications* 192 (2), 525-531
- (61) Kitamoto, T., Ohta, M., Doh-ura, K., Hitoshi, S., Terao, Y., Tateishi, J. (1993) Novel Missense Variants of Prion Protein in Creutzfeldt - Jakob disease or Gerstmnn-Sräussler Syndrome. *Biophysical Research Communications* 191 (2), 709-714

- (62) McKinley, M., Bolton, D.C., Prusiner, S.B. (1983) A Protease-Resistant Protein is a Structural Component of the Scrapie Prion. *Cell* 35, 57-62
- (63) Sparkes, R.S., Simon, M., Cohn, V.H., Fournier, R.E.K., Lem, J., Klisak, I., Heinzmann, C., Blatt, C., Lucero, M., Mohandas, T., DeArmond, S.J., Westaway, D., Prusiner, S.B. (1986) Assignment of the human and mouse prion protein genes to homologous chromosomes. *Proceedings of the National Academy of Science USA* 83, 7358-7362
- (64) Aguzzi, A. (1996) Between cows and monkeys. *Nature* 381, 734-735
- (65) Büeler, H., Aguzzi, A., Sailer, A., Greiner, R.A., Autenried, P., Aguet, M., Weissmann, C. (1993) Mice Devoid of PrP are Resistant to Scrapie. *Cell* 73, 1339-1347
- (66) Telling, G.C., Scott, M., Masterianni, J., Gabizon, R., Torchia, M., Cohen, F.E., DeArmond, S.J., Prusiner, S.B. (1995) Prion Propagation in Mice Expressing Human and Chimeric PrP Transgenes Implicates the Interaction of Cellular PrP with Another Protein. *Cell* 83, 79-90
- (67) Jarrett, J.T. and Lansbury, P.T. (1993) Seeding "One-Dimensional Crystallization" of Amyloid: A Pathogenic Mechanism in Alzheimer's Disease and Scrapie? *Cell* 73, 1055-1058
- (68) Kocisko, D.A., Priola, S.A., Raymond, G.J., Chesebro, B., Lansbury, P.T., Cauphey, B. (1995) Species specificity in the cell-free conversion of prion protein to protease-resistant forms: A model for the scrapie species barrier. *Proceedings of the National Academy of Science USA* 92, 3923- 3027
- (69) Kocisko, D.A., Lansbury, P.T., Cauphey, B. (1996) Partial Unfolding and Refolding of Scrapie-Associated Prion Protein: Evidence for a Critical 16-KDa C-Terminal Domain. *Biochemistry* 35, 13434-13442
- (70) Bessen, R.A., Kocisko, D.A., Raymond, G.J., Nandan, S., Lansbury, P.T., Cauphey, B. (1995) Non-genetic propagation of strain-specific properties of scrapie prion protein. *Nature* 375, 698-700
- (71) Bessen, R.A., Raymond, G.J., Cauphey, B. (1997) In Situ Formation of Protease-Resistant Prion Protein in Transmissible Spongiform Encephalopathy-Infected Brain Slices. *The Journal of Biological Chemistry* 272 (24), 15227-15231
- (72) DeArmond, S.J., Sanchez, H., Yehiely, F., Qiu, Y., Ninchak-Casey, A., Daggett, V., Camerino, A.P., Cayetano, J., Rogers, M., Groth, D., Torchia, M., Tremblay, P., Scott, M.R., Cohen, F.E., Prusiner, S.B. (1997) Selective Neuronal Targeting in Prion Disease. *Neuron* 19, 1337-1348
- (73) Bessen, R.A. and Marsh, R.F. (1994) Distinct PrP Properties Suggest the Molecular Basis of Strain Variation in Transmissible Mink Encephalopathy. *Journal of Virology* 68 (12), 7859-7868

- (74) Prusiner, S.B. (1997) Prion Diseases and the BSE Crisis. *Science* 278, 245-251
- (75) Prusiner, S.B., Scott, M., Foster, D., Pan, K-M, Groth, D., Mirenda, C., Torchia, M., Yang, S-L, Serban, D., Carlson, G.A., Hoppe, P.C., Westaway, D., DeArmond, S.J. (1990) Transgenic Studies Implicate Interactions between Homologous PrP Isoforms in Scrapie Prion Replication. *Cell* 63, 673-686
- (76) Barmada, S., Piccardo, P., Yamaguchi, K., Ghetti, B., Harris, D.A. (2004) GFP-tagged prion protein is correctly localized and functionally active in brains of transgenic mice. *Neurobiology of Disease* 16, 527-537
- (77) Barmada, S. and Harris, D.A. (2005) Visualization of Prion Infection in Transgenic Mice Expressing Green Fluorescent Protein-Tagged Prion Protein. *The Journal of Neuroscience* 25 (24), 5824-5832
- (78) Masters, C.L., Gajdusek, D.C., Gibbs, C.J. (1981) Creutzfeldt-Jakob Disease Virus Isolations from the Gerstmann-Sträussler Syndrome with Analysis of the Various Forms of Amyloid Plaque Deposition in the Virus-induced Spongiform Encephalopathies. *Brain* 104, 559-588
- (79) Masters, C.L., Gajdusek, D.C., Gibbs, C.J. (1981) The Familial Occurrence of Creutzfeldt - Jakob disease and Alzheimer's disease. *Brain* 104, 535-558
- (80) Prusiner, S.B., (1991) Molecular Biology of Prion Diseases. *Science* 252, 1515-1522
- (81) Peretz, D., Williamson, R.A., Matsunaga, Y., Serban, H., Pinilla, C., Bastidas, R.B., Rozenshteyn, R., James, T.L., Houghten, R.A., Cohen, F.E., Prusiner, S.B., Burton, D.R. (1997) A Conformational Transition at the N Terminus of the Prion Protein Features in Formation of the Scrapie Isoform. *Journal of Molecular Biology* 273, 614-622
- (82) Kaneko, K., Zulianello, L., Scott, M., Cooper, C.M., Wallace, A.C., James, T.L., Cohen, F.E., Prusiner, S.B. (1997) Evidence for protein X binding to a discontinuous epitope on the cellular prion protein during scrapie prion propagation. *Proceedings of the National Academy of Science USA* 94, 10069-10074
- (83) Raymond, G.J., Hope, J., Kocisko, D.A., Priola, S.A., Raymond, L.D., Bossers, A., Ironside, J., Will, R.G., Chen, S.G., Peterson, R.B., Gambetti, P., Rubenstein, R., Smits, M.A., Lansbury, P.T., Cauphey, B. (1997) Molecular assessment of the potential transmissibilities of BSE and scrapie to humans. *Nature* 388, 285-288
- (84) Gajdusek, D.C., Gibbs, C.J., Alpers, M. (1966) Experimental Transmission of a Kuru-like Syndrome to Chimpanzees. *Nature* 209 (5025), 794-796

- (85) Gajdusek, D.C. and Gibbs, C.J. (1971) Transmissin of Two Subacute Spongiform Encephalopathies of Man (Kuru and Creutzfeldt - Jakob disease) to New World Monkeys. *Nature* 230, 588-591
- (86) Will, R.G. (1993) Epidemiology of Creutzfeldt-Jakob disease. *British Medical Bulletin* 49 (4), 960-970
- (87) Guiroy, D.C., Yanagihara, R., Gajdusek, D.C. (1991) Localization of amyloidogenic proteins and sulfated glycosaminoglcans in nontransmissible and transmissible cerebral amyloidoses. *Acta Neuropathologica* 82, 87-92
- (88) Pocchiari, M. (1994) Spongiform Encephalopathies: An Introduction to the Mysterious Etiological Agent. *Molecular Aspects of Medicine* 15 (3), 195-291
- (89) Lasmezas, C.I., Deslys, J.P., DEmaimay, R., Adjou, K.T., Lamoury, F., Dormont, D., Robain, O., Ironside, J., Hauw, J.J. (1996) BSE transmission to macaques. *Nature* 381, 743-744
- (90) Lasmezas, C.I., Fournier, J.G., Nouvel, V., Boe, H., Marce, D., Lamoury, F., Kopp, N., Hauw, J.J, Ironside, J., Bruce, M., Dormont, D., Deslys, J.P. (2001) Adaptation of the bovine spongiform encephalopathy agent to primates and comparison with Creutzfeldt-Jacob disease: Implications for human health. *Proceedings of the National Academy of Science USA* 98 (7), 4142- 4147
- (91) Telling, G.C., Scott, M., Hsiao, K.K., Foster, D., Yang, S-L, Torchia, M., Sidle, K.C.L., Collinge, J., DeArmond, S.J., Prusiner, S.B. (1994) Transmission of Creutzfeldt-Jacob disease from humans to transgenic mice expressing chimeric human-mouse prion protein. *Proceedings of the National Academy of Science USA* 91, 9936-9940
- (92) Asante, E.A., Linehan, J.M., Desbruslais, M., Joiner, S., Gowland, I., Wood,A.L., welch, J., Hill, A.F., Lioyd, S.E., Wadsworth, J.D.F., Collinge, J. (2002) BSE prions propagatate as either variant CJD-like or sporadic CJD-like prion strains in transgenic mice expressing human prion protein. *The EMBO Journal* 21 (23), 6358-6366
- (93) Calzolari, L., Lysek, D., Güntert, P., Schroetter, C., Riek, R., Zahn, R., Wüthrich, K. (2000) NMR structures of three single-residue variants of the human prion protein. *Proceedings of the National Academy of Science USA* 97 (15), 8340-8345
- (94) Garcia, F.L., Zahn, R., Riek, R., Wüthrich, K. (2000) NMR structure of the bovine prion protein. *Proceedings of the National Academy of Science USA* 97 (15), 8334-8339
- (95) Chiesa, R., Piccardo, P., Ghetti, B., Harris, D.A. (1998) Neurological Illness in Transgenic Mice Expressing a Prion Protein with an Insertional Mutation. *Neuron* 21, 1339-1351

- (96) Prusiner, S.B., Telling, G., Cohen, F.E., DeArmond, S.J. (1996) Prion disease of humans and animals. *Seminars in Virology* 7, 159-173
- (97) Parchi, P., Chen, S.G., Brown, P., Zou, W., Capellari, S., Budka, H., Hainfellner, J., Reyes, P.F., Golden, G.T., Hau, J.J., Gajdusek, D.C., Gambetti, P. (1998) Different patterns of truncated prion protein fragments correlate with distinct phenotypes in P102L Gerstmann-Sträussler-Scheinker disease. *Proceedings of the National Academy of Science USA* 95, 8322-8327
- (98) Peden, A.H., Head, M.W., Richie, D.L., Bell, J.E., Ironside, J.W. (2004) Preclinical vCJD after blood transfusion in a PRNP codon 129 heterozygous patient. *The Lancet* 364, 527-529
- (99) Palmer, M.S., Dryden, A.J., Hughes, J.T., Collinge, J. (1991) Homozygous prion protein genotype predisposes to sporadic Creutzfeldt-Jacob disease. *Letters To Nature* 352, 340-342
- (100) Almer, G., Hainfellner, J.A., Brücke, T., Jellinger, K., Kleinert, R., Bayer, G., Windl, O., Kretschmar, H.A., Hill, A., Sidle, K., Collinge, J., Budka, H. (1999) Fatal familial insomnia: a new Austrian family. *Brain* 112, 5-16
- (101) Taraboulos, A., Scott, M., Semenov, A., Avrahm, D., Laszlo, L., Prusiner, S.B. (1995) Cholesterol Depletion and Modification of COOH-Terminal Targeting Sequence of the Prion Protein Inhibit Formation of the Scrapie Isoform. *The Journal of Cell Biology* 129 (1), 121-132
- (102) Scott, M., Groth, D., Foster, D., Torchia, M., Yang, S-L, DeArmond, S.J., Prusiner, S.B. (1993) Propagation of Prions with Artificial Properties in Transgenic Mice Expressing Chimeric PrP Genes. *Cell* 73, 979-988
- (103) Cousens, S.N., Vynnycky, E., Zeidler, M., Will, R.G., Smith, P.G. (1997) Predicting the CJD epidemic in humans. *Nature* 385, 197-198
- (104) Collinge, J., Poulter, M., Davis, M.B., Baraitser, M., Qwen, F., Crow, T.J., Harding, A.E. (1991) Presymptomatic Detection or Exclusion of Prion Protein Gene Defects in Familis with Inherited Prion Diseases. *American Journal of Human Genetics* 49, 1351-1354
- (105) Hsiao, K., Dlouhy, S.R., Farlow, M.R., Cass, C., Costa, M., Conneally, P.M., Hodes, M.E., Ghetti, B., Prusiner, S.B. (1992) Mutant prion proteins in Gerstmann-Sträussler-Scheinker disease with neurofibrillary tangles. *Nature genetics* 1, 68-71
- (106) Dicknison, A.G. (1968) Some Factors Controlling The Incidence Of Scrapie In Sheep Injected With A Cheviot-Passaged Scrapie Agent. *Journal of Comparative Pathology* 78, 313-321
- (107) Towbin, H., Staehelin, T., Gordon, J. (1979) Electrophoretic transfer of proteins from polyacrylamide gels to nitrocellulose sheets: Procedure and

some applications. Proceedings of the National Academy of Sciences USA 76 (9), 4350-4354

- (108) Saiki, R.K., Gelfand, D.H., Stoffel, S., Scharf, S.J., Higuchi, R., Horn, G.T., Mullis, K.B., Erlich, H.A. (1988) Primer-Directed Enzymatic Amplification of DNA with a Thermostable DNA Polymerase. *Science* 239, 487-491
- (109) Lee, V.M-L, Goedert, M., Trojanowski, J.Q. (2001) Neurodegenerative Tauopathies. *Annual Review of Neurosciences* 24 (1), 121-159
- (110) Jeffery, M., Goodsir, C.M., Bruce, M.E., McBride, P.A., Scott, J.R., Halliday, W.G. (1992) Infection specific prion protein (PrP) accumulates on neuronal plasmalemma in scrapie infected mice. *Neuroscience Letters* 147, 106-109
- (111) Jeffery, M., Goodsir, C.M., Bruce, M.E., McBride, P.A., Fowler, N., Scott, J.R. (1994) Murine scrapie-infected neurons in vivo release excess prion protein into the extracellular space. *Neuroscience Letters* 174, 39-42
- (112) DeArmond, S.J., McKinley, M.P., Barry, R.A., Braunfeld, M.B., McColloch, J.R., Prusiner, S.B. (1985) Identification of Prion Amyloid Filaments in Scrapie-Infected Brain. *Cell* 41, 221-235
- (113) DeArmond, S.J. (2004) Discovering the Mechanisms of Neurodegeneration in Prion Diseases. *Neurochemical Research* 29 (11), 1979-1998
- (114) Arnold, J.E., Tipler, C., Laszlo, L., Hope, J., London, M., Mayer, J. (1995) The Abnormal Isoform Of The Prion Protein Accumulates In Late-Endosome-Like Organelles In Scrapie-Infected Mouse Brain. *Journal of Pathology* 176, 403-411
- (115) Fournier, J.G., Escaig-Haye, F., Grigoriev, V. (2000) Ultrastructural Localization of Prion Proteins: Physiological and Pathological Implications. *Microscopy Research and Technique* 50, 76-88
- (116) Kovacs, G.G., Puopolo, M., Ladogana, A., Pocchiari, M., Budka, H., Dijn, C., Collins, S.J., Boyd, A., Giulivi, A., Coulthart, M., Delasnerie-Lauorette, N., Brandel, J.P., Zerr, I., Kretzschmar, H.A., Pedro-Cuesta, J., Calero-Lara, M., Glatzel, M., Aguzzi, A., Bishop, M., Knight, R., Belay, G., Will, R., Mitrova, E. (2005) Genetic prion disease: the EUROCD experience. *Human Genetics* 118, 166-174
- (117) Herms, J., Tings, T., Gall, S., Madlung, A., Giese, A., Siebert, H., Schürmann, P., Windl, O., Brose, N., Kretzschmar, H.A. (1999) Evidence of Presynaptic Location and Function of the Prion Protein. *The Journal of Neuroscience* 19 (20), 8866-8875
- (118) Ivanova, L., Barmada, S., Kummer, T., Harris, D.A. (2001) Mutant Prion Proteins Are Partially Retained in the Endoplasmic Reticulum. *The Journal of Biological Chemistry* 276 (45), 42409-42421

- (119) Laine, J., Marc, M-E, Sy, M-S, Axelrad, H. (2001) Cellular and subcellular morphological localization of normal prion protein in rodent cerebellum. *European Journal of Neuroscience* 14, 47-56
- (120) Liu, T., Zwingman, T., Li, R., Pan, T., Wong, B-S, Peterson, R.B., Gambetti, P., Herrup, K., Sy, M-S (2001) Differential Expression of cellular prion protein in mouse brain as detected with multiple anti-PrP monoclonal antibodies. *Brain Research* 896, 118-129
- (121) Lorenz, H., Windl, O., Kretzschmar, H.A. (2002) Cellular Phenotyping of Secretory and Nuclear Prion Proteins Associated with Inherited Prion Diseases. *The Journal of Biological Chemistry* 277 (10), 8508-8516
- (122) Ma, J., Lindquist, S. (2001) Wild-type PrP and a mutant associated with prion disease are subject to retrograde transport and proteasome degradation. *Proceedings of National Academy of Sciences USA* 98 (26), 14955-14960
- (123) Ma, J., Lindquist, S. (2002) Conversion of PrP to a Self-Perpetuating PrP^{Sc}-like Conformation in the Cytosol. *Science* 298, 1785-1788
- (124) Ma, J., Wollmann, R., Lindquist, S. (2002) Neurotoxicity and Neurodegeneration When PrP Accumulates in the Cytosol. *Science* 298, 1781-1785
- (125) Magalhaes, A.C., Silva, J.A., Lee, K.S., Martins, V.R., Prado, V.F., Ferguson, S.S.G., Gomez, M.V., Brentani, R.R., Prado, M.A.M. (2002) Endocytic Intermediates Involved with the Intracellular Trafficking of a Fluorescent Cellular Prion Protein. *The Journal of Biological Chemistry* 277 (36), 33311-33318
- (126) Mayor, S. and Maxfield, F.R. (1995) Insolubility and Redistribution of GPI-anchored Proteins at the Cell Surface after Detergent Treatment. *Molecular Biology of the Cell* 6, 929-944
- (127) Mayor, S., Rothberg, K.G., Maxfield, F.R. (1994) Sequestration of GPI-Anchored Proteins in Caveolae Triggered by Cross-Linking. *Science* 264, 1948-1951
- (128) Mironov, A., Latawiec, D., Wille, H., Bouzamondo-Bernstein, E., Legname, G., Williamson, R.A., Burton, D., DeArmond, S.J., Prusiner, S.B., Peters, P.J. (2003) Cytosolic Prion Protein in Neurons. *The Journal of Neuroscience* 23 (18), 7183-7193
- (129) Moya, K.L., Sales, N., Hässig, R., Creminon, C., Grassi, J., Giamberardino, L.D. (2000) Immunolocalization of the Cellular Prion Protein in Normal Brain. *Microscopy Research and Technique* 50, 58-65
- (130) Moya, K.L., Hässig, R., Creminon, C., Laffont, I., Giamberardino, L.D. (2004) Enhanced detection and retrograde axonal transport of PrP^C in peripheral nerve. *Journal of Neurochemistry* 88, 155-160

- (131) Negro, A., Ballarin, C., Bertoli, A., Massimino, M.L., Sorgato, M.C. (2001) The Metabolism and Imaging in Live Cells of the Bovine Prion Protein in Its Native Form or Carrying Single Amino Acid Substitutions. *Molecular and Cellular Neuroscience* 17, 521-538
- (132) Sales, N., Rodolfo, K., Hässig, R., Faucheux, B., Giamberardino, L.D., Moya, K.L. (1998) Cellular prion protein localization in rodent and primate brain. *European Journal of Neuroscience* 10, 2464-2471
- (133) Yedidia, Y., Horonchik, L., Tzaban, S., Yanai, A., Taraboulos, A. (2001) Proteasomes and ubiquitin are involved in the turnover of the wild-type prion protein. *The European Molecular Biology Organization Journal* 20 (19), 5383-5391
- (134) Lemaire-Vieille, C., Schulze, T., Podevin-Dimster, V., Follet, J., Bailly, Y., Blanquet-Grossard, F., Decavel, J-P, Heinen, E., Cesbron, J-Y (2000) Epithelial and endothelial expression of the green fluorescent protein reporter gene under the control of bovine prion protein (PrP) gene regulatory sequences in transgenic mice. *Proceedings of National Academy of Sciences USA* 97 (10), 5422-5427
- (135) Giaccone, G., Tagliavini, F., Verga, L., Frangione, B., Farlow, M.R., Bugiani, O., Ghetti, B. (1999) Neurofibrillary tangles of the Indiana Kindred of Gerstmann-Sträussler-Scheinker disease share antigenic determinants with those of Alzheimer disease. *Brain Research* 530, 325-329
- (136) Collinge, J., Harding, A.E., Owen, F., Poulter, M., Lofthouse, R., Boughey, A.M., Shah, T., Crow, T.J. (1989) Diagnosis of Gerstmann-Sträussler Syndrome in Familial Dementia With Prion Protein Gene Analysis. *The Lancet* Juli 1, 15-17
- (137) Beringue, V., Mallinson, G., Kaiser, M., Tayebi, M., Sattar, Z., Jackson, G., Anstee, D., Collinge, J., Hawke, S. (2003) Regional heterogeneity of cellular prion protein isoforms in the mouse brain. *Brain* 126, 2065-2073
- (138) Borchelt, D.R., Kolatsos, V.E., Guarnieri, M., Pardo, C.A., Sisodia, S.S., Price, D.L. (1994) Rapid Anterograde Axonal Transport of the Cellular Prion Glycoprotein in the Peripheral and Central Nervous Systems. *The Journal of Biological Chemistry* 269 (20), 14711-14714
- (139) Courtoy, P.J., Picton, D.H., Farquhar, M.G. (1983) Resolution and Limitations of the Immunoperoxidase Procedure in the Localization of Extracellular Matrix Antigens. *The Journal of Histochemistry and Cytochemistry* 31 (7), 945-951
- (140) Dotti, C.G., Parton, R.G., Simons, K. (1991) Polarized sorting of glypiated proteins in hippocampal neurons. *Letters to Nature* 349, 158-161
- (141) Drisaldi, B., Stewart, R.S., Adles, C., Stewart, L.R., Quaglio, E., Biasini, E., Fioriti, L., Chiesa, R., Harris, D.A. (2003) Mutant PrP Is Delayed in Its Exit from the Endoplasmic Reticulum, but Neither Wild-type nor Mutant PrP

Undergoes Retrotranslocation Prior to Proteasomal Degradation. The Journal of Biological Chemistry 278 (24), 2732-21743

- (142) Ford, M.J., Burton, L.J., Li, H., Graham, C.H., Frobert, Y., Grassi, J., Hall, S.M., Morris, R.J. (2002) A Marked Disparity Between The Expression of Prion Protein And Its Message By Neurons Of The CNS. Neuroscience 11 (3), 533-551
- (143) Haeberle, A.M., Ribaut-Barassin, C., Bombarde, G., Mariani, J., Hunsmann, G., Grassi, J., Bally, Y. (2000) Synaptic Prion Protein Immuno-Reactivity in the Rodent Cerebellum. Microscopy Research and Technique 50, 66-75
- (144) Manson, J.C., Jamieson, E., Baybutt, H., Tuzi, N.L., Barron, R., McConnell, I., Somerville, R., Ironside, J., Will, R., Sy, M-S, Melton, D.V., Hope, J., Bostock, C. (1999) A single amino acid alteration (101L) introduced into murine PrP dramatically alters incubation time of transmissible spongiform encephalopathy. The European Molecular Biology Organization Journal 18 (23), 6855-6864
- (145) Speer, M.C., Goldgaber, D., Goldfaber, L.G., Roses, A.D., Pericak-Vance, M.A. (1991) Support of Linkage of Gerstmann-Sträussler-Scheinker Syndrome to the Prion Protein Gene on Chromosome 20p12-pter. Genomics 9, 366-368
- (146) Hill, A.F., Joiner, S., Wadsworth, J.D.F., Sidle, K.C.L., Bell, J.E., Budka, H., Ironside, J.W., Collinge, J. (2003) Molecular classification of sporadic Creutzfeldt-Jakob-disease. Brain 126, 1333-1346
- (147) Lee, H-S, Broun, P., Cervenakova, L., Garruto, R.M., Alpers, M.P., Gajdusek, D.C., Goldfarb, L.G. (2001) Increased susceptibility to kuru of carriers of the *PRNP* 129 Methionine/Methionine genotype. The Journal of Infectious Diseases 183, 192-196
- (148) Wodsworth, J.D.F., Joiner, S., Linehan, J.M., Desbruslais, M., Fox, K., Cooper, S., Cronier, S., Asante, E.A., Mead, S., Brandner, S., Hill, A.F., Collinge, J. (2008) Kuru prions and sporadic Creutzfeldt-Jakob disease prions have equivalent transmission properties in transgenic and wild-type mice. Proceedings of National Academy of Sciences USA 105 (10), 3885-3890
- (149) Wodsworth, J.D., Asante, E.A., Desbruslais, M., Linehan, J.M., Joiner, S., Gowland, I., Welch, J., Stone, L., Lloyd, S.E., Hill, A.F., Brandner, S., Collinge, J. (2004) Human prion protein with valine 129 prevents expression of variant CJD phenotype. Science 306 (5702), 1692-1693.
- (150) Lopez, G.F., Zahn, R., Riek, R., Wuthrich, K. (2000) NMR structure of the bovine prion protein. Proceedings of National Academy of Sciences USA 97, 8334-8339
- (151) Parchi, P.P., Castellani, R., Capellari, M.D., Ghetti, B., Young, K., Chen, S.G., Farlow, M., Dickson, D.W., Sima, A.F., Trojanowski, J.Q., Peterson,

- R.B., Gambetti, P. (1996) Molecular Basis of Phenotypic Variability in Sporadic Creutzfeldt-Jakob Disease. *Annals of Neurology* 39 (6), 767-778
- (152) Mullis, K., Faloona, F., Scharf, S., Saiki, R., Horn, G., Erlich, H. (1986) Specific Enzymatic amplification of DNA in vitro: the polymerase chain reaction. *Cold Spring Harbor Symposia on Quantitative Biology* 51 (1), 263-273
- (153) Kyhse-Anderson, J. (1984) Electrophotting of multiple gels: a simple apparatus without a buffer tank for rapid transfer of proteins from polyacrylamide to nitrocellulose. *Journal of Biochemical and Biophysical Methods* 10, 203-209
- (154) Harlow, E.D. and Lane, D. (1999) *Using Antibodies*. Cold Spring Harbor, New York: Cold Spring Harbor Laboratory Press
- (155) Hames, B.D. and Rickwood, D. (1998) *Gel Electrophoresis of Proteins: A Practical Approach 3rd Edition*, The Practical Approach Series, Oxford University Press
- (156) Bolt and Mahoney (1997) High-efficiency blotting of proteins of diverse sizes following sodium dodecyl sulfate-polyacrylamide gel electrophoresis. *Analytical Biochemistry* 247, 185-192
- (157) Stahl, N., Baldwin, M.A., Teplow, D.B., Hood, L., Gibson, B.W., et al. (1993) Structural studies of the scrapie prion protein using mass spectrometry and amino acid sequencing. *Biochemistry* 32, 1991-2002
- (158) Alpers, M.P. (1987) Epidemiology and clinical aspects of kuru. Cited in: Will, R.G. (2003) Acquired prion disease: iatrogenic CJD, variant CJD, kuru. *British Medical Bulletin* 66, 255-265
- (159) Piccardo, P., Dlouhy, S.R., Lievens, P.M.J. et al. (1998) Phenotypic variability of Gerstmann-Sträussler-Scheinker disease is associated with prion protein heterogeneity. *J. Neuropathol. Exp. Neurol.* 57, 979-988
- (160) Collinge, J. (1999) Variant Creutzfeldt-Jakob disease. *Lancet* 354, 317-323. Cited in: Mead, S. (2006) Prion Disease Genetics. *European Journal of Human Genetics* 14, 273-281
- (161) Goldfarb, L.G., Haltia, M., Brown, P., et al. (1991) New mutations in scrapie amyloid precursor gene (at codon 178) in Finnish Creutzfeldt-Jakob kindred. *Lancet* 337, 425
- (162) Medori, R., Tritschler, H.J., LeBlanc, A., et al. (1992) Fatal familial insomnia, a prion disease with a mutation at codon 178 of the prion protein gene. *New England Journal of Medicine* 326, 444-449
- (163) Bruce, M. E., Fraser, H., McBride, P. A., Scott, J.R., and Dickson, A.G (1992) The basis of strain variation in scrapie, in *Prion Diseases of Humans*

and Animals (Prusiner, S. B., Collinge, J., Powell, J., and Anderton, B., eds.), Ellis Horwood, Chichester, pp. 497–508

- (164) Cauphey, B. (2001) Interaction between prion protein isoforms: the kiss of death. *Trends in Biochemical Sciences* 4, 235-242
- (165) www.abcam.com/technical: SDS-PAGE and Western Blot Analysis.
- (166) [www.eBioscience BestProtocols Immunofluorescent Staining of Cell Surface Antigens for Flow Cytometric Analysis \(FACS Analysis\).htm](http://www.eBioscience.com/BestProtocols/Immunofluorescent%20Staining%20of%20Cell%20Surface%20Antigens%20for%20Flow%20Cytometric%20Analysis%20(FACS%20Analysis).htm)

8. Curriculum Vitae

Name: Mohamed Karmi Hussien Mahmoud
Birth date: 08/05/1972
Birth place: Aswan, Egypt
Social state: Married
Nationality: Egyptian
Profession: Assistant Lecturer in the Faculty of Veterinary Medicine,
South Valley University, Qena, Egypt
E.mail: Karmy99@yahoo.com

Education:

1980-1986 Primary school, Edfu Baneen, Aswan, Egypt
1986-1988 Preparatory school, Edfu El-Hadetha, Aswan, Egypt
1988-1990 Secondary school, Edfu El-Thanawia, Aswan, Egypt
1990-1995 Faculty of Veterinary Medicine, Assiut University, Egypt
June-2001 Master in Food Hygiene and Diseases, Faculty of Veterinary
Medicine, Assiut University, Egypt
2007-2008 PhD studies in the Faculty of Veterinary Medicine, LMU,
Munich, Germany and in the Center of Neuropathology
and Prion Research, LMU, Munich, Germany

Languages: Arabic (mother language)
English (good)
German (good)

PC Skills: ICDL certificate (Windows, Word, Excel, Access, Power Point, Internet and IT)

Experiences:

2000 Training courses in Molecular Biology, PCR technique, Assiut
1999 Workshop on Practical applications of PCR technique in Molecular Biology Research Center, Assiut
2004 Course (Theoretical Lectures) on recent techniques of Molecular Biology, Recombinant DNA, Gene-Expression, Proteomics, Human Genome, Assiut

Courses:

2000 Course in HPLC (Well-skillful)
2002 Course in Laboratory Quality Control Assurance
1998 Course in Statistics
1998 Course of Zoonotic Diseases (Viral, Bacterial & Parasitic)
1998 Course of Microbiology
1998, 2002 Courses in Food Hygiene, Microbiology and Technology

9. Acknowledgment

Ultimate thanks are to GOD who gives me strength to complete this work.

I wish to express my sincere gratitude and deep thanks to Prof. Dr. Hans Kretzschmar, Professor of neuropathology, ZNP, LMU, Munich, for suggestion of theme, kind supervision and continuous support.

Sincere thanks to Prof. Dr. Walter Hermanns, professor of veterinary pathology, faculty of veterinary medicine, LMU, Munich, for cooperative, uncomplicated supervision and support.

I am greatly indebted to Dr. Sabina Eigenbrod, assistant in ZNP, LMU, Munich for her learning, continuous support, help and advice, a lot of thanks to Dr. Marko Maringer and Dr. Niklas Piening, Dr. Martin Fuhrmann, Prof. Dr. Jochen Herms for their help in mouse transgenesis, tissue culture and FACS analysis. The HuMM and HuVV mice were a gift from Prof. Jean Manson, Edinburg, UK.

Also, deepest appreciation to Dr. Petra Weber, ZNP, LMU, for her help in planning and laboratory work.

I would like to thanks Dr. med. vet. Gerda Mitteregger and Dr. med. vet. Mehdi Shakarami for their help in animal breeding, management and infection.

Deep thanks to Mr. Michael Schmidt, Mrs. Gertrud Kwiatkowski, Mrs. Veronika Kaltenbrunn and all staff members of the ZNP, LMU, Munich for their technical assistance, help and valuable advice.

Special thanks to my family and my wife for their continuous support, encouragement and patience.

Sincere thanks should be offered to the Egyptian government for its support of my doctor study in Germany for two years.